REPUBLIQUE DU CAMEROUN
Paix – Travail – Patrie
****

UNIVERSITE DE YAOUNDE I
FACULTE DES SCIENCES
DEPARTEMENT DE CHIMIE INORGANIQUE
****

REPUBLIC OF CAMEROUN
Peace – Work – Fatherland
****

UNIVERSITY OF YAOUNDE I
FACULTY OF SCIENCES
DEPARTMENT OF INORGANIC CHEMISTRY
****

MICROSTRUCTURE AND THERMOMECHANICAL PROPERTIES OF GEOPOLYMERS FROM SOME CAMEROON'S VOLCANIC ASHES

Doctor of
Philosophy in Chemistry

Par :

LEMOUGNA NINLA Patrick
DEA in Inorganic Chemistry

Sous la direction
Uphie CHINJE MELO
Associate professor

Année Académique
2014-2015

TABLE OF CONTENTS

Acknowledgements

The completion of this work would not have been possible without the financial support of the Local Materials Promotion Authority (MIPROMALO), Cameroon, the MacDiarmid Institute for Advanced Materials and Nanotechnology, School of Chemical and Physical Sciences, Victoria University of Wellington in New Zealand and the Department of Physical Chemistry and Polymer Science, Faculty of Engineering Science, Vrije Universiteit Brussel in Belgium. I am also grateful to VLIR-UOS for the short research grant which supported part of this work. I hereby express my sincere gratitude to all these Institutions.

I am very grateful to:

Prof Uphie Chinje Melo of the University of Yaoundé I for the thesis topic provided as well as the interesting comments and orientations helpful to achieve this work. Her rigor and dynamism have always been a source of motivation for me. She followed this work step by step and the time has come now to say thank you.

Prof. Kenneth MacKenzie and Prof. Hubert Rahier of Victoria University of Wellington and Vrije Universiteit Brussel respectively, to have accepted and supervised my research internships in New Zealand and Belgium. Their kind support, their encouragement and their observations were very helpful in the completion of this work and I wish to say thank you.

Prof. Jan Wastiels of Vrije Universiteit Brussel, for the interesting comments;

Prof. Daniel Njopwouo and Prof. Antoine Elimbi of the University of Yaoundé I, for their encouragement to pursue my studies after my Master degree;

Prof. Henk Nugteren of TU Delft University and Technology, for his advice and the interesting exchanges.

I am also grateful to:

Dr. Elie Kamseu, Dr. Ndigui Billong, Dr. André Njoya, Dr Tchaptchep and Dr. Chantale Djangang for their advice, interesting exchanges and moral support;

My colleagues in MIPROMALO, especially those from the Technical Department, for their moral support;

My family for their moral and financial support;

The members of jury for their critical comments to improve the work;

All those not mentioned here, but who contributed in one way or the other in the achievement of this piece of work.

List of figures

List of photographs

List of tables

Abreviations

A.S.T.M:	American Society for Testing and Materials
CSH:	Calcium Silicate Hydrate
DMA:	Dynamic Mechanical Analysis
DSC:	Differential Scanning Calorimetry
DTA:	Differential Thermal Analysis
EDS:	Energy Dispersive X-ray Spectroscopy
FTIR:	Fourier Transform Infrared Spectroscopy
GGBS:	Ground granulated blast slag
IRL	Industrial Research Limited (New Zealand)
L.T.G.S:	Low Temperature Geopolymeric Setting
MAS-NMR:	Magic-Angle Spinning -Nuclear Magnetic Resonance spectroscopy
MPa:	Mega Pascal
OPC:	Ordinary Portland Cement
PCDS:	Polycyclodisialate
PS:	Poly(sialate)
PSDS:	Poly(sialate-disiloxo)
PSS:	Poly(sialate-siloxo)
TG or TGA:	Thermogravimetry Analysis
SEM:	Scanning Electron Microscopy
Va:	Volcanic ash
Va1 :	Va from Foumbot Petponun
Va1 :	Va from Foumbot Lac Mfou
Va 3 :	Va from Djoungo (Black feature)
Va 4 :	Va from Djoungo (Red feature)
VUB:	Vrije Universiteit Brussel
VUW:	Victoria University of Wellington
XRD:	X-ray diffraction

ABSTRACT

This study deals with the alkaline activation of volcanic ashes to produce structural materials with potential application in construction or as refractories. Four Cameroonian volcanic ashes (Va1, Va2, and Va3, Va4 respectively from Foumbot and Djoungo) were used. For practical reasons the volcanic ashes were ground and sieved to a grain size less than 400 µm. The alkaline activator solutions used were sodium hydroxide, potassium hydroxide, and a mixture of both, with or without amorphous silica. The reactivity of the systems was studied by Differential Scanning Calorimetry (DSC).

Several techniques were used to characterize the raw materials and products: X-ray fluorescence (XRF), X-ray diffraction (XRD), Fourier Transform Infrared Spectroscopy (FTIR), Scaning Electron Miscroscopy (SEM), Digital Optical Microscopy (DOM), Mossbauer Spectroscopy (MS), Differential Scaning Calorimetry (DSC), Thermogravimetry and Differential Thermal Analyses (TGA/DTA) Mechanical and Dynamic Mechanical Analyses (DMA).

The results obtained showed that NaOH solution was the fastest activator, though the reaction is still very slow at room temperature. The samples were treated at 90 °C for 7 days, but the mechanical strength increased substantially up to 21days at 90 °C.

The X-ray spectra showed a mixture of amorphous and crystalline phases in both volcanic ashes and synthesized materials. Scanning electron microscopy showed a homogenously distributed mixture of lath-shaped and agglomerated morphologies, with a homogeneous distribution of Si, Al and O in the geopolymer matrix. The largest particles acted as filler while smaller particles dissolved in the activating solution forming the glassy aluminosilicate matrix. The reactivity of the volcanic ashes was found to increase with their content in amorphous phases. The wet strength at lowest NaOH concentration also increased with the amount of amorphous phase in the volcanic ashes. For the high NaOH concentrations, no correlation could be established between the amount of amorphous phase in the starting materials and the final strength.

Curing conditions, the Na_2O/SiO_2 or the Na_2O/Al_2O_3 molar ratio were found to influence the development of compressive strength of the geopolymers. Dry curing conditions led to better strengths (in the range 14-63 MPa). However, the strength decreased (1-28 MPa) after specimens' immersion overnight in water, but was partly or totally recovered after overnight drying. The formation of a mortar by the addition of 40 wt% sand to the optimized

composition reduced the compressive strength from 55 to 30 MPa, still within the useful range for construction applications.

The geopolymers were relatively stable to heat, shrinking only slowly and retaining about 60% of their as-synthesized compressive strength on heating to 900 °C. However the more thermally stable materials were found to be specimens from KOH solution.

The results obtained suggest the possible use of the synthesized materials for building applications and low temperature refractories up to about 700-900 °C.

Key words: Volcanic ash, Alkaline activation, Amorphous phase, Geopolymers, Compressive strength, Thermal properties, Construction.

RESUME

Cette étude porte sur l'activation alcaline des scories volcaniques pour produire des matériaux ayant une application potentielle dans la construction ou les réfractaires de basse température. Quatre scories volcaniques camerounaises (Va1, Va2 et Va3, Va4 en provenance de Foumbot et Djoungo respectivement) ont été utilisées. Pour des raisons pratiques, les scories volcaniques ont été broyées et tamisées à une granulométrie inférieure à 400 micromètres. Les solutions d'activation alcaline utilisées sont l'hydroxyde de sodium, l'hydroxyde de potassium, un mélange des deux, avec ou sans silice amorphe. La réactivité des systèmes a été étudiée par Calorimétrie Différentielle à Balayage (DSC).

Plusieurs techniques ont été utilisées pour la caractérisation des matières premières et des produits de synthèse: Fluorescence X (XRF), Diffraction des rayons X (XRD), Spectroscopie Infrarouge à Transformée de Fourier (FTIR), Miscroscopie Electronique à Balayage (SEM), Microscopie optique numérique (DOM), Spectroscopie Mössbauer (MS), Calorimetrie Différentielle à Balayage, Analyses Thermogravimétrique et Thermique Différentielle (TGA/DTA), Analyses mécaniques et thermomécaniques (DMA).

Les résultats obtenus montrent que la solution de NaOH est l'activateur alcalin le plus rapide, mais la réaction demeure très lente à la température ambiante. Les échantillons ont été traités à 90 °C pendant 7 jours, mais les résistances mécaniques augmentent sensiblement après 21 jours à 90 °C.

Les spectres de rayons X des matériaux montrent un mélange de phases amorphes et cristallines aussi bien pour les scories pures que dans les matériaux de synthèse. La Microscopie électronique à balayage montre un mélange homogène de morphologies sous forme de plaquettes et d'agglomérés, avec une répartition homogène de Si, Al et O dans la matrice géopolymèrique. Les grosses particules se sont beaucoup plus comportées comme matériaux de remplissage tandis que les petites particules se sont dissoutes dans la solution d'activation formant la matrice geopolymérique. Les réactivités des cendres volcaniques augmentent avec leur teneur en phase amorphe. La résistance mécanique humide, à faible concentration de NaOH, augmente également avec la teneur en phase amorphe dans les cendres volcaniques. Pour les concentrations élevées de NaOH, aucune corrélation entre la quantité de phase amorphe dans les matières premières et la résistance finale des produits n'a pu être établie.

Les conditions de synthèse, les rapports molaires Na_2O/SiO_2 ou Na_2O/Al_2O_3 influencent le développement de la résistance à la compression des géopolymères. La synthèse dans un

environement sec conduit à de meilleures résistances mécaniques (de l’ordre de 14-63 MPa). Toutefois, les résistances mécaniques diminuent (1-28 MPa) après immersion des spécimens pendant 24 heures dans l'eau, mais augmentent à nouveau partiellement ou totalement après 24 heures de séchage. L’addition de 40 % en masse de sable à la meilleure formulation a réduit la résistance à la compression de 55 à 30 MPa, encore suffisante pour des applications de construction.

Les géopolymères sont relativement stables à la chaleur, présentant un faible retrait et maintenant environ 60 % de leur résistance initiale à la compression après chauffage à 900 °C. Toutefois, les matériaux plus stables thermiquement sont les spécimens à base de la solution de KOH.

Les résultats obtenus suggèrent la possibilité d'utiliser les matériaux synthétisés pour des applications de construction et réfractaires à basse température jusqu'à environ 700-900 °C.

Mots clés: Cendres volcaniques, activation alcaline, phase amorphe, géopolymères, résistance à la compression, propriétés thermiques, construction.

GENERAL INTRODUCTION

GENERAL INTRODUCTION

Geopolymers are new materials with applications as coatings and adhesives, binders for fiber composites, waste encapsulation, new cements for structural purposes etc. In France, their initial applications between 1973 and 1976 were oriented towards construction, following a series of fires in buildings worsened by the flammability of plastic insulating materials (Davidovits, 1991; 1994a; 2008). Subsequently, their properties and uses were explored by several scientific and industrial disciplines including modern inorganic chemistry, physical chemistry, colloidal chemistry, geological sciences and various engineering and technology approaches (Duxson et al., 2007a; Davidovits, 1991, 2008; MacKenzie et al., 2009; Nugteren, 2010; Rahier et al., 1996a; 1996b). Today, the vast diversity of their potential applications include fire-resistant materials, decorative stone, insulation, low-technology building materials, low energy production of ceramic tiles, various types of refractories, foundry materials, high-tech composites for aircraft and automobiles, high-tech resins, encapsulation of radioactive waste, art and archeology (Davidovits and James, 1984; Barbosa and MacKenzie, 2002; Boutterin and Davidovits, 2003; Davidovits, 2008; Rahier et al., 2007; O'Connor and MacKenzie, 2010). The synthesis methods of geopolymer materials have the advantage of being environmentally-friendly, producing very little greenhouse gas (Davidovits, 1994a; Barbosa et al., 2000; Nugteren, 2010). Their chemistry generally involves mechanisms such as dissolution of silicates and aluminates in a strongly basic medium, followed by polymerization of surface active groups of particles with the dissolved species to form a solid geopolymer structure. This consists of a network of more or less amorphous SiO_4 and AlO_4, where silicon and aluminum are in IV-fold coordination with oxygen. The presence of alkaline ions such as Na^+, K^+, Li^+ in the network is necessary to compensate the negative charge of Al^{3+} in IV-fold coordination (Barbosa et al., 2000; Xu and van Deventer, 2000; Davidovits, 2002; Barbosa and MacKenzie, 2002; Kamseu et al., 2009; Temuujin et al., 2010).

In Cameroon, despite the wide availability of adequate minerals potentially suitable for the synthesis of these materials, the benefits of this technology remain unexploited. There are no factories producing low-temperature refractories and insulators, despite the large consumption of these products by companies such as local bakeries. Moreover, the construction materials sector is dominated by a monopoly company producing Portland cement, the price of which has increased by about 51% in the last decade. This price increase, coupled with the lack of

companies producing construction materials has the effect of reducing access to affordable houses for a large fraction of the population with low income. It also leads to a fall in currency because of the need to import construction materials, producing negative impact on the trade balance.

Recognizing the role and importance of research for industrial and technological development and with the aim of improving the population's living conditions, the Laboratory of Physico-chemistry of Inorganic Materials of the University of Yaounde 1 and the Materials Analysis Laboratory of the Local Materials Promotion Authority (MIPROMALO) have been involved since 2007 in research activities to develop more ecological and affordable building materials from local resources.

The objective of this study is to continue the preliminary work already carried out on geopolymers in Cameroon, by developing improved low cost and environmentally-friendly synthesis protocols for manufacturing viable geopolymer products from local aluminosilicate raw materials such as volcanic ashes that are readily available in the Littoral, Adamawa, West and South-west Regions. Previous work (Lemougna, 2008; Kamseu et al., 2009) has shown these to be suitable for geopolymers syntheses. Following from this, mineralogical, microstructural, Fourier Transform Infrared Spectroscopy (FTIR), thermal and mechanical analytical methods will be used to characterize the geopolymer products obtained from optimised formulations and processes to allow their properties to be mastered and to highlight the possibilities of their potential application in the fields of construction, or low temperature refractories.

This thesis is divided into three chapters:

- Chapter I provides a literature review of the various aluminosilicate raw materials and geopolymer chemistry;
- Chapter II presents the characteristics of the materials studied and the experimental methods used;
- Chapter III presents and discusses the results of this study and makes suggestions and observations on their future prospects. It is subdivided into 5 subparts:

Subpart III-1 investigates the influence of the chemical and mineralogical composition of four volcanic ashes (from different deposits) on their reactivity for geopolymers synthesis;

Subpart III-2 investigates the influence of the activating solution composition on the thermomechanical properties of geopolymers made from the more reactive ash;

In the subpart III-3, the influence of processing conditions and the thermal stability of geopolymers made from the more reactive ash are investigated;

Subpart III-4 presents a brief enquiry on environmental concerns and economic practicability of geopolymer binders versus ordinary Portland cement in Cameroon and the suggestions and prospects are presented in the subpart III-5.

CHAPTER I: STATEMENT OF THE PROBLEM AND LITERATURE REVIEW

Introduction

This section starts with a statement of problem situating the work in its context. It provides a review on geopolymer chemistry. The different types of possible raw materials for geopolymer synthesis are presented. The synthesis processes and parameters influencing the final properties are highlighted with the different analytical methods used for geopolymers characterization. Zeolites are also briefly described due to their similarities in raw materials and synthetic routes with geopolymer materials.

I-1: STATEMENT OF THE PROBLEM

Ordinary Portland Cement (OPC) is the most commonly used construction material. It is used by communities across the globe and is second only to water (Habert et al., 2011). Customarily, concrete is produced by using Ordinary Portland Cement (OPC) as the binder. Portland cement constitutes one of the most important technological advances in the history of humanity. Thanks to this material the twentieth century saw the consolidation and acceleration of the reconstruction and even the redefinition of many of the world's major cities (C. Shi et al., 2011). However, OPC is a high energy intensive product which releases great quantities of carbon dioxide (CO_2) during its production. G. (Habert et al., 2011). Beyond the pollution associated to OPC production, the limited durability, the limited resistance to heat and corrosion were also reported as handicaps of OPC binders (F. Pacheco-Torgal et al., 2008; D.L.Y. Kong, J.G. Sanjayan., 2010). Due to a world-wide increase in the demand of OPC, the production and pollution associated to OPC manufacturing have also increased, negatively affecting the global warming and the living conditions of human beings. So far, research works carried out in developing alkali activated binders (geopolymers) show that these new binders are likely to have enormous potentials to become an environmental-friendly alternative to OPC (F. Pacheco-Torgal et al., 2008 C. Shi et al., 2011). Geopolymers can be synthesized from a wide range of Si and Al rich materials which can be naturally occurring or by-products of industrial processes. Despite the huge number of reports on geopolymers chemistry and applications, these binders are still at the early stage of development and, hence, need further research work in order to become technically and economically viable construction materials (F. Pacheco-Torgal et al., 2008). In addition, due to the high difference in chemical and mineralogical composition of naturally occurring aluminosilicates materials, somewhat linked to their geological history, new investigations are always needed before

designing a possible pathway for the synthesis of geopolymer building materials from a particular source of naturally occurring aluminosilicate material.

Beyond the concern of global warming, the high cost and the scarcity of OPC is still a great preoccupation in many developing countries including Cameroon, hence the need to develop new alternative building materials, not only for environmental issues, but also to increase the offer of building materials in the local market. The broad aim of the thesis is to investigate and provide information on the possibilities to produce geopolymers for structural and high temperature applications from Cameroon's volcanic ashes. The output of the thesis is also expected to bring out useful technical and scientific data that may facilitate the production of geopolymers in Cameroon with the related advantages.

I-2: SOME ALUMINOSILICATE RAW MATERIALS FOR GEOPOLYMERS SYNTHESIS

Raw materials for geopolymerization can be naturally occurring minerals such as clays. These are all minerals containing Si, Al and O with possibly other elements such as H, Na, K, Ca and Mg. They are classified as aluminosilicates (Davidovits, 1988). The earth's crust chemical composition is rich in silica and alumina (about 59% of SiO_2% and 16 % of Al_2O_3 in the outer most 20 km) (Sigg, 1991) and is therefore an important source of raw materials available for geopolymerization reactions.

I-2-1: Pozzolanas

Pozzolanas are natural or artificial materials rich in silica and alumina which may react with lime in the presence of water to form products exhibiting binding properties (Davidovits, 1994a; Melo and Ndigui, 2004). They are used in cement production for their hydraulic properties; namely, their ability to fix lime at room temperature and form compounds with hydraulic properties (Melo and Ndigui, 2004). The main pozzolanas are vitreous pyroclastic materials produced by violent eruptive volcanic action, power plant ash (fly ash), slag from blast furnaces, ash from rice husks, bagasse from sugar cane, and calcined clay (Davidovits, 1994a; Melo and Ndigui, 2004).

During volcanic eruptions, particularly of the Strombolian-type, pozzolanas are ejected on the surface of the earth, forming layers of several meters thick. Throughout the world there are

volcanoes (eg. Mount St. Helens in the U.S.A., Etna in Italy, Tinatubo in the Philippines, Tarawera in New Zealand, Santiaguito and Pacaya in Guatemala, Fuego in Costa Rica) which have produced huge quantities of pozzolanas (Kamseu et al., 2009).

In Cameroon, most volcanic eruptions over millions of years in the tertiary period were accompanied by the ejection of pozzolanas. Consequently, many cones of volcanic ash exist along the'Cameroon line' oriented N30°E, specially at the side of mount Cameroon, mount Manenguba, the Tombel plain around Djoungo, the Noun plain around Foumbot, the Kumba plain, the region of lake Nyos and the Adamaoua plateau. The latest eruption of mount Cameroon in 1999, as with previous eruptions, resulted in millions of tonnes of volcanic materials covering vast areas with nonmetallic minerals deposits. These deposits are readily accessible and have the advantage that they can be naturally mined with the enormous benefit of low cost methods which have limited negative environmental impact compared with traditional open pit quarry type clay mining (Ntep Gweth et al., 2001; Leonelli et al., 2007).

Wandji and Tchoua (1989) studied the geochemistry and petrography of volcanic projections from Foumbot. They observed that there is no petrographical and geochemical difference between tephras and lavas. Their mineralogy as the quasi totality of Cameroon volcanism involves minerals of alkaline series, from alkaline basalt with olivine to rhyolites and anorthose or minerals from sanidine-anorthose series (Wandji and Tchoua, 1989).

The pozzolanic properties of Foumbot and Djoungo volcanic deposits studied by Wandji and Tchoua (1988) and Bijocka et al. (1993) have shown their suitability for the production of Portland cement and concrete. The mineralogical content of these ashes includes plagioclase, diopside, enstatite, anorthite, pyroxene and olivine (Leonelli et al., 2007; Bijocka et al., 1993). Djoungo and Foumbot volcanic ashes have also been shown to be suitable raw materials for geopolymer syntheses (Lemougna, 2008; Kamseu et al., 2009).

Some Cameroon's pozzolanas are used in road improvement works or as additives in the production of Portland cement and concrete mortar. However, several large deposits remain undeveloped or unexplored (Ntep Gweth et al., 2001).

I-2-2: Clay minerals

Clay minerals (phyllosilicates) are hydrous aluminosilicates, with large lattice structures (Sigg, 1991; Karfa, 2003). These minerals are made up of tetrahedral, silicon-oxygen units interspersed with octahedral sheets containing aluminum (or magnesium) surrounded by six oxygen atoms in 6- fold coordination (Sigg, 1991).

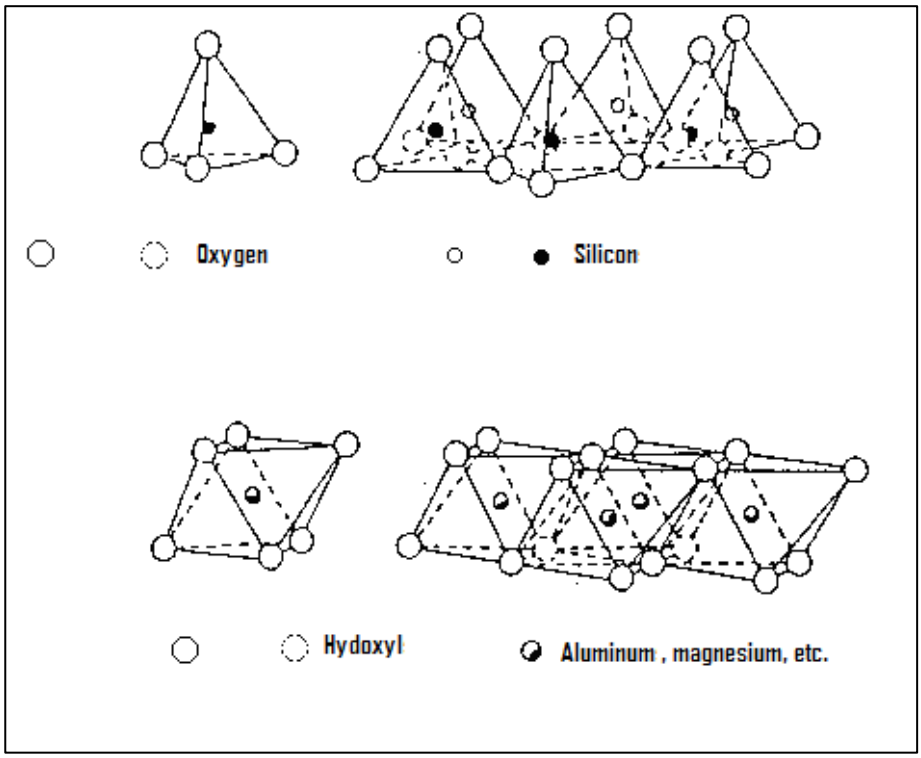

Figure 1: Structural elements of clay minerals (Sigg, 1991).

Top- single silica tetrahedron and sheet structure of silica tetrahedra arranged in a hexagonal network; Bottom- single octahedral unit and sheet structure of octahedral units.

Atom substitutions are common in the crystalline layers and may disrupt the crystal structure. Clays can be classified as 1 / 1 layer silicates, containing a repeating sequence of one tetrahedral layer and one octahedral layer or 2 / 1 layer silicates containing two tetrahedral layers and one octahedral layer and 2/1/1 (two tetrahedral layers and two octahedral layers) (Aliprandi, 1979; Karfa, 2003). Cameroon's soil is rich in unmined clay deposits, but little use is made of them for pottery and bricks production. Figure 2 and Table 1 show respectively the structure of a type 1 / 1 clay mineral and the classification of clay minerals.

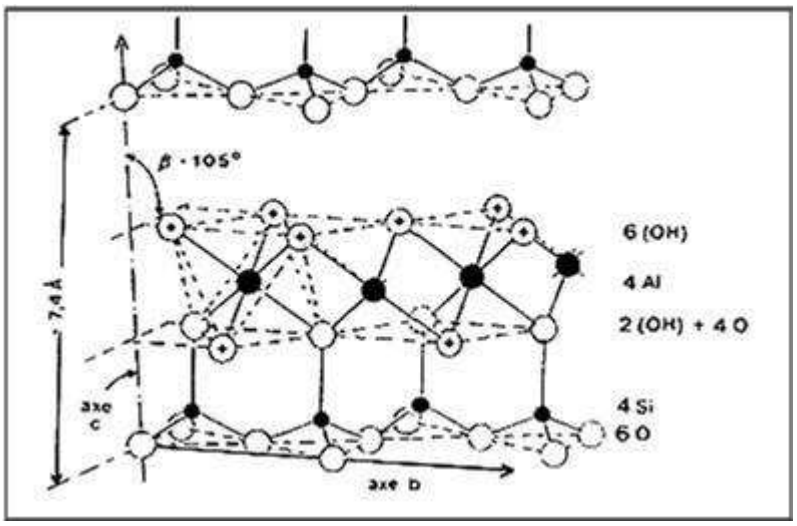

Figure 2: Structure of kaolinite (clay mineral type 1 / 1) (Karfa, 2003).

Table 1: Classification of clay minerals (the first number designating the number of tetrahedral layers, the second and third, those of octahedral layers (dioctahedral or trioctahedral) (Aliprandi, 1979).

Type	Group	Sub-group	Species	Formula
1/1	Kaolin	Kaolinite	Dickite	$Si_2O_5Al_2(OH)_4$
			Nacrite	$Si_2O_5Al_2(OH)_4$
			Kaolinite	$Si_2O_5Al_2(OH)_4$
			Metahalloysite	$Si_2O_5Al_2(OH)_4$
			Halloysite	$Si_2O_5Al_2(OH)_4\ 4H_2O$
		Serpentine	Antigorite	$Si_2O_5Mg_3(OH)_4$
2/1	Talc	Pyrophyllite	Pyrophyllite	$Si_4O_{10}Al_2(OH)_2$
		Talc	Talc	$Si_4O_{10}Mg_3(OH)_2$
	Smectite	Dioctahedral Smectite	Montmorillonite	$Si_4O_{10}(Al_{1,67}Mg_{0,33})(OH)_2$
		Trioctahedral Smectite	Saponite	$(Si_{3,67}Al_{0,33})O_{10}Mg_3\ (OH)_2$
	Vermi-culite	Dioctahedral Vermiculite	Vermiculite dioctahedral	$(Si,Al)_4O_{10}(Al,Fe...)_2(OH)_2$
		Trioctahedral Vermiculite	Vermiculite	$(Si,Al)_4O_{10}(Mg,Fe...)_2(OH)_2$
	Micas	Dioctahedral Micas	Muscovite	$K(Si_3Al)O_{10}Al_2(OH)_2$
		Trioctahedral Micas	Phlogopite	$K(Si_3Al)O_{10}Mg_3(OH)_2$
2/1/1	Chlorite	Dioctahedral Chlorite	Sudoite	$(Si,Al)_4O_{10}Al_4(OH)_8$
		Trioctahedral Chlorite	Different species	$(Si,Al)_4O_{10}(Mg,Fe...)_6(OH)_8$

Clay minerals conventionally used for geopolymer synthesis are of the kaolinite type, dehydroxylated by heat treatment to form metakaolinite. The transformation of kaolinite into metakaolinite (for geopolymer synthesis) involves the loss of structural water, increasing the reactivity of the silicate and aluminate units and converting the octahedral aluminium into a mixture of 4, 5 and 6-fold coordination with higher reactivity (MacKenzie, 2009).

I-2-3: Other aluminosilicate materials

In theory, all aluminosilicate materials can be used as source of raw materials for geopolymers synthesis (Duxson et al., 2007a). However, apart from the high number of studies using kaolinite (Davidovits, 1979; Cioffi et al., 2003; Ka-bik, 2004; Singh et al., 2004; Wang et al., 2005; Singh et al., 2005; Dedecek et al., 2008; Okada et al., 2009; Zuhua et al., 2009; 2009b; Mackenzie and O'Leary, 2009), other reports are for fly ash, ground granulated blast slag (GGBS) and feldspar (Swanepoel et al., 2002; Lee William, 2002; Lee and van Deventer, 2003; Sindhunata, 2006; Wallah and Rangan, 2006; Sumajouw and Rangan, 2006; Andini et al., 2007; Provis et al., 2009; Temuujin, 2010; Zhang et al., 2009; Ravikumar et al., 2010).

a) Fly ash

Fly ashes are very fine residues from the combustion of coal during the operation of thermal power plants. They are fine spherical particles composed of minerals containing silicon, aluminum, iron, calcium, magnesium and traces of titanium and organic materials such as carbon. Their chemical composition depends on the nature of the coal from which they originate. Class F fly ash consists of 80-85 wt% silica + alumina and less than 10 wt% calcium oxide, whereas class C fly ash contains less alumina and silica, but 20-40 wt% calcium oxide (Lee William, 2002; Swanepoel et al., 2002; Sindhunata, 2006).

From a technological point of view and in terms of strength properties, up to 25 wt% of fly ash may be blended with Portland cement. In 1998, world production of electricity generated 290 million tonnes of fly ash, of which only 10 % to 15 % has been used in blended cements. There are several reasons for the relatively low percentage of fly ash used in cements. The most relevant is the non-uniform nature of the fly ash, which also restricts its use for geopolymers synthesis and applications. In addition, the tendency in world electricity generation is away from coal fuelled power plants, in line with the trends towards reduced CO_2 emissions (Davidovits, 1994a).

b) Ground granulated blast slag (GGBS)

Ground Granulated Blast furnace Slag (GGBS) as the name suggests is granulated blast furnace slag, ground to very high fineness. Blast furnace slag is formed in processes such as pig iron manufacture from iron ore, combustion residue of coke, and fluxes such as limestone or serpentine, and other materials. If the molten slag is fast-cooled by highpressure water, a

vitreous Ca–Al–Mg silicate fine grain glass is formed. Generally, the way to utilize granulated blast furnace slag is in partially replacing Portland cement (Cheng and Chiu, 2003).
GGBS was suggested to be highly reactive and low cost for geopolymer preparation, compared to fly ash and metakaolin (Zhang et al., 2009).

I-3: GEOPOLYMERS

I-3-1: Geopolymer history and terminology

a) History

In the ancient times, synthetic rocks were formed by mixing kaolinite, dolomite or limestone with Na_2CO_3 or K_2CO_3 (obtained from plant ashes or salt lakes) and silica. This mixture produces NaOH and KOH when mixed with water, which dissolves some of the silica and reacts strongly with the other components to form a geopolymeric binder (van Jaarsveld and van Deventer, 1996). In the 1950's Victor Glukhovsky and Pavel Krivenko developed alkaline systems containing activated calcium silicate hydrate (CSH) and aluminosilicate phases that were used to create large buildings in Ukraine. Glukhovsky was the first to associate the geological processes of transformation at low temperature and pressure of some volcanic rocks in zeolite with cement system models (Komnitsas and Zaharaki, 2007). These research activities were pursued by Berg et al., (1970), who developed uncalcined ceramic materials based on kaolinite for building purposes. In 1978, Davidovits coined the term geopolymer to describe the inorganic polymers with tridimensional structures formed by low temperature polycondensation of aluminosilicates. Subsequently, due to the flammability of plastic building materials causing major fires in France, this led to the development of geopolymers for construction applications. Today, multiple applications of geopolymer materials continue to grow through numerous research activities carried out in the chemical and geological sciences (Xu and Van Deventer, 2000; Komnitsas and Zaharaki, 2007; Rahier et al., 2007; Davidovits, 2008; MacKenzie, 2009; Bell et al., 2009a; Nugteren, 2010; Ruscher et al., 2011).

.

b) Terminology

Davidovits (1994b; 2002) described three classes of inorganic polymers, according to the ratio (R) of SiO_2/Al_2O_3 in the monomer unit

- Poly(sialate), PS, with the monomer unit (-Si-O-Al-O-), and R = 1;
- Poly(sialate-siloxo), PSS, with the monomer unit (-Si-O-Al-O-Si-O-), and R = 2;
- Poly(sialate-disiloxo), PSDS, with the monomer unit (-Si-O-Al-O-Si-O-Si-O-), and R = 3.

Despite the fact that Davidovits describes geopolymers as having a three-dimensional network structure, the polysialate nomenclature proposed by Davidovits inherently does not entirely describe the full connectivity of each silicon and aluminum center or how they relate to one another in a continuous network. However, this nomenclature is commonplace in the field of geopolymer research and is frequently used more to describe the nominal Si/Al ratio rather than the molecular structure and does not provide for description of systems with noninteger Si/Al ratios (Duxson et al., 2005).

The notation Q^n (mAl), where $0 \leq m \leq n \leq 4$; n is the coordination number of the central silicon and m the number of Al neighbors is used to describe the connectivity of a silicon tetrahedron bridged through oxygen to aluminum and to other silicon centers. This notation as first described by Engelhardt in 1982 is used universally for explicitly characterizing aluminosilicate systems including glasses, zeolites, gels, and minerals in experimental and modeling investigations. The three-dimensional structure of Q^n (mAl) notation is illustrated in Figure 3, where n = 4, corresponding to the tetrahedral geometry observed in geopolymers. The links represent oxygen bridges. This notation is quite flexible and aluminosilicate materials can be described regardless of the order degree (Duxon, 2006).

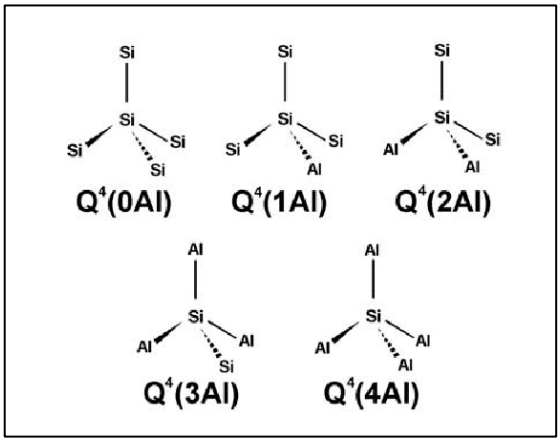

Figure 3: Coordination of three-dimensional silicon centers describing the notation Q^4 (mAl) (Duxson, 2006).

I-3-2: Mechanism of geopolymerization

Geopolymerization is an exothermic reaction which involves the polycondensation of monomers to form a three-dimensional macromolecular structure (Xu and van Deventer, 2000, Rahier et al.,1997). Figure 4 presents the DSC thermograms of metakaolin with different silicate solutions, showing exothermal reaction with peak max between 60- 120°C. The heats of reaction of these mixtures were in the range 260- 580 J per gram of metakaolinite (Rahier et al., 1997).

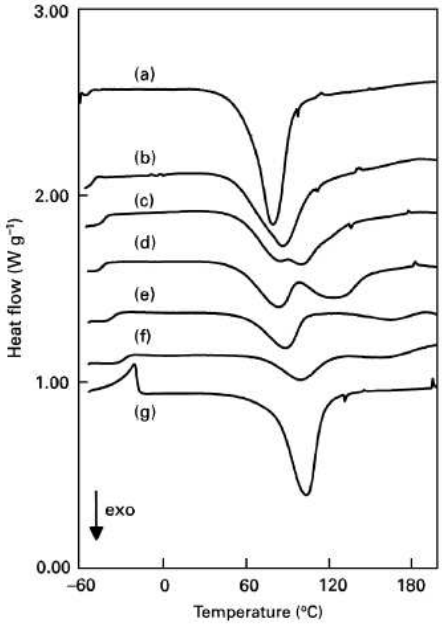

Figure 4: Comparison of DSC thermograms for the reaction of metakaolinite with Na-silicate solutions at H_2O/R_2O = 10.0): with variable SiO_2/R_2O : (a) 1.0, (b) 1.4, (c) 1.6, (d) 1.7, (e) 1.9, (f) 2.3 and (g) K-Silicate solution at H_2O/R_2O = 10.0 with SiO_2/R_2O *of* 1.4. R=Na or K (Rahier et al., 1997).

The equations I.1 and I.2 present an overview of geopolymerisation reactions (Xu and van Deventer, 2000):

$$n\,(Si_2O_5, Al_2O_2) + 2n\,SiO_2 + 4n\,H_2O + NaOH \text{ or } (KOH) \longrightarrow Na^+, K^+ + n\,(OH)_3\text{-Si-O-Al}^-\text{-O-Si-}(OH)_3 \quad \text{(I.1)}$$

Aluminosilicate

$(OH)_2$

Geopolymeric precursor

$$n\,(OH)_3\text{-Si-O-Al}^-\text{-O- Si-}(OH)_3 + NaOH \text{ or } (KOH) \longrightarrow (Na^+, K^+)\text{-(-Si-O-Al}^-\text{-O-Si-O-)} + 4nH_2O \quad \text{(I.2)}$$

$(OH)_2$

Geopolymeric network

A theory of ion pairs was proposed (Xu and van Deventer, 2000) to explain the mechanism of dissolution of aluminosilicate minerals and the mechanism of geopolymerization. The possible chemical process of dissolution of aluminosilicate minerals and silicates in alkaline medium is presented in the following three equations (I.3 - I.5).

$$\text{Al-Si (particulate solid)} + OH^- \text{ (aqueous)} \longleftrightarrow \underset{\text{Monomer}}{Al(OH)_4^-} + \underset{\text{Monomer}}{{}^-OSi(OH)_3} \quad \text{(I.3)}$$

$${}^-OSi(OH)_3 + OH^- \longleftrightarrow {}^-OSi(OH)_2O^- + H_2O \quad \text{(I.4)}$$

$$\begin{array}{l} \\ {}^-OSi(OH)_2O^- + OH^- \end{array} \longleftrightarrow \begin{array}{l} O^- \\ | \\ {}^-OSi(OH)O^- \end{array} + H_2O \quad \text{(I.5)}$$

The reactions between the alkali metal M^+ with divalent and trivalent ortho silicic acid leading to compensate the electrostatic repulsion are presented in the equations I.6 - I.9 (Xu and van Deventer, 2000):

$$\underset{\text{Monomer}}{M^+ + {}^-OSi(OH)_3} \longleftrightarrow \underset{\text{Monomer}}{M^+ {}^-OSi(OH)_3} \quad \text{(I.6)}$$

$$\underset{\text{Monomer}}{2M^+ + {}^-OSi(OH)_2O^-} \longleftrightarrow \underset{\text{Monomer}}{M^+ {}^-OSi(OH)_2O^- M^+} \quad \text{(I.7)}$$

$$\begin{array}{l} O^- \\ | \\ 3M^+ + {}^-OSi(OH)O^- \\ \text{Monomer} \end{array} \longleftrightarrow \begin{array}{l} O^- M^+ \\ | \\ M^+ {}^-OSi(OH)O^- M^+ \\ \text{Monomer} \end{array} \quad \text{(I.8)}$$

$$\underset{\text{Monomer}}{M^+ + Al(OH)_4^-} + OH^- \longleftrightarrow \underset{\text{Monomer}}{M^+ {}^-OAl(OH)_3^-} + H_2O \quad \text{(I.9)}$$

The condensation reactions of cations with anions are presented in equations I.10 - I.13 (Xu and van Deventer, 2000):

$$^{-}OSi(OH)_3 + M^{+}\,^{-}OSi(OH)_3 + M^{+} \longleftrightarrow M^{+}\,^{-}OSi(OH)_2\text{-}O\text{-}Si(OH)_3 + MOH \quad \text{(I.10)}$$

Monomer Monomer Dimer

$$^{-}OSi(OH)_2O^{-} + M^{+}\,^{-}OSi(OH)_3 + M^{+} \longleftrightarrow M^{+}\,^{-}OSi(OH)_2\text{-}O\text{-}Si(OH)_2\text{-}O^{-} + MOH \quad \text{(I.11)}$$

Monomer Monomer Dimer

$$^{-}OSi(OH)O^{-} + M^{+}\,^{-}OSi(OH)_3 + M^{+} \longleftrightarrow M^{+}\,^{-}OSi(OH)\text{-}O\text{-}Si(OH)_2\text{-}O^{-} + MOH \quad \text{(I.12)}$$

Monomer Monomer Dimer

2 silicates monomers^{-} +2 silicates dimers^{-} + $2M^{+} \longleftrightarrow$ M^{+}+ trimer cyclic^{-} +M^{+} linear trimer + 2O H^{-} (I.13)

Amorphous to semi-crystalline geopolymers are therefore formed by the co-polymerisation of individual alumino and silicate species, which originate from the dissolution of silicon and aluminium-containing source materials at a high pH in the presence of soluble alkali metal silicates (van Jaarsveld et al., 2002).

I-3-3: Sol-gel synthesis

Typical starting materials for the melt-quench preparation of geopolymers include industrial wastes, calcined clays, melt–quenched aluminosilicates, natural materials, or mixtures of these materials (Tsai et al., 2010). With these materials, it is very difficult to employ the conventional approach to prepare geopolymers which can meet the stringent requirements for sensitive applications. In addition, due to competing reactions associated to the presence of impurities in these materials during syntheses, the elucidation of the chemistry of geopolymer formation from precursors such as fly ash and slag-based materials remains a challenge (Tsai et al., 2010; Brew and MacKenzie, 2007).

These observations have led to the development of sol-gel chemistry synthetic protocol to prepare geopolymers with well defined chemical composition from simpler chemical system involving solid aluminosilicates.

Brew and MacKenzie (2007) prepared monolithic geopolymers by sol–gel condensation reactions between sodium aluminate and sodium silicate formed in-situ by dissolution of silica fume particles in an alkaline solution. The products obtained presented typical characteristics of geopolymers: the materials setting and hardening at ambient temperature, presenting amorphous X-ray, tetrahedral aluminium co-ordination and a range of Q^3 environments corresponding to cross-linked silicate bonds.

Tsai et al. (2010) have also successfully developed a sol–gel method preparation protocol for geopolymer using synthetic kaolinite as aluminosilicate precursor. These geopolymers presented spectroscopic properties similar to those obtained with natural kaolinite.

Compared with the traditional approach that employed natural kaolinite as the starting material, the synthetic approach can help prepare geopolymers with more diversified chemical compositions and can offer a good opportunity for medical applications of geopolymers (Tsai et al., 2010).

I-3-4: Structure of geopolymers

Barbosa et al., (2000) used ^{29}Si, ^{27}Al MAS solid-state NMR and X-ray diffraction to study various compositions of geopolymers derived from metakaolinite. They observed that irrespective of the curing and drying properties of a particular composition, all geopolymer mixes studied showed a lack of long-range atomic order. Their materials showed structural characteristics similar to glasses or hydrated silicate minerals, having a range of Si environments, but predominantly those of framework structures saturated in Al. The semi-schematic structural models which satisfy these requirements are shown in Figure 5.

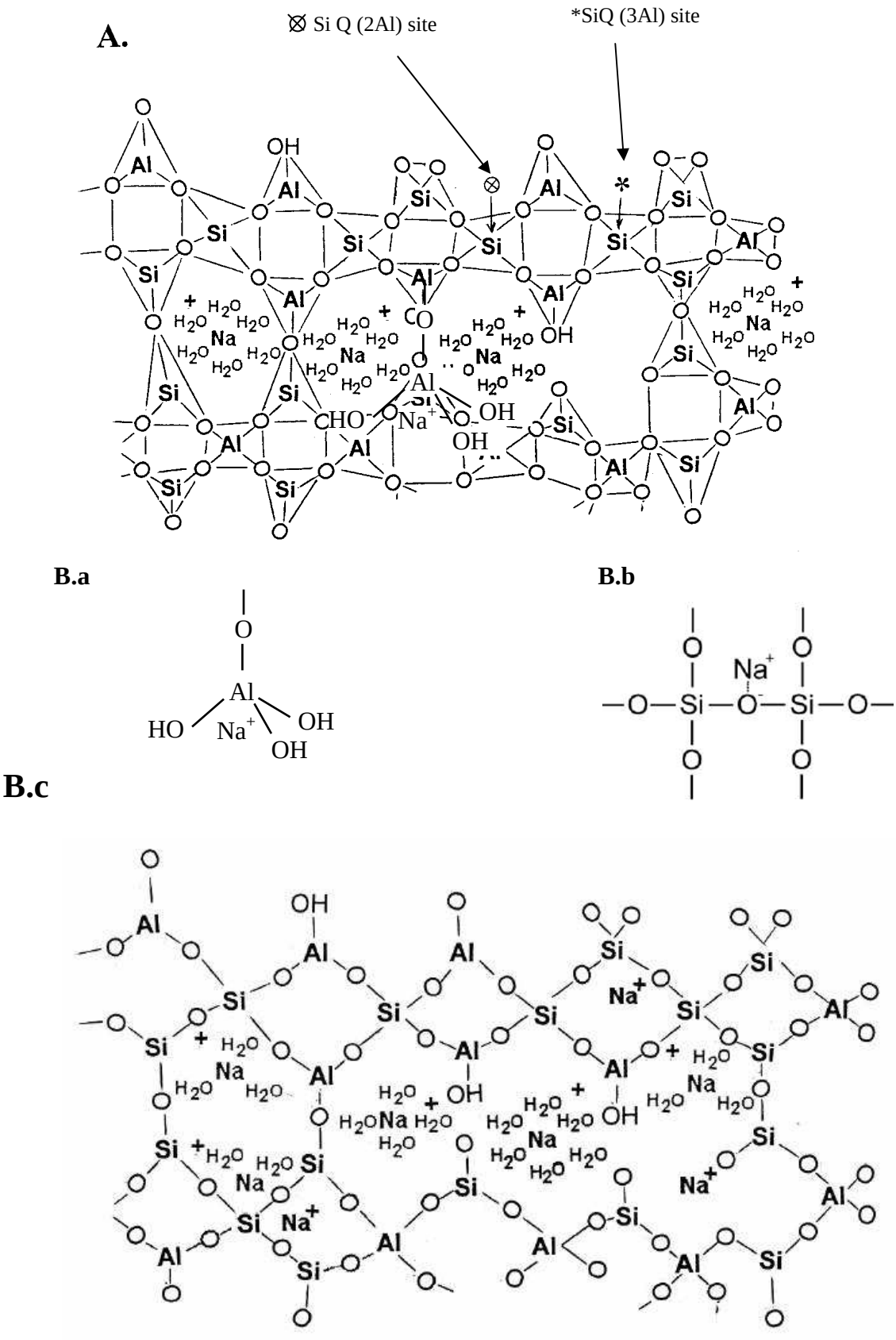

Figure 5: (A) Proposed semi-schematic structure for Na–polysialate polymer (Barbosa et al., 2000). (B.a) Proposed model for the location of the charge-balancing Na^+ cation which assumes the form of a semiattached Na aluminate species; (B.b) Proposed model for the location of the charge-balancing Na^+ cation which assumes the form of a modified bridging network. (B.c), Proposed schematic model structure based on an original model by Barbosa et al., (2000), but which attempts to incorporate the new elements mentioned above, Rowles et al.,(2007). *SiQ (3Al) site; ⊗ Q (2Al) site.

The structure contains Si and Al tetrahedra randomly distributed along the polymer chains which are cross linked so as to provide cavities of sufficient size to accommodate the charge-balancing hydrated sodium ions. This arrangement leads to Si environments such as Q (2Al) and Q (3Al), but with the latter predominating. All the Al atoms have Si nearest neighbours.
The cavities shown in the structural model of Figure 5 A (Barbosa et al.,2000) present solely Na in a hydrated form. The structures presented in Figure 5 B.a, b and c show that Na is present in a range of hydrated states and sometimes shows short-range order, which suggests that the role of Na solely as a charge-balancing cation is understating its purpose and that it may be active in forming and modifiying the polymer network (Rowles et al., 2007).

I-3-5: Factors influencing geopolymerization

a) Raw materials

The chemical and mineralogical composition of the raw materials, their particle size distribution and the concentration of the activators greatly influence the geopolymer properties (Komnitsas and Zaharaki, 2007; Xu and van Deventer, 2000). Kaolinite and other clays were initially used in 1974 and 1975 as the source of aluminosilicate for the manufacture of geopolymers used in the encapsulation of radioactive waste (Komnitsas and Zaharaki, 2007). Kaolinite has a suitable structure for geopolymerization process, but during the synthesis, much of this mineral may not participate in geopolymerization reactions (Schmücker and Mackenzie, 2005). The calcined materials generally react better than non-calcined materials and impurities present in the raw materials can undergo secondary reactions affecting both the reaction kinetics and mechanical properties of resulting products (Komnitsas and Zaharaki, 2007). The geopolymers derived from metakaolinite require more water due to an increase in porosity and become less useful as building materials. However, metakaolinite is beneficial as an additive mineral in geopolymer cements because it improves the mechanical strength. It is also used in manufacturing geopolymers for adhesive applications (Komnitsas and Zaharaki, 2007).

Xu and van Deventer (2000) have done extensive research on the use of 16 different aluminosilicate minerals with the addition of kaolinite to synthesize geopolymers. They observed that for most aluminosilicate minerals, the addition of kaolinite was necessary for

the formation of gels, and when kaolinite was used alone, the mechanical properties were poor. This result suggests that a synergy between the various aluminosilicate minerals may have beneficial effects on geopolymerization reactions.

The influence of aggregates on geopolymer paste has been studied by many authors (Subaer, 2004; Temuujin et al., 2010; Barbosa and Mackenzie, 2003a). Temuujin et al., 2010 studied the influence of sand agregates on the compressive strength and Young's modulus of fly ash-based geopolymers. They observed that adding up 50 wt% of sand aggregate did not significantly affect mechanical properties; the compressive strength of the mortar remained essentially constant with varying aggregate content in the mortars up to 50 wt%. Motars containing 10–30 wt % of aggregate exhibited acceptable flowability while motars containing 40 and 50 wt % aggregate were stiff and difficult to pack into the plastic moulds. Sectioning the mortar by diamond saw did not cause any interfacial cracks between the sand and geopolymer binder at a macro level, suggesting that the interfacial bonding between the aggregate and geopolymer was comparable in strength to the geopolymer and/or the sand aggregate by itself. These results are at variance with those obtained by Barbosa and MacKenzie, (2003a) who observed a reduction on compressive strength while adding 10-20 vol % of various granular inorganic fillers on metakaolinite-based geopolymer. The mechanical properties of the geopolymer mortar may therefore depend on the strength of the geopolymeric gel, the interfacial bonding between the geopolymeric gel and aggregate and the aggregate itself (Subaer, 2004; Temuujin et al., 2010).

b) Alkali ions

Theoretically, any alkaline or alkaline earth such as Na^+, K^+ or Ca^{2+} may be used in the activating solution for geopolymerization reactions. However, most studies have focused on the effects of sodium and potassium ions. The choice of alkaline ion used for the geopolymeric synthesis depends on several factors, of which the most importants are the origin of the aluminosilicate raw material and applications of the geopolymer (Komnitsas and Zaharaki, 2007). The cations present in the basic raw materials or added as alkaline hydroxides are considered to be important because of their catalytic role (Komnitsas and Zaharaki, 2007). Using Na^+ as the charge balancing ion, optimal geopolymer properties are obtained when the concentration of sodium is sufficient to compensate for the charge imbalance caused by the substitution of silicon by tetrahedral aluminum, but not in such

excess as to form sodium carbonate in the presence of atmospheric CO_2 (Barbosa et al., 2000). The large cation size of K^+ promotes the formation of silicate oligomers with which $Al(OH)^{4-}$ prefers to bind. Therefore, when a solution of KOH is used, more geopolymeric precursor is formed, facilitating better curing and better compressive strength than geopolymers synthesized with NaOH (Cioffi et al., 2003; Komnitsas and Zaharaki, 2007).

Potassium ions appear to be responsible for a greater degree of condensation compared to sodium ions under the same conditions. Since K^+ is more basic, it promotes greater dissolution of silicates. The radii of alkaline metals increase from Li^+ to Cs^+ (181pm, 227 pm, 275 pm, 303 pm and 343 pm, for Li, Na, K, Rb, and Cs respectively). This trend is at variance with the hydration sphere of these cations which is more linked to the charge density. Consequently the hydration sphere of K^+ being smaller than for Na^+, allows polycondensation reactions to be more intimate. The addition of KOH tends to improve the degree of polycondensation in solutions of alkali silicate ion whereas the addition of NaOH will increase the amount of silicate monomers (Cioffi et al., 2003; Komnitsas and Zaharaki, 2007). Na^+ also seems to promote faster reaction compared to K^+. With Differential Scanning Calorimetry, the isothermal reaction at 60°C of Metakaolin with a NaOH solution compared to a KOH solution shows a larger heat flow signal with NaOH solution, returning earlier to the baseline (Figure 6), suggesting a faster reaction for the sodium solution (Rahier et al., 2007).

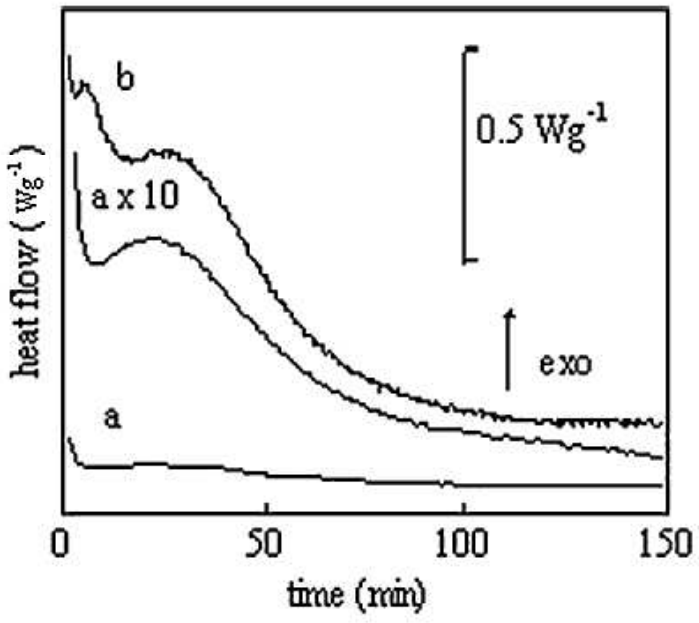

Figure 6: DSC heat flow of isothermal cure at 60°C of Metakaolin with: (a) KOH solution and (b) NaOH solution (Rahier et al., 2007)

The widespread use of Na^+ and K^+ as charge-balancing ions is probably due to their low cost compared with other alkali ions. However there are a few published reports of cesium and lithium-based geopolymers. Using Cs^+ as the alkaline reagent with metakaolin produces more refractory compounds compared to the homologues synthesised with Na^+ and K^+ (Bell et al., 2009a; 2009b). The use of Li^+ and dehydroxylated halloysite forms a zeolite structure instead of the conventional amorphous geopolymer obtained with Na^+ or K^+ (O'Connor and MacKenzie, 2010).

It is therefore clear that the type of alkaline reagent used as the charge-balancing ion greatly influences the geopolymer structure and properties and must be considered when designing synthesis pathways for manufacturing geopolymer products.

c) Calcium ions

The presence of calcium ions in raw materials may improve the mechanical properties of the geopolymer gel by forming an amorphous Ca-Al-Si gel. When the CaO content is high, the porosity decreases due to the resultant microstructural formation of gels (Komnitsas and Zaharaki, 2007). The addition of high amounts of calcium hydroxide to fly ash-based geopolymers improves their early strength, whereas the addition of small amounts of calcium improves the strength at later stages. For both fly ash and metakaolinite binders, exchanging about 10% of the alumosilicate material with calcium hydroxide appears to be optimal (Komnitsas and Zaharaki, 2007; Diaz et al., 2010). Yip et al., (2008) studied the influence of calcium in geopolymerization by synthetising samples with 0%, 20%, 40%, 60%, 80% and 100% replacement of metakaolin by calcite and dolomite. They observed that the addition of a moderate amount (20 mass %) of calcite or dolomite extended a positive effect on the mechanical strength of a metakaolinite-based geopolymeric binder. Excessive addition of calcite or dolomite to the geopolymeric gel (>20 mass %) was found to be detrimental, likely due to a low degree of geopolymeric gel formation and connectivity. A significant degree of shrinkage was also experienced in these systems and it was noted that the addition of calcite tended to produce a stronger geopolymeric material than when dolomite was used. This is unlikely to be due to simple micro-aggregate effects, which suggests that the small amount of dissolution of the carbonate minerals that is observed is sufficient to release enough Ca^{2+} or Mg^{2+} to have a significant effect on the geopolymer gel structure, coupled eventually with

potential differences induced by the different surface structures of the two minerals (Yip et al. 2008).

The effect of calcium on the final reaction product can be determined by the level of dissolved silicate in the activating solution through pH control. When the solid raw material is deficient in calcium, $CaCO_3$ and CaO can be introduced in the form of an aqueous suspension to improve the physical and mechanical properties of geopolymers (van Jaarsveld et al., 2003; Komnitsas and Zaharaki, 2007).

MacKenzie el al., 2007 studied the influence of up to 50 wt % of different calcium compounds ($Ca(OH)_2$, $CaCO_3$, $Ca_3(PO_4)_2$, amorphous nanosized calcium silicate, and α-$CaSiO_3$) on Na and K metakaolinite based-geopolymer. They observed that all the samples cured and hardened to viable strong materials, showing the general ^{27}Al NMR, ^{29}Si NMR and XRD features of conventional geopolymer composites containing additional crystalline fillers. These spectra showed that calcium silicate and calcium hydroxide enter into the geopolymer network, by contrast to calcium carbonate and calcium phosphate which act as fillers rather than entering into the geopolymer network. Thus, the form in which the calcium is added influences the structure of the final geopolymer and therefore the properties of the resulting product, and should be taken into account when planning and tailoring geopolymer properties.

d) Iron ions

The presence of iron ions in raw materials may have a negative effect. It was suggested that when dissolving basaltic glasses containing significant levels of network-forming Fe^{3+} under slightly alkaline conditions, reprecipitation of dissolved Fe was much faster than the reprecipitation of Si and Al (Provis, 2006). It is therefore likely that the iron present in raw materials used for aluminosilicate geopolymerization will react similarly, removing OH^- by forming hydroxides and consequently, slow down the dissolution of residual aluminosilicate (Provis , 2006). These results are however subject to discussion.

Perera et al., (2007) studied the speciation of Fe added as ferric nitrate solution or freshly precipitated ferric (oxy) hydroxide to metakaolin based-geopolymers. They observed that in the freshly cured geopolymers, the Fe was present in octahedral sites, either as isolated ions in dilute samples or as oxyhydroxide aggregates in samples richer in Fe. Heating to 900°C formed nepheline, with partial substitution of Fe^{3+} for the tetrahedral Al in addition to glass which also incorporated Fe^{3+} in tetrahedral coordination.

The conclusion is that the presence of iron could be positive or negative according to the nature of the initilal components in the geopolymer mixtures.

e) Water

The presence of water is essential for geopolymerisation reactions to take place. It provides the medium for the dissolution of aluminosilicates and the transfer of various ions, hydrolysis of Al^{3+} and Si^{4+} compounds and polycondensation of different aluminate and silicate-hydroxyl species. As a result, water has a major effect on geopolymer formation, the structure of the geopolymer gels and the properties of the products (Barbosa et al., 2000; van Jaarsveld et al., 2002; Zuhua et al., 2009).

It has been suggested (Zuhua et al., 2009) that geopolymerisation can be approximately partitioned into two periods (dissolution–hydrolysis, and hydrolysis–polycondensation) which probably occur simultaneously once the solid material is mixed with the liquid activator. It is found that during the first period, higher liquid/solid ratios result in faster reaction rates. In the second period, the main reaction may change from hydrolysis (consuming water) to polycondensation (releasing water). Water acts as a product in this period and if too much is present, it will hinder the polycondensation kinetics. Systems with lower liquid/solid ratios show higher polycondensation rates.

Pure water cannot activate the solid material in the absence of significant concentrations of OH^- ions. High alkalinity is necessary for the destruction of the raw material (Zuhua et al., 2009) and excess water may favor sedimentation or dilute the reaction, leaching out the more soluble ions, transporting them away from the reaction zone (Rahier et al., 1997; Barbosa et al., 2000).

The role of water is therefore critical even in the final stages of geopolymerisation because the polycondensation processes occur concomitantly with dissolution (Zuhua et al., 2009).

f) Curing condition

Curing parameters include temperature, humidity, the air circulating around the geopolymer mixtures during setting and the ageing time. Temperature and air circulation are the two main factors determining whether the geopolymeric products have high mechanical strength or contain cracks (Xu, 2002).

It has been reported that for metakaolinite and fly ash-based systems, the temperature at which samples are cured greatly affects their final compressive strength. It is however suggested that initial curing at higher temperatures does not increase the compressive strength substantially above that achieved by curing at room temperature. Curing at higher temperatures for more than a couple of hours does seem positively to affect the development of compressive strength. It is of interest to note that curing for longer periods of time at elevated temperatures appears to weaken the structure, suggesting that small amounts of structural water need to be retained in order to reduce cracking and maintain structural integrity. It seems that prolonged curing at elevated temperatures breaks down the gel structure of the geopolymer synthesis mixture, resulting in dehydration and excessive shrinkage as the gel contracts without transforming to a more crystalline form (van Jaarsveld et al., 2002).

Longer curing times have been reported to not significantly affect the crystalline regions of the geopolymer, but changes affecting structural integrity take place within the amorphous gel structure. Samples cured at higher humidity in sealed plastic bags do not exhibit improved compressive strengths, in contrast with the curing of conventional cementitious products. It has been proposed that the saturated atmosphere in the bags results in conditions more suitable to the formation of slightly weaker bonds (van Jaarsveld et al., 2002). These results are not in accordance with those obtained by Izquierdo et al. (2010) who observed that open curing conditions produce solid bodies characterized by high porosity, low compressive strength and exacerbated leaching of certain oxyanionic metalloids, whereas protected curing promotes the binder development, giving rise to higher strength and less porous systems. It has been also shown (Zuhua et al., 2009) that humidity in the curing environment may allow producing crack-free geopolymers. These effects are, however, very subtle (van Jaarsveld et al., 2002).

Together with the properties of the starting materials and other parameters, curing temperatures have varied from room temperature (Singh et al., 2005) to about 80 °C (Kon and Sanjayan, 2008; Buchwald et al., 2009) and even 400°C Kamseu et al., (2009). This last author observed an increase of compressive strength of about 40% upon increasing the curing temperature of volcanic ash based-geopolymer from 25 to 400°C. Similar results have been obtained by Kon and Sanjayan (2008) who showed that higher curing temperatures may promote the polymerization reactions, producing an increase of about 53 % in the compressive strength after heating fly ash-based geopolymer at 800°C. Buchwald et al., (2009) showed that increasing the temperature up to 60 °C shortened the dissolution time

from 90 days (at 20 °C) to about 14 days (at 60 °C) for thermally activated illitte/ smectite clay-based geopolymers. Yip et al., (2008) studied the strength development of metakaolinite and calcium based geopolymers at 2 days (d), 7d, 28 d, 90 d, 360 d, and 560 d after synthesis, found out that strength development was generally almost complete within 2 d, whereas Kon and Sanjayan (2008) observed a small increase in the compressive strength of fly ash-based geopolymer specimens when the age was extended from 3 to 7 d.

All these observations indicate that curing conditions and ageing time are important parameters to be considered when manufacturing geopolymer materials from a particular aluminosilicate raw material.

I-3-6: Factors influencing compressive strength

Compressive strength has been used by many researchers as a measure of the "success" of the geopolymerization process (Komnitsas and Zaharaki, 2007). Compressive strength depends on many factors including the strength of the gel phase, the ratio of the gel phase to undissolved Al-Si particles and the distribution and hardness of any undissolved Al-Si particles. It is also depends on the nature of the amorphous phase of the geopolymer, its degree of crystallinity and surface reaction between the gel phase and any undissolved Al-Si particles (van Jaarsveld et al., 2003; Komnitsas and Zaharaki, 2007). However other factors such as the percentage of CaO, K_2O, and the type of alkali correlate strongly with compressive strength (Komnitsas and Zaharaki, 2007). After geopolymerization, undissolved particles remain bound in the matrix, which means that the hardness of these minerals shows a positive correlation with the compressive strength. During the geopolymerization of natural minerals, it is known that when aggregates such as fine sand are added to the geopolymer mixture, the compressive strength increases (Xu and van Deventer, 2000; Komnitsas and Zaharaki, 2007). Alkaline activation of metakaolin using a solution containing sodium silicate and sodium hydroxide gives better mechanical properties than when activated with only sodium hydroxide (Komnitsas and Zaharaki, 2007). The best compressive strength is obtained when the molar ratios of SiO_2/Al_2O_3 and Na_2O/Al_2O_3 are respectively 3.0-3.8 and about 1 respectively (Silva et al., 2007). However, these optimum ratios can depend on the type of material used as the source of Al_2O_3 and SiO_2 (van Jaarsveld et al., 2003).

I-3-7: Characterization methods of geopolymers

a) X-Ray Diffraction

Geopolymers are amorphous and therefore difficult to study by X-ray diffraction (XRD). The X-ray diffraction patterns of (Na, K)-Poly(sialate-siloxo), (Ca, K)-Poly(sialate-siloxo) and K-Poly(sialate-siloxo) present in the commercial geopolymer binder "Geopolymite" show they consist of a disordered lattice of materials ordered on a short scale with a structure similar to feldspathic glasses or crystallized zeolites (Davidovits, 1991). Figure 7 below shows that the poly(sialate-siloxo) contains a diffuse halo at around 3.05 to 3.30 A (27-29°, 2Θ max, Cu K_α).

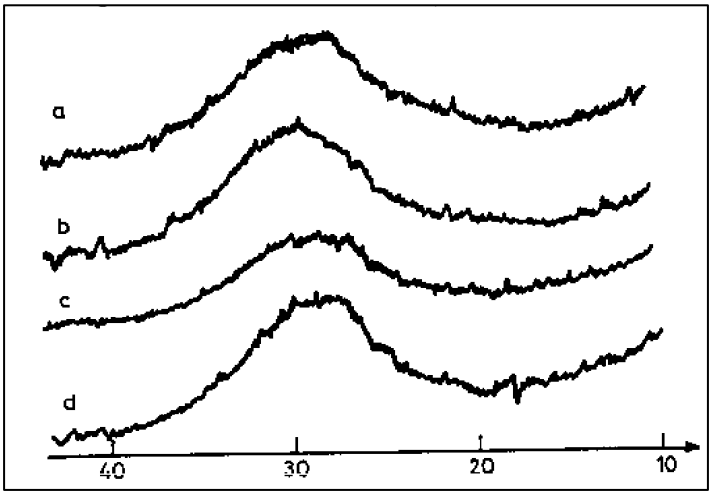

Figure 7: X-ray diffraction (Na, K)-PSS and K-PSS (Davidovits, 1991).

a) (Na,K)-PSS , Na_2O+K_2O/SiO_2=0,235 and SiO_2/Al_2O_2 = 4,02
b) (Na,K)-PSS , Na_2O+K_2O/SiO_2=0,380 and SiO_2/Al_2O_2 = 3,98
c) K-PSS , Na_2O+K_2O/SiO_2=0,296 and SiO_2/Al_2O_2 = 3,39
d) K-PSS , Na_2O+K_2O/SiO_2=0,366 and SiO_2/Al_2O_2 = 4,11

Comparison of the values of 2Θ max for (Na, K)-PSS and K-(PSS) (Figure 7) with the values of the 2Θ of natural and synthetic crystalline aluminosilicates (Table I-2) shows that the geopolymers (Na, K)-PSS and K-PSS are equivalents of most amorphous aluminosilicate crystalline except hydrosodalite and analcime (Davidovits, 1991). It should be noted that these results comply with the chemical mechanism set forth for poly(sialate-siloxo) (Si-O-Al-O-Si-O-)n species. The three-dimensional framework assigned to (Na,K)-PSS is Phillipsite and Leucite for the K-PSS geopolymers. Practical experience suggests that the formation of the Analcime framework necessitates the presence of soluble Ca^{++} ions in complement to Na^{++} or K^{+} ions.

Table 2: Values of 2Θ max diffraction rays for natural crystalline aluminosilicates (Davidovits, 1991)

Aluminosilicate mineral network		**mol Na_2O+K_2O/SiO_2**	**mol Si_2O_2/Al_2O_2**	**Cu (Kα) 2Θ max**
Leucite	$K(Si_2AlO_6)$	0,25	4,0	27,24°
Nepheline	$(Na,K)(SiAlO_4)$	0,50	2,0	29,46°
Orthose	$K(Si_3AlO_8)$	0,16	6,0	27,70°
Albite	$Na(Si_3AlO_8)$	0,16	6,0	27,86°
Analcime	$Na(Si_2AlO_6)H_2O$	0,25	4,0	26-30°
Phillipsite	$(K,Na)(Si_2AlO_6)H_2O$	0,25	4,0	27,90°
Hydrosodalite	$Na(SiAlO_4)\ H_2O$	0,50	2,0	24,20°
Zeolite W (K-M)	$K(Si_{1.8}AlO_6)\ H_2O$	0,27	3,6	27,42°
Zeolite W (K-G)	$K(Si_{1.95}AlO_6)\ H_2O$	0,26-0,37	2,6-4,15	30,00°
Zeolite W (K-F)	$K(SiAlO_4)\ H_2O$	0,4	2,3	28,70°

b) High Resolution Solid State Nuclear Magnetic Resonance

Solid state NMR spectroscopy is a powerful technique capable of providing information both about the structure of materials and the dynamics of processes occuring within these materials, such as the formation of intermediate phases when minerals react or transform to other phases upon heating or mechanical grinding; these materials often lack the long-range order necessary for conventional diffraction studies (MacKenzie and Smith, 2002). ^{27}Al and ^{29}Si MAS-NMR, and also ^{23}Na MAS-NMR are particularly powerful tools for structural analysis of zeolites, clays, ceramics, cements, and geopolymers (Davidovits, 1991; Duxson, 2006; Barbosa and Mackenzie 2003a).

^{29}Si MAS-NMR is capable of distinguishing SiO_4 tetrahedra of cross-linked density ranging from 0 to 4, the relative concentration of which may be estimated from the integrated peak intensities (Singh et al., 2005). It can also show correlations between the chemical shift (δ) of the silicon resonance and the bond angle and/or bond length of the Si-O group, or the total cation-oxygen bond strength (MacKenzie and Smith, 2002). In addition, cross-polarization experiments with the ^{1}H nucleus provide information specifically about silicon atoms close to the proton-bearing species such as in hydroxyl-containing minerals (Meinhold et al., 1985). For each replacement of Si by Al in the second coordination sphere of a Si atom, a

characteristic shift is observed in the ^{29}Si MAS-NMR resonance position which makes it possible to determine the number of tetrahedral Al atoms connected via oxygen bridges to a given SiO_4 tetrahedron (Singh et al., 2005). Therefore ^{29}Si MAS-NMR can provide valuable information on the types of the cross-linked SiO_4 tetrahedra present.

Recent researches have shown that the aluminate anion containing tetra coordinated Al resonates at 60-80 ppm, and that in aluminosilicates, tetra coordinated Al resounds at approximately 50 ± 20 ppm while the hexa coordinated aluminum $[Al(H_2O)_6]^{3+}$ resounds at around 0 ± 10 ppm (Davidovits, 1991; MacKenzie and Smith, 2002).

The Lowenstein principle in aluminosilicates states that when two tetrahedra are linked by an oxygen bridge, only one can contain aluminum, i.e an Al-O-Al bond is thermodynamically unfavorable and the environment of each aluminum atom is Al (4Si). The Lowenstein rule is obeyed by aluminosilicate anions, limiting the number of possibilities of AlQ_n (nSi) to 5 structural units where n = 0, 1, 2, 3 and 4. Some AlQ_n (nSi) units are shown in Figure 8.

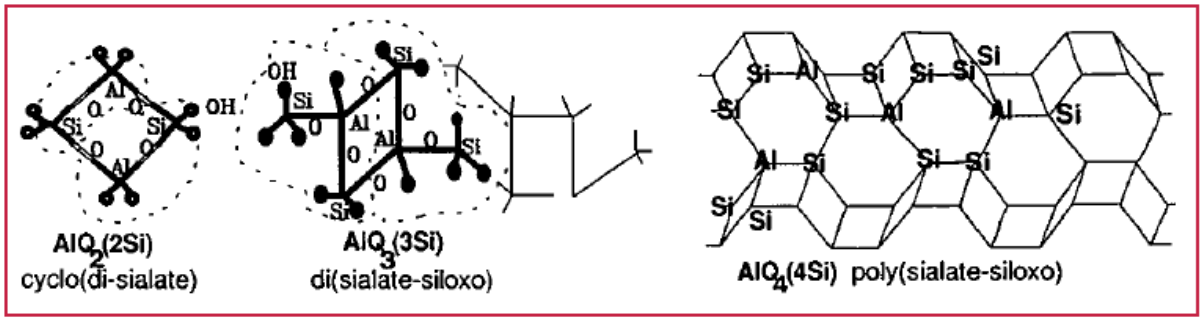

Figure 8: Some structural units AlQ_n (nSi) involved in geopolymerization reactions (Davidovits, 1991).

The ^{27}Al NMR spectra of (Na, K)-PSS and K-PSS show that the chemical shift of ^{27}Al from $[Al(H_2O)_6]^{3+}$ is about 55 ppm (Figure 9) which indicates that the aluminium is AlQ_4(4Si) and is tetra-coordinated. The absence of other resonances and the sharp peak at 55 ppm excludes any residual units of molecules of small size such as dimmers and trimmers (Davidovits, 1991).

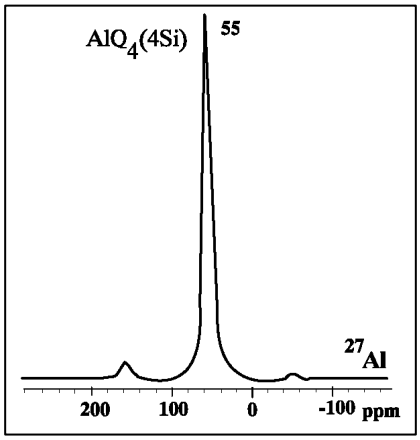

Figure 9: ^{27}Al NMR spectrum of K-PSS (Davidovits, 1991).

However ^{27}Al NMR does not differentiate between the different structures proposed for geopolymer materials based on poly (sialate) (Si-O-Al-O-)n, poly (sialate-siloxo) (Si-O-Al -O-Si-O)n or poly (sialate-disiloxo) (Si-O-Al-O-Si-O-Si-O-)n. This differentiation can be done by ^{29}Si NMR spectroscopy. As shown in Figure 10, K-PSS gives a broad resonance at -94.5 ppm associated with a signal at -87 ppm, a small resonance at -81.5 ppm and a small peak at -79 ppm. The last resonance at -79 ppm (SiQ_1) is tapered, which means it comes from an orderly environment, different from the disordered environment of the other peaks of the matrix (Davidovits, 1991).

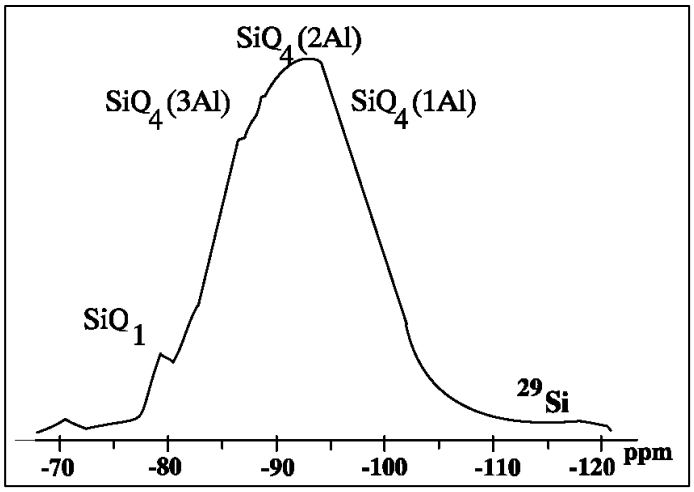

Figure 10: ^{29}Si NMR spectrum of K-PSS of GEOPOLYMITE (Davidovits, 1991).

For ideal silicate glasses, the ^{29}Si chemical shifts of Q^m_n units are given in Table 3 where 'n' is the number of Al atoms connected by oxygen bridges to SiO_4 tetrahedra.

Table 3: Chemical compositions and ^{29}Si chemical shifts of ideal silicate glasses containing only one type Q^m_n unit (Singh et al., 2005)

Q^m_n unit	Composition (mol%)			$-\delta$ (ppm)
	M_2O	Al_2O_3	SiO_2	
Q^4_0	0	0	100	109
Q^4_1	10	10	80	104
Q^4_2	16.7	16.7	66.7	97
Q^4_3	21.4	21.4	57.2	90
Q^4_4	25	25	50	88
Q^3_0	33.3	0	66.7	90
Q^3_1	41.7	8.3	50	82
Q^3_2	46.7	13.3	40	80
Q^3_3	50	16.7	33.3	77
Q^2_0	50	0	50	80
Q^2_1	58.3	8.3	33.3	73
Q^2_2	62.5	12.5	25	73
Q^1_0	60	0	40	74
Q^1_1	70	10	20	70
Q^0	66.7	0	33.3	70

$M_2 = Ca$.

Barbosa and Mackenzie (2003a) studied the evolution of ^{23}Na MAS-NMR spectra of Na-PSS geopolymer heated up to 1300°C (Figure 11). They observed a chemical shift of -5.5 to -7 ppm, for hydrated Na^+ in an unheated geopolymer framework. When heated, the ^{23}Na resonance moved progressively upfield to -14 ppm at 800°C and -19 ppm at 1100-1300°C, which is a typical chemical shift value of unhydrated sodium aluminosilicate and rhyolite glasses. This shift is due to the loss of hydration water from the charge-balancing Na^+ ion (Barbosa and Mackenzie, 2003a).

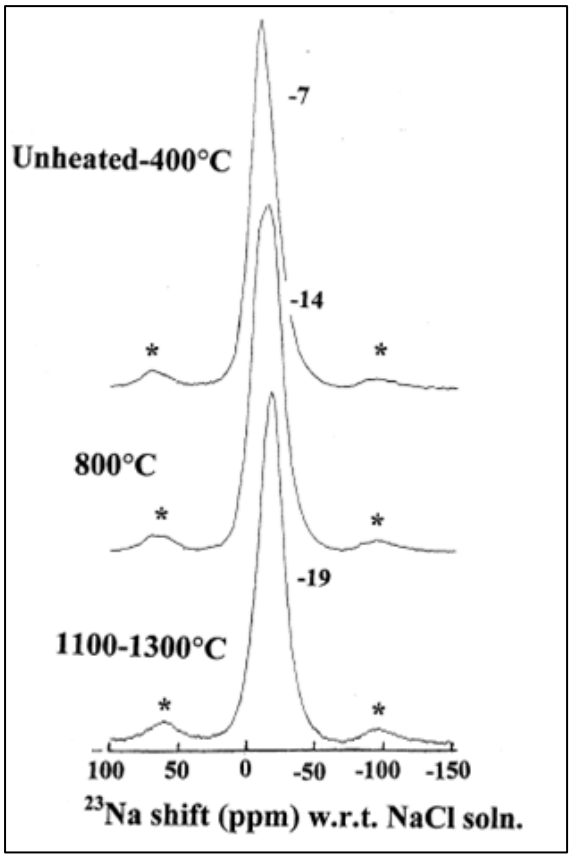

Figure 11: ^{23}Na MAS-NMR spectra of Na-PSS heated for 1 h at the indicated temperatures (Barbosa and Mackenzie, 2003a).

c) Infrared Spectroscopy

The IR spectra of polysialate and polysialate-siloxo and for geopolymer precursors contain the strongest vibrations found in all aluminosilicates, assigned to the internal vibrations of Si-O-Si, Si-O-Al at 950-1250 cm^{-1} and 420-500 cm^{-1} respectively. The stretching modes are sensitive to the Si: Al composition of the framework and may shift to a lower frequency with increasing number of tetrahedral aluminum atoms (Davidovits, 2008). Barbosa et al. (2000) studied the FTIR spectra of a starting metakaolinite and various polymer compositions. They observed:

- a typical metakaolinite spectrum with broad bands at about 3450 cm^{-1} and 1650 cm^{-1} from adsorbed atmospheric water;
- an Si–O stretching vibration at 1088 cm^{-1};
- an Si–O–Al vibration at 810 cm^{-1} ;
- an Si–O bending vibration at about 450 cm^{-1} and a shoulder near 1000 cm^{-1} arising from quartz impurity.

On the formation of the polymer, they observed the following changes in the spectra:

(a) The presence of the added water increases the intensity of the bands at about 3500 and 1650 cm^{-1}.

(b) Major disruption of the Al environment is indicated by the loss of the Si–O–Al band at 810 cm^{-1} which is replaced by several weaker bands in the range 600–800 cm^{-1}.

(c) The presence of sodium carbonate is indicated by the band at about 1460 cm^{-1} in all the polymers except the well-cured sample Na–PSS1 (Figure 12. B), in which, however, the carbonate peak appears when the solid polymer is dried for about 30 h to constant weight after curing (Figure 12.C). This interesting result suggests that during prolonged drying of the cured polymer slab, the passage of water through the bulk carries with it a high concentration of sodium to the surface, where it then carbonates.

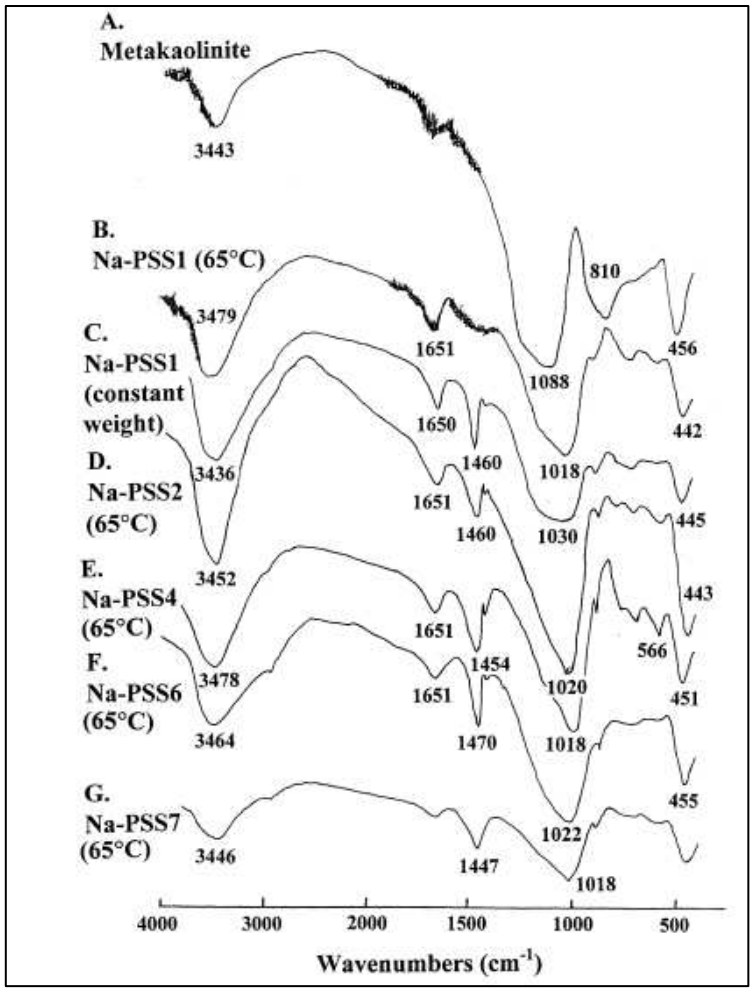

Figure 12: IR spectra of metakaolinite and different geopolymers compositions (Barbosa et al. 2000).

However, for the characterization of geopolymer materials, analysis by IR spectroscopy is generally complementary to analyses by X-ray and NMR spectroscopy.

d) Electron microscopy

A detailed knowledge of the microstructure of geopolymers with an aluminosilicate framework is of fundamental interest for a deeper understanding of the polymer formation process as well as of their mechanical properties (Singh et al., 2005). Duxson et al., (2007) studied the relationship between geopolymer composition, microstructure and mechanical properties, and observed a rapid evolution of the microstructure with increasing silicon content within the small compositional region ($1.40 \leq Si/Al \leq 1.65$) of metakaolin-based geopolymers. This change in microstructure, observed by nitrogen adsorption, was shown to be a result of an increased volume of gel in specimens as the skeletal density of the gel decreases; the variation in the lability of silicate species within the sodium silicate activating solutions controls the rate of structural reorganization and densification during geopolymerization. Greater mobility allows extensive gel reorganization and densification, and facilitates pores to aggregate, resulting in a microstructure of dense gel particles and large interconnecting pores, whereas reduced mobility promotes decreased localized gel density and distributed porosity (with higher mobility promoted by low silicon concentration). It has also been demonstrated that strength development is not only linked to improvement in the strength of the binder, but also to a homogeneity increase of the microstructure (Duxson et al., 2005a). Kovalchuk et al., (2007) have shown that curing and synthesis conditions (the ratio of liquid / solid phase) exerted an influence on the microstructure of geopolymer materials, and consequently on their mechanical properties. The microstructure can also be used to provide an indication of the amount of undissolved phases in the geopolymer matrix (Duxson, 2006).

The microstructure of geopolymers is important in view of the possible inhomogeneity suggested by their high temperature behavior. However, the study and understanding of the microstructure of geopolymer materials is hampered by impurities in the raw starting aluminosilicate that can be found dispersed in the gel (Schmücker and MacKenzie, 2005).

The Figure 13 shows the microstructure of geopolymer materials obtained from different aluminosilicate materials (fly ash and metakaolin) (Duxson, 2006). Large difference is observed. In the fly ash based sample, remaining fly ash particles can be observed.

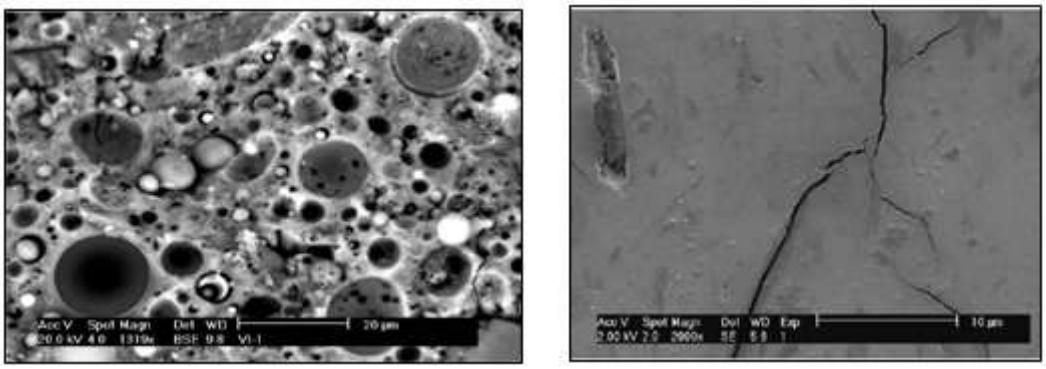

a) b)

Figure 13: Geopolymer microstructures: from fly ash (a) from metakaolin (b) (Duxson, 2006).

I-3-8: Thermal properties of geopolymers

A study of the thermal behavior and properties of materials during or after heating has been proven to be a fundamental indicator of their refractory properties (Aliprandi, 1979). Since the need for refractory materials is growing with industrial and technology development, increasingly research is focussing on the evolution of geopolymer properties when exposed to high temperatures.

Geopolymers generally have a higher thermal stability than Portland cement, because of their similar properties to those of ceramic materials. Kong and Sanjayan, (2008) showed that fly ash-based geopolymer is consolidated further when exposed to elevated temperatures up to 800 °C. They attributed this behavior to continued polymerization reactions at higher temperatures, leading to improvement in the mechanical properties. Davidovits (1991), Barbosa and MacKenzie (2003a) and Elimbi et al., (2014) showed that geopolymers prepared with sodium or potassium alkaline reagents and metakaolin are resistant to fire, with thermal stability up to at least 900 °C.

Provis et al., (2009) have studied the correlation between the thermal and mechanical properties of fly ash-based geopolymer and reported that the samples that showed very high or very low expansion from 700 to 800 ° C generally showed poor mechanical properties. The optimum mechanical properties were obtained with formulations that gave small expansions in this temperature range. They suggested that such behavior would result from a correlation between the physical properties of formulations rather than a strict relationship of cause and effect, but concluded that the use of dilatometric analysis could be helpful to select certain

geopolymer precursors where the production of large specimens for mechanical measurements would be difficult to achieve due to lack of raw materials.

Barbosa and MacKenzie (2003a) studied the X-ray diffraction of metakolin-based geopolymers after heating at different temperatures and observed that the cured and dried polymers were X-ray amorphous, displaying a typical background with a superimposed sharp major reflection of quartz impurity present in the original kaolinite. The polymer remained amorphous between 400 and 1100°C, but the quartz peak became much less distinct, possibly reflecting a degree of dissolution under the alkaline condition prevailing within the polymer (Figure 14).

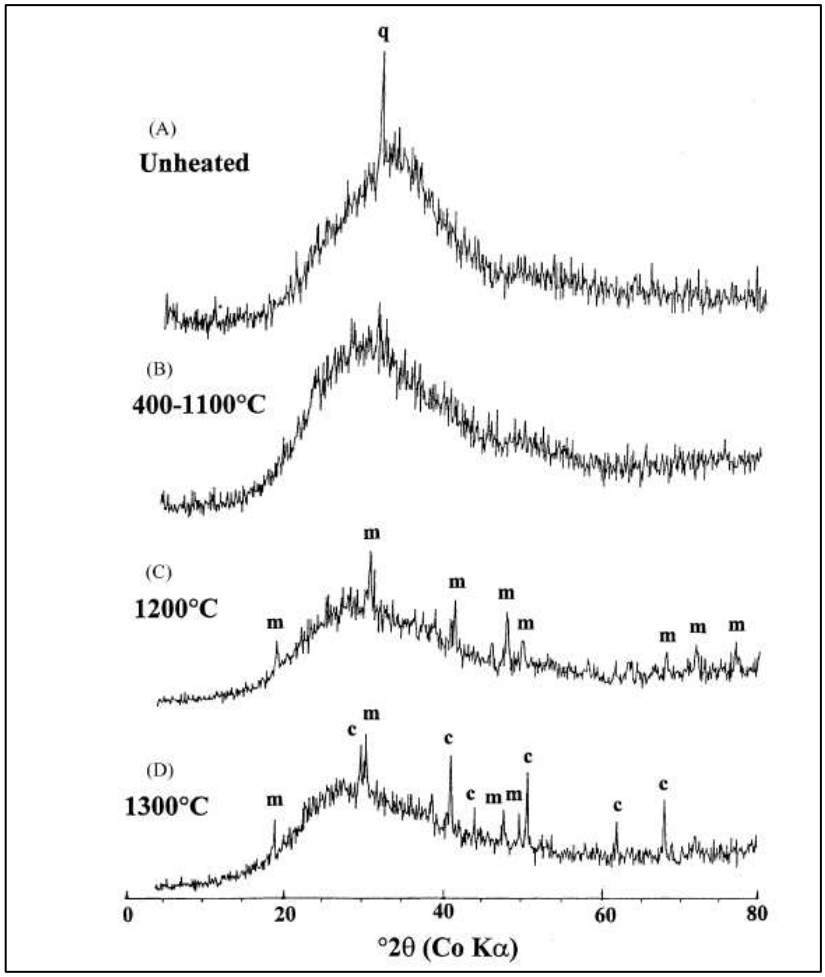

Figure 14: X-ray powder diffractions of Na-PSS heated for 1 h at the indicated temperature. Key: q, quartz; m, mullite; c, corundum (Barbosa and MacKenzie, 2003a)

Mullite and corundum which appear at 1200-1300 °C, are suggested to arise from the presence of a small amounts of unreacted metakaolinite starting material.

This result has been discussed by Schmücker and MacKenzie (2005) who attributed the origin of mullite in heated metakaolin-based geopolymer as resulting from the geopolymer matrix

itself and not from the metakaolinite relicts. They studied the microstructural evolution of metakaolin-based geopolymer and observed that SEM micrograph showed evidence that the needle-like grains of mullite are formed within the geopolymer matrix rather than within the metkaolinite relicts which are still identifiable by their angular shape (Figure 15)

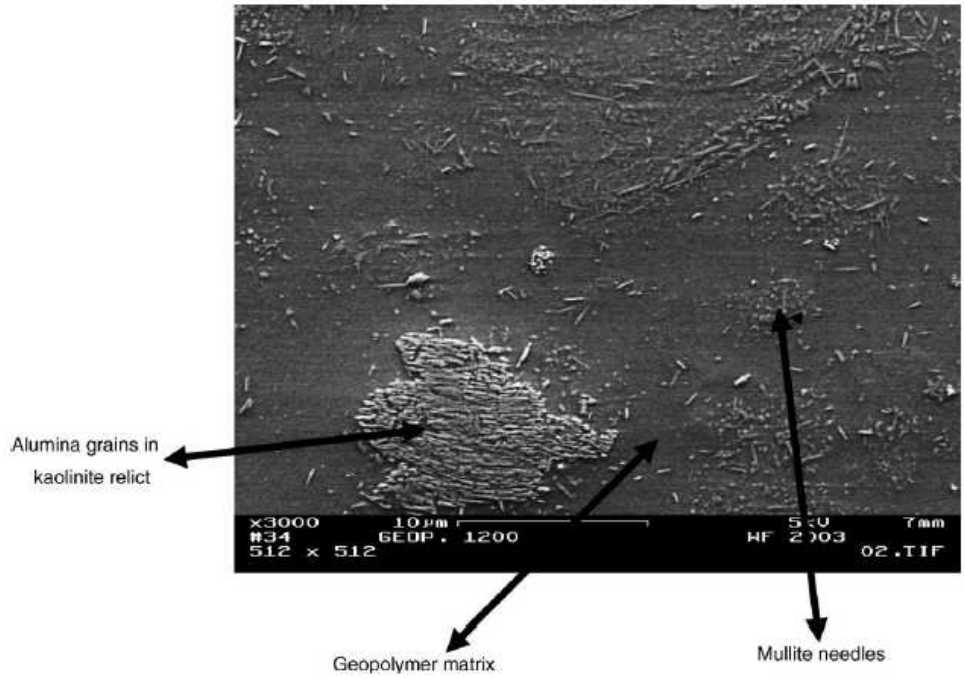

Figure 15: SEM of geopolymer heated at 1200°C (Schmücker and MacKenzie, 2005)

The thermal stability of glassy geopolymer matrix was suggested by the fact that its composition is maintained (within the limits of the analysis) after heating in areas in which mullite formation had not occurred. This was attributed to a mechanism involving a balance between the high-temperature reactions that tend to increase the silica content (dissolution of the labile silica component of the unreacted metakaolinite and the quartz impurities) and the removal of silica by the crystallization of mullite (Schmücker and MacKenzie, 2005).

The thermal stability of geopolymer materials is also greatly influenced by the nature of the alkaline metal reagent used in the synthesis. Bell et al., (2009a; 2009b) observed that metakaolin Cs-based geopolymer was more refractory than Na and K-based geopolymers. Cs-based geopolymers crystallized to pollucite ($Cs_2O.Al_2O_3.4SiO_2$), which is the most refractory silicate known, on gradual heating. Pollucite has exceptional creep resistance between 1400 and 1500 °C and melts at above 1900°C. An exothermic reaction was observed over the range 900°C-1250°C and a density of 3.18 g/ cm^3 (about 98 % of the theoretical density of pollucite) was obtained after heating the sample at 1600°C (Bell et al, 2009a).

The thermal evolution of geopolymers has been divided into four regions on the basis of shrinkage behavior (Bell et al, 2009a; 2009b; Duxson et al., 2006).

The shrinkage in Region I is minimal (Figure 16). Region II begins with the onset of initial shrinkage, lasting until the rate of shrinkage decreases and evaporation of free water is completed. The shrinkage in this region is also minimal as only free water from large pores and surfaces is lost. Region III is marked by a gradual weight loss and shrinkage due to dehydroxylation. The amount of shrinkage is much greater in this region and the water loss is due to desorption of water from small pores and the release of chemically bound water in the form of silanol and aluminol groups. Region IV begins with the onset of densification by viscous sintering with considerable shrinkage. The temperature range of these four regions varies according to the Si/Al ratio and alkaline cation (Bell et al., 2009a; 2009b; Duxson et al., 2006).

The thermal evolution of Cs-based geopolymers studied by Bell et al., (2009a) showed that Region I extended from approximately 25 to 100°C and involved rapid loss of freely evaporable water and minimal shrinkage. Nearly 50% of the overall weight loss occurred within this region and was due to water loss. In Region II, weight loss and shrinkage occurred concomitantly over the range 100–300°C. Shrinkage in this region was much higher than in Region I and about 94% of the remaining water was lost. Region III involved nominal weight loss and shrinkage but there was considerable shrinkage in Region IV (Figure 16).

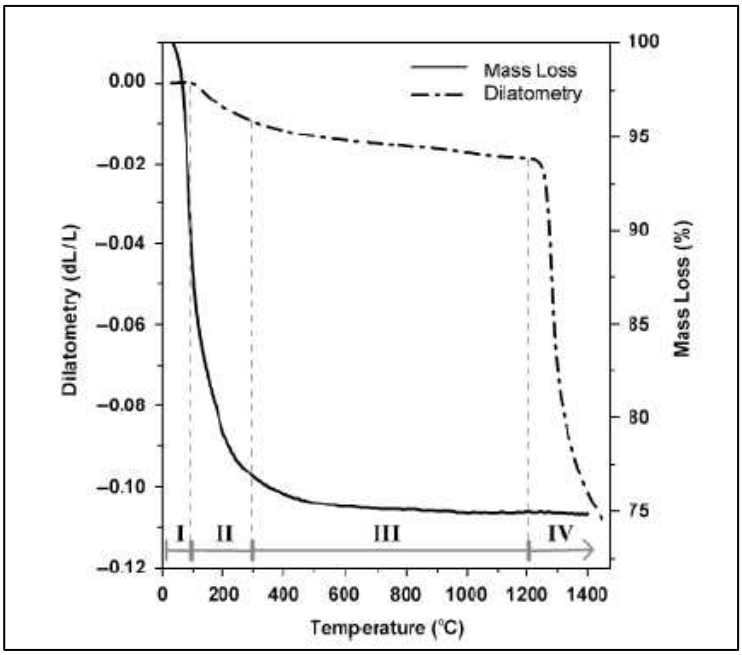

Figure 16: Dilatometry and thermal gravimetry (TG) results for Cs-Geopolymer heated at 10°C/min up to 1450°C in air (Bell et al, 2009a).

Duxson et al., (2006) observed the onset temperature of Region I for K-geopolymers at approximately 70°C, 90 °C and 115 °C for specimens with Si/Al ratios of 1.15, 1.40 and ≥1.65 respectively. Region II shrinkage extended from the onset of shrinkage until about 250–300 °C; nominal thermal shrinkage was observed in Region III and densification in Region IV was observed from 700 °C to 1000 °C. Similar studies by Barbosa and MacKenzie, (2003a) on Na-PSS geopolymer indicates that material dried at 65°C retains about 15 % water, of which 12% is lost below about 230°C; the remainder more tightly bound or less able to diffuse to the surface continuing to evolve gradually up to about 500°C. Once heated up to 1000°C, they observed a small degree of shrinkage associated with water loss below 250 °C and densification at about 800°C, the polymer dimensions remaining stable between 250 and 800°C.

The thermal stability of geopolymer is attributed to the formation of crystalline mineral phases at high temperatures, e.g. pollucite from Cs-based geopolymers (Bell et al, 2009a), leucite ($KAlSi_2O_6$), kalsilite ($KAlSiO_4$) or mullite ($Si_2Al_6O_{13}$) from potassium based geopolymer (Barbosa, and MacKenzie, 2003b; Duxson et al., 2006; Schmücker and MacKenzie, 2005) and mullite from Na-based geopolymer (Barbosa, and MacKenzie, 2003a).

The presence of aggregate in geopolymer matrices generally influences their thermal behavior. Barbosa and Mackenzie (2003a) studied the properties of Na-PSS geopolymer composites with a variety of inorganic fillers ranging from waste mining and demolition materials to high-technology ceramics. They observed these products to be thermally stable when heated and concluded that the effect of the fillers on the thermal reactions is not necessarily detrimental, and may even contribute to enhance mechanical properties of the composite by processes akin to reaction bonding. The thermal stability of geopolymer composites however greatly depends on the compatibility between the aggregates used and the geopolymer gel. Quartz aggregates have been found to reduce shrinkage upon heating, but also cause an abrupt expansion between 500 and 600°C, due to the α-β quartz phase change, followed by further shrinkage as the temperature is increased (Subaer, 2004). Kong and Sanjayan, (2008) showed that the mechanical properties of fly ash geopolymer with aggregates such as basalt, granite, siltstone, slag were reduced by about 65 % when the temperature was increased to 800 °C, due to differential thermal expansion behavior between the aggregates and geopolymer matrix, leading to destruction of the mechanical properties. The ideal aggregate is therefore one which may react with the geopolymer matrix upon heating or which may possess thermal behavior very close to that of the geopolymer gel.

I-3-9: Geopolymers from unheated clays

a) Processes producing similar effects to thermal activation

Conventional geopolymerisation processes require the availability of free alumina and silica for the polymerization reaction. The common method of producing these compounds from a 1/1clay material is to thermally dehydroxylate it, which increases the amount of energy required for geopolymerisation. More ecologically-friendly processes to produce geopolymers, have been sought, by increasing the clay reactivity without the need for thermal activation. Some of these alternative activation methods are mechanochemical processing (high energy grinding) and chemical pretreatment (MacKenzie, 2009).

Mechanochemical processing has been found to produce a similar effect to thermal activation, by destroying the crystalline structure and converting the aluminium coordination of halloysite clay from 6-fold to a mixture of 4, 5 and 6 fold, thereby producing viable geopolymers. Chemical pretreatment of halloysite in acid did not produce good results, but pretreatment in alkali produced a sufficient amount of tetrahedral aluminium to allow the mixtures to set and harden, although they contained crystalline compounds.

However, mechanochemical processing requires an input of energy and, in terms of convenience, may not present a significant advantage over thermal pre-treatment whereas pre-treatment of the clay with alkali solution seems to represent the best of these methods for reducing the energy consumption of geopolymerisation (MacKenzie, 2009).

b) Low temperature geopolymeric setting (LTGS)

The Low Temperature Geopolymeric Setting (LTGS) is a geopolymerization process which may take place in the presence of unheated clay in alkaline medium. Nearly all clay soils are capable of reacting with alkali (e.g. caustic soda). With different clay materials (kaolinite, montmorillonite, muscovite, chlorite, etc.) ceramic setting is obtained at temperatures between 50°C and 200°C (Davidovits and James, 1988). With kaolinite, the geopolymer of the Poly (sialate) (-Si-O-Al-O-) type which is formed is of the sodalite type, hydrosodalite (Si_2O_4,$Al2O_4$,2Na,3H_2O) (Davidovits and James, 1988; Davidovits and Bouterin, 2003).

The reaction of kaolinite with NaOH at 100°C-150°C can be written (J. Davidovits, 1988):

$$\underset{\text{Kaolinite}}{Si_2O_5,Al_2(OH)_4} + 2\ NaOH \longrightarrow \underset{\text{Hydrosodalite Na-PCDS}}{(Si_2O_4,Al_2O_4,2Na),\ 3H_2O} \qquad (I.14)$$

The Na-PCDS (Sodium Poly (sialate cyclodisialate)) obtained is a tridimensional poly(aluminosilicate) stable to water and possessing strong mechanical resistance.

The industrial application of this technique has been called the "SILIFACE Process" and the products are generally shaped by pressing (Davidovits and Bouterin, 2003; Davidovits, 1988). The working temperatures for LTGS processing generally vary between 50 and 500 ° C. The density of the resulting ceramics is around 1.9 g/cm^3 and their apparent porosity is around 30%. Their compressive strengths can be up to 40 MPa (Subaer, 2004).

For example, a SILIFACE Q obtained from 40 g kaolinite, 60 g quartz, 8 g NaOH, and 10g H_2O has a bulk density of 1.9 g/cm^3, a Mohs hardness varying from 4 to 6, flexural strength of 6 to 25 MPa, calculated minimum open porosity of 15 vol.% and measured porosity (water absorption) of 15% to 40%, depending on the experimental conditions involved in the cold-densification and thermo-setting steps. The higher the applied pressure, the lower the porosity. LTGS have proved to be useful for the production of low energy consuming building materials (bricks, tiles, etc.) and also the reproduction of archeological objects (Davidovits and Bouterin, 2003; Davidovits, 2008).

c) Solid-state synthesis

An alternative method of preparation of geopolymer by the direct calcination of low-quality kaolin with Na/K hydroxides was investigated by Kolousek et al., (2007). In this method, the formation of geopolymer matrix does not require activation by alkaline silicate solution. The compact and hardened material is obtained only by adding a small amount of water to the calcined mixture. The product of this reaction was largely X-ray amorphous, with aluminium in predominantly tetrahedral coordination and SiO_4 units in predominantly $Q^4(4Al)$ and $Q^4(3Al)$ environments. Although the mechanical properties observed (about 1MPa) was relatively low for building applications, the resulting product still can be applied as solidifier of dangerous and powdered substances (Kolousek et al., 2007). From an energy conservation point of view, the solid state synthesis offers no advantage since although it utilises an undehydroxylated starting material, the solid-state reaction is carried out at a typical dehydroxylation temperature. Nevertheless, this process represents a synthetic route to

geopolymers that are difficult to make by the conventional Davidovits method such as the formation of lithium geopolymers from metakaolinite (MacKenzie, 2009).

I-3-10: OPC and Geopolymer binders

Geopolymers are sometimes referred to as alkali-activated aluminosilicate binders. These materials differ substantially from Ordinary Portland Cements (OPC), because geopolymers use a totally different reaction pathway in order to attain structural integrity. Whereas Portland cements depend on the presence of calcium, geopolymers do not utilise the formation of calcium–silica-hydrates (CSHs) for matrix formation and strength. Instead, geopolymers utilize the polycondensation of silica and alumina precursors and a high alkali content to attain structural strength (van jaarsveld et al., 2002).

One of the primary advantages of geopolymers over traditional cements from an environmental perspective is the much lower CO_2 emission rate from geopolymer manufacture compared to OPC production. This is mainly due to the absence of the high temperature calcination of limestone when geopolymers are synthesised from ashes and/or slags, reducing the overall CO_2 emmission of the process (Rahier et al., 1996a; Davidovits, 2002; Duxson et al., 2007b; Tailby and Mackenzie, 2010; Nugteren, 2010). The largest growth in carbon emissions is from electricity generation, transport, industries and from building operations (Radhi, 2009). Cement (OPC) results from the calcination of limestone (calcium carbonate) and silico-aluminous materials. The production of 1 ton of cement generates 0.55 tons of CO_2 and needs the combustion of carbon-fuel into 0.40 tons of CO_2 (Davidovits, 1991).

In addition to greenhouse gas benefits, geopolymer technology also provides the opportunity for the utilization of waste streams that may not be of any benefit in OPC-blending applications. For example, magnesia-iron slags, ferronickel slags, and tungsten mine waste, have been shown to be effectively geopolymerised, but they are of little or no benefit in OPC (Duxson et al., 2007a). The possibility of immobilizing toxic and/or radioactive wastes also provides potential significant environmental benefits of geopolymers when compared to OPC (Duxson et al., 2007a; van Jaarsveld and van Deventer, 1996).

Portland cement clinker contains four major phases: tricalcium silicate (C_3S), β-dicalcium silicate (β-C_2S), tricalcium aluminate (C_3A), and ferrite solid solution ($C_4(A,F)$) (in the cement nomenclature, C= CaO, S = SiO_2, A=Al_2O_3, H=H_2O, F=Fe_2O_3). The main hydratation

product of Portland cement is a very poorly crystalline calcium silicate hydrate known as C-S-H. It is produced by hydration of C_3S and β-C_2S and is often described as a gel when there are other phases admixed on a sub-micrometre scale (Lecomte et al., 2006). In these structural models, silicate groups are organized in linear finite chains (principally dimmers, but also some pentamers and octamers), composed mainly of SiQ^1 and SiQ^2 species (Lecomte et al., 2006). On the contrary, geopolymers contain essentially three-dimensional cross-linked sites [SiQ^4(2Al) and SiQ^4(3Al)], which reflects a highly polymerized structural aluminosilicate framework (Barbosa et al., 2000; Lecomte et al., 2006; Davidovits, 2008).

In terms of durability, geopolymer binders are more acid resistant materials than OPC, with zeolitic properties that may allow them to encapsulate toxic wastes such as heavy metals. One of the weaknesses of OPC compared to geopolymers is the rapid decrease in mechanical properties when exposed to elevated temperatures. Indeed, when heating, OPC generally loses its mechanical properties at around 400°C whereas geopolymers generally maintain them up to 700-800°C and above (Davidovits, 2008). Geopolymer binders are also characterized by a rapid setting at room temperature and may attain compressive strengths of the order of 20 MPa after 4 hours. The final strength after 28 days may reach 70 to 100 MPa (Davidovits, 2002; Sofi et al., 2007).

I-4: ZEOLITES

Zeolites are aluminosilicates with a range of three-dimensional structures consisting of (Si, Al) O_4 tetrahedra coordinated by sharing all their oxygen atoms in the network (Subaer, 2004; Miladinovic et al., 2007; Nugteren, 2010). The tetrahedra make up a three-dimensional network, with lots of voids and open spaces. It is these voids that define many special properties of zeolites, such as adsorption of molecules in the huge internal channels. The substitution of Si (IV) by Al (III) in the tetrahedron accounts for a negative charge of the structure (Figure 17) which may give rise to a high Cation Exchange Capacity (up to 5 meq.g^{-1}) when the open spaces allow the access of cations (Nugteren, 2010; Ahmaruzzaman, 2010).

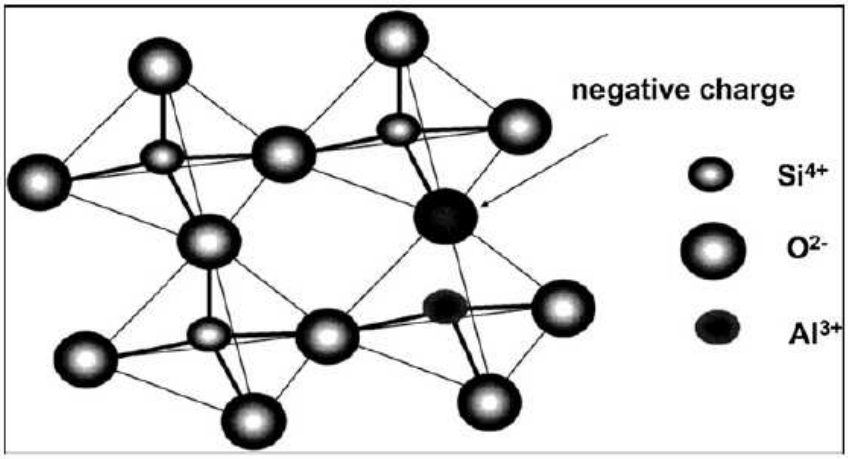

Figure 17: Idealized structure of zeolite framework of tetrahedral $[SiO_4]^{4-}$ with a Si/Al substitution ($[AlO_4]^{5-}$) yielding a negative charge, and consequently a cation exchange capacity (Ahmaruzzaman, 2010).

The stœchiometry of zeolites can be represented by the general formula (Subaer, 2004): $M^{n+}_{1/n}[(AlO_2)(SiO_2)_x]^- z\ H_2O$,

where x is the Si /Al molar ratio, z the number of water molecules physically linked. Cations (M) such as Li^+, Na^+, K^+, (where the valence n = 1) are necessary to compensate the tetrahedral aluminate charges.

I-4-1: Synthesis

Zeolites may be found in natural deposits, generally associated with alkaline activation of glassy volcanic rocks, but can also be synthesized from a wide variety of high-Si and Al starting materials (Subaer, 2004; Ahmaruzzaman, 2010). Many patents and technical articles proposed different hydrothermal activation methods for the synthesis of different zeolites. However most of them were based on the dissolution of Al–Si-bearing material phases with alkaline solutions (mainly NaOH and KOH solutions) and subsequent precipitation of zeolitic material (Ahmaruzzaman, 2010). The synthesis of type A zeolites for example is by hydrothermal treatment of kaolinite in alkaline solution at 100 ° C according to reaction (Subaer, 2004):

$$\underset{\text{Kaolinite}}{Al_2O_3.2SiO_2.2H_2O} + 2NaOH \longrightarrow \underset{\text{Zeolite A}}{Na_2O.Al_2O_3.2SiO_2} + 3H_2O \qquad \text{(I.15)}$$

Within the stability field of a given zeolite, increasing the alkalinity at constant temperature influences the kinetics, as does increasing the temperature at constant alkalinity. Both these factors decrease the nucleation time and enhance the rate of crystal growth of the zeolite. The effect of increasing the alkalinity is believed to be due at least in part to much greater concentrations of dissolved Al and Si species which assist the nuclei to develop more quickly from the more numerous encounters between the precursor species in solution.

I-4-2: Applications

As a consequence of the peculiar structural properties of zeolites, they have a wide range of industrial applications mainly based on ion exchange (exchange inherent $Na^+/K^+/Ca^{2+}$ for other cations on the basis of ion selectivity), gas adsorption (selective absorption of specific gas molecules), water adsorption (reversible adsorption of water without any desorption chemical or physical change in the zeolite matrix), adsorbents for removal, such as, wastewaters, radioactive wastes and gases, catalysts and molecular sieving (Ahmaruzzaman, 2010, Nugteren, 2010).

I-4-3: Comparison between zeolites and geopolymers

It has been found that temperature, pH and cations are three major factors affecting zeolites synthesis. These factors also affect geopolymerization. The formation of geopolymeric materials follows much the same route as that of most zeolites: (1) dissolution with the formation of mobile precursors through the complexing action of hydroxide ions, (2) partial orientation of mobile precursors as well as the partial internal restructuring of the alkali polysilicates and (3) reprecipitation where the whole system hardens to form an inorganic polymeric gel (van Jaarsveld et al., 2002).

However there are some fundamental differences between zeolites and geopolymers. Geopolymers have no long-range order as in the case of zeolites. Zeolites have certain stoichiometric compositions and crystalline structure. Geopolymer products do not have stoichiometric composition and consist of a mixture of amorphous to semi-crystalline structures. The hardening step occurring in geopolymerisation differs from the crystallisation step in zeolite synthesis. During this step in zeolite synthesis, no chemical reaction is involved, only the evaporation of water. However, during the hardening of geopolymers, although there is no obvious movement of particles at this stage, leaching and diffusion between particle surfaces and the gel phase may still occur and a slight movement of paste in the capillary pores may also take place (Xu, 2002).

The structural unit of zeolite A is identical to that of Na-poly(sialate). However, the zeolite A comes from the polycondensation of a cyclo-tetrasialate while Na-poly(sialate) comes from the polycondensation of a cyclo-disialate (Davidovits, 1991) (Figure 18).

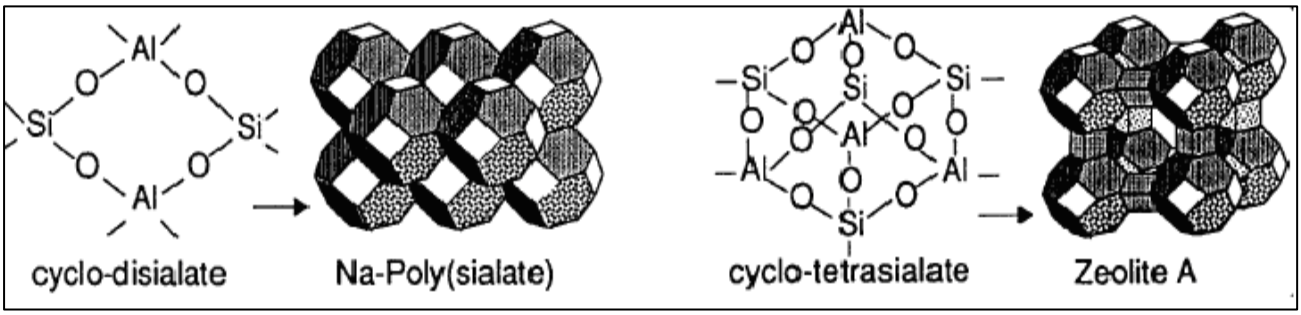

Figure 18: Network structure of Na-poly (sialate) and zeolite A (Davidovits, 1991).

Conclusion

Material containing sufficient amount of alumina and silica such as natural pozzolana (volcanic ashes), clayey materials, fly ash, etc., are suitable to be used as raw materials for geopolymers synthesis. Factors such as the type of alkali cation, the processing temperature and the water/solid ratio are able to affect the final properties of geopolymer materials. Geopolymers are more stable at elevated temperature than OPC and could be a possible alternative for supplying environmentally-friendly building materials due to less CO_2 emissions involved in their manufacturing processes. In addition, geopolymer technology also provides the opportunity for the utilization of waste streams that may not be of any benefit in OPC-blending applications.

CHAPTER II: MATERIALS AND EXPERIMENTAL METHODS

II-1: Introduction

The aluminosilicate materials used in this work were volcanic ashes, and the alkaline activators were sodium hydroxide, potassium hydroxide, a mixture of both, with or without amorphous silica. The experimental part of the work was performed in the Laboratory of Materials Analysis of the Local Materials Promotion Authority, Cameroon, the MacDiamid Institute for Advanced Materials and Nanotechnology at Victoria University of Wellington in New Zealand, the Industrial Research Limited in New Zealand and the Department of Physical Chemistry and Polymers of Vrije University of Brussel in Belgium. The present chapter presents the synthetic and natural materials used, the synthesis processes, the analytical methods and equipments for materials and products characterization.

II-2: MATERIALS

II-2-1: Natural materials

The volcanic ashes used were from Foumbot and Djoungo. Four samples were used: two from Foumbot and two from Djoungo.

a) Volcanic ashes from Foumbot deposits

Foumbot is situated at the left side of the Noun plain. This region had been subjected to important volcanic activities, from fissural events to explosive through strombolian activity. This has resulted in the deposit of huge quantities of scoria, lapillis and bombs. Most of the deposits consist only of lapillis and scoria. Globally, these are black materials often with a purplish iridescence, but in certain deposits, the materials tend to be grey or red. In the first case, the deposits are iron-poor, whereas in the second case the colour denotes the oxidation of Fe^{2+} to Fe^{3+}, either by surface phenomena or in the fumaroles (Wandji and Tchoua, 1988; 1989). The Foumbot samples come from the Petponoun and the Lac Mfou sites. Particles from the Petponoun deposit are gravelly (scoria) and black while the particles from the Lac Mfou deposit are finer and can be either black or red, with a predominance of black (Photos II-1 to II-4). Only black feature was collected for this study. Little part of pouzzolan from both sites is exploited for paving roads and masonry in addition with sand.

b) Volcanic ashes from Djoungo deposits

Djoungo is located in the Littoral Region. The Djoungo samples are in form of scoria. One is black while the other is poorly red (**Photo 5 and 6**). Part of Djoungo's pozzolana deposit is currently being exploited by the Douala "CIMENCAM" plant. The main reasons are the quantitative importance of the deposit and its location near the railway linking Douala, the

largest industrial city of Cameroon (Bidjoka, et al., 1993). Some part of this pouzzolan is also exploited for paving roads and masonry in addition with sand.

The geographic coordinates of all the samples' deposits used are presented in the Table 4.

Table 4: Geographic coordinates of the four samples' sites

Sample	N Latitude	E Longitude	Altitude
Petponoun (Va or Va1)	N5°37'46"	E10°37'56"	1145 m
Lac Mfou (Va2)	N5°32'17"	E10°41'39"	1301 m
Djougo scoria black (Va3)	N : 04 ° 35' 18''	E : 09° 37' 48''	147 m
Djoungo scoria red (Va4)	N 04°34'43''	E 09° 37''36''	

Photo 1: Panoramic view of the Petponoun site (Va1)

Photo 2: Black gravelly volcanic ash particles in the Petponoun deposit (Va1)

Photo 3: Panoramic view of the Lac Mfou deposit (Va2)

Photo 4: Fine particles in the Lac Mfou deposit showing red and black features (Va2)

Photo 5: Black sample from Djoungo deposit (Va3)

Photo 6: Poor red sample from Djoungo deposit (Va4)

c) Aggregate sand

The aggregate used was New Zealand natural sand, provided by the Industrial Research Limited (IRL), New Zealand.

II-2-2: Synthetic materials

The alkaline activators used in this study were sodium hydroxide, from Applichem Company (pH (1M, H_2O): 12-13 and solubility: 1090 g/l (H_2O) at 20°C) for the investigation carried out at Victoria University of Wellington (VUW). The work performed at Vrije Universiteit Brussel (VUB) was with NaOH and KOH (pro analysis) from Merck. The amorphous silica was of the AEROSIL 200 type from Degussa Company.

The Figure 19 globally presents the approach used for the experiments in the thesis.

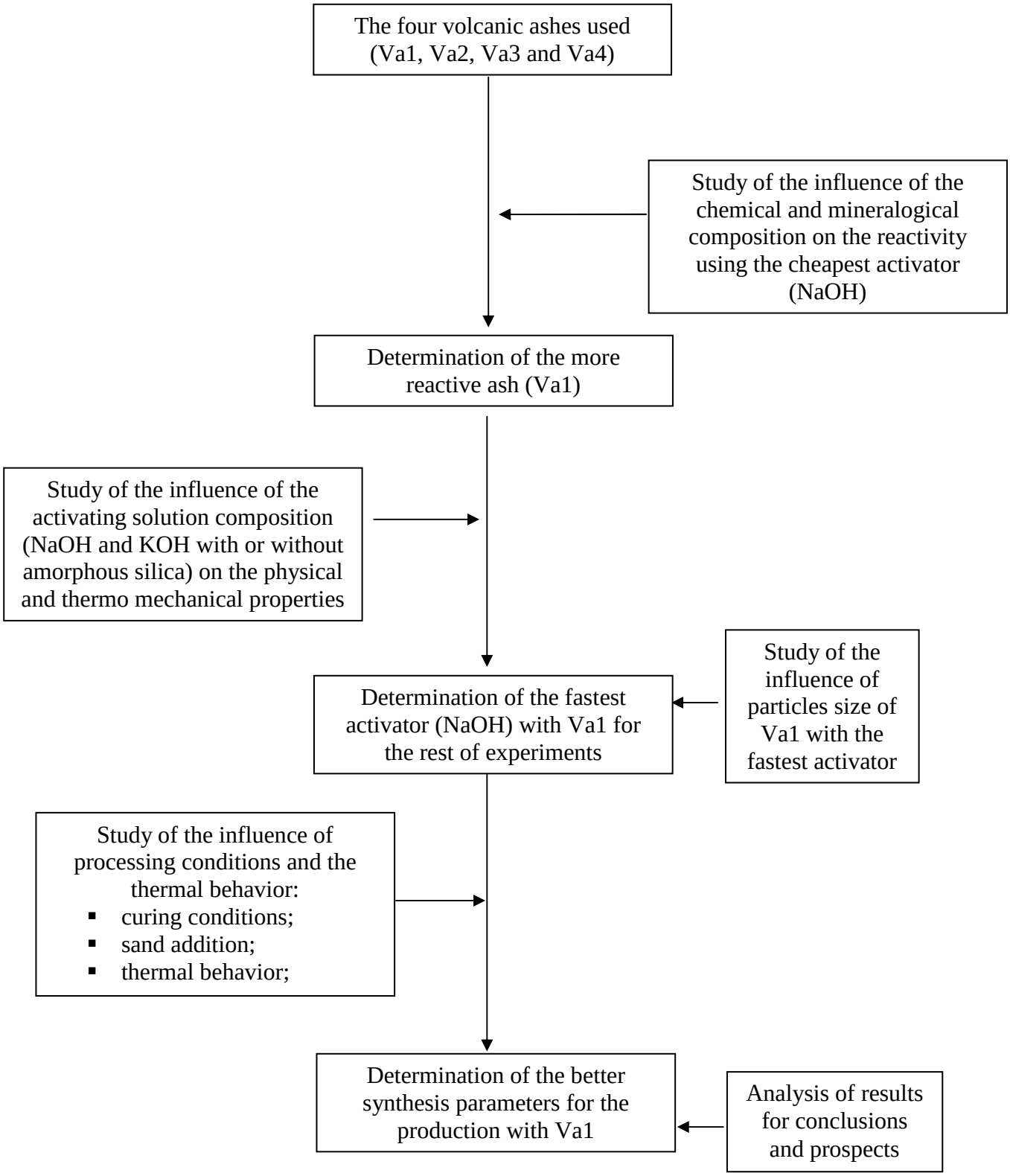

Figure 19: Approach used for the experiments

II-3: RAW MATERIALS CHARACTERIZATION

II-3-1: Particle size distribution

The particle size distribution of the sand was determined according to ASTM C 778-00 by shaking the sand through a sieve set with sizes of 1180, 850, 600, 425, 300 and150 µm. The volcanic ash was ground up to total passing through a 400µm sieve. The particle size distribution was then determined using a Shimadzu Sald-2001 Laser diffraction particle size analyser. A representative set of particles was sent through a broadened beam of laser light which scatters the incident light onto a Fourier lens. This lens focuses the scattered light onto a detector array and, using an inversion algorithm, a particle size distribution is inferred from the collected diffracted light data. These analyses were carried out at VUW in New Zealand. Sieving and then sedimentation technique using the Stoke's Law was also used for particle size analysis at VUB in Belgium.

II-3-2: Chemical and X-ray diffraction analyses

Chemical analyses were carried out by X-ray fluorescence at IRL and VUB. For X-ray diffraction, samples were powdered in a porcelain bowl using a Philips PW1700 with computer controlled goniometer and graphite monochromator using CoK_{α} at VUW and a D500 Bruker diffractometer, generating a Cu K_{α} radiation at VUB. An applied voltage of 40 kV and a current of 30 mA were used. XRD scans were measured from 5° to 70° 2-theta at a scan rate of 1°/min.

II-4: PREPARATION OF GEOPOLYMERS

The preparation of volcanic ash raw materials was conducted in the laboratory of materials analysis at MIPROMALO. The field samples were dried and ground in a ball mill up to total passing through a 400µm sieve. The powdered materials obtained were then stored in plastic bags to prevent the fixation of atmospheric water.

II-4-1: Influence of the chemical and mineralogical composition on the reactivity of the four volcanic ashes for geopolymer synthesis

The four volcanic ashes (Va1, Va2, Va3 and Va4) used in this section were from Foumbot (Va1, Va2) and Djoungo (Va3, Va4), situated respectively in the West and Littoral Regions of

Cameroon. The inorganic polymer formulations were obtained by adding while stirring volcanic ash into a solution obtained by dissolving in distilled water, NaOH, as to obtain in the mixtures a Na_2O/Al_2O_3 molar ratio ranging from 1.00 to 1.75, with 0.25 intervals. This has resulted in four compositions for each of the ashes Va1, Va2, Va3 and Va4. The ratio water/ash was maintained at 0.21 for all the compositions. The mixed pastes were placed in polyethylene cubic moulds (4x4x4 cm), and then vibrated for 5 min to remove air bubbles. The molded samples were then placed at 40°C for 2 days, then, the samples were demolded and placed at 90°C for 5 days.

II-4-2: Effect of the activating solution composition on the stability and thermomechanical properties of geopolymers from Va1

The inorganic polymer formulations were obtained by adding while stirring volcanic ash from Foumbot Petponun site (Va1 here simply called Va) into a solution obtained by dissolving in distilled water NaOH, KOH with or without amorphous silica, in order to obtain in the mixtures, a M_2O/SiO_2 molar ratio of 0.30 for mixtures without amorphous silica and 0.29 for mixture with amorphous silica. This has resulted in six compositions; three of them without amorphous silica named Va-Na, Va-Na+K and Va-K corresponding to mixtures containing added sodium, sodium+potassium and potassium respectively. Their counterparts with amorphous silica were named Va-NaSil, Va-(Na+K)Sil and Va-KSil. For Va-Na+K and Va-(Na+K)Sil preparation, the molar concentration of potassium and sodium added were equal. The water/ash ratio (weight) was maintained at 0.21 for all the mixtures. However, as the Va-K composition presented a lower viscosity, a water/ash ratio of 0.18 called Va-K0.18 was also made.

The influence of particle size distribution on the reactivity and compressive strength was investigated with the fastest activator (NaOH) by removing the coarser particles (40 wt% of the initial ash sieved at 400μm) while sieving at 125 μm. The specimens made with this fraction and sodium hydroxide were named Va(<125μm)-Na. All the mixtures made in this section are summarized in Table 5. The mixed pastes were placed in the cylindrical plastic moulds (50 mm height x 2.5mm diameter), then vibrated for 5 min to remove air bubbles before being treated at 90°C for 7 and 21 days.

Table 5: Mixtures composition

Formulations	**SiO_2/Al_2O_3** (molar)	***M_2O/SiO_2** (molar)	**H_2O/solid ash** (weight)
Va-Na	4.84	**0. 30**	0.21
Va-NaSil	5.18	**0.28**	0.21
Va-Na+K	4.84	**0.30**	0.21
Va-(Na+K)Sil	5.18	**0.28**	0.21
Va-K	4.84	**0.30**	0.21
Va-KSil	5.18	**0.28**	0.21
Va-K0.18	4.84	**0.30**	0.18
Va(<125µm)-Na	4.84	**0.30**	0.21

* M=Na or K

II-4-3: Impact of processing conditions and thermal behavior of geopolymers from Va1

The inorganic polymers were synthesized by stirring the volcanic ash from Foumbot Petponun (Va1 here simply called Va) in a solution of NaOH (Applichem Co.) in distilled water, to give five compositions with Na_2O/SiO_2 molar ratios of 0.15 to 0.35. The weight ratio (H_2O: volcanic ash) was maintained at 0.21 in all the formulations. The mixed pastes were stirred for 5 min, placed in 50x50x50 mm^3 polyethylene moulds and vibrated for 5 min. to remove air bubbles. One of the mixtures (Na_2O/SiO_2 = 0.25) was subjected to various curing procedures as follows: 40°C for 24 hr. sealed, then unsealed at 40°C for 24 hr. This initial curing was the same for all the samples, and was followed by post-curing for five days, either in water or in open air at 40, 70 and 90°C. The post-curing environment that produced the best compressive strength (dry curing at 90°C) was then adopted for the remaining experiments. An addition of 10, 25 and 40 wt % of sand on the basis of the volcanic ash was also made on the geopolymer formulation which gives the best compressive strength.

II-5: GEOPOLYMERS CHARACTERIZATION

II-5-1: Influence of chemical and mineralogical composition on the reactivity of the four volcanic ahses

All the analyses performed in this session were carried out at VUB, except the Mössbauer spectroscopy analyses carried out at IRL in New Zealand.

The reactivity of the systems was studied with Differential Scanning Calorimetry. The resulting products were characterized by Scanning Electron Microscopy (SEM), Infrared spectroscopy (IR), X-ray diffraction (XRD), Differential Thermal Analysis and Thermogravimetry Analysis (DTA/TGA). The products stability was assessed by dry, wet and wet-dry compressive strength measurements.

a) Differential scanning calorimetry (for reativity assessment)

Differential scanning calorimetry (non-isothermal and isothermal measurements) was performed on a DSC 822e Mettler Toledo instrument using Helium at 25 mL/min as a purge gas. The samples were mixed in small quantities (800 mg) with a spatula before placing in the sample pan. Reusable high pressure stainless steel sample pans (Mettler) were used. The sample (about 30 mg) was heated from 0°C to 240°C at 5°C/min. Temperature calibration was done with cyclohexane and indium. The latter was also used for enthalpy calibration. For isothermal measurements the samples were heated at 90°C for 700 min.

At least two measurements were performed for each formulation and the error on the reaction enthalpy was below 10%.

b) Fourier Transform Infrared Spectroscopy

IR spectra were obtained with a NICOLET 6700 FTIR. For each spectrum, 32 scans with a resolution of 2 cm^{-1} were used in transmission mode on KBr pellets made with about 2 mg sample and 200 mg KBr.

c) Miscrostructure

Scanning electron micrographs and maps of polished samples coated with about 20 nm of carbon for second electron imaging were determined using a Jeol JSM 6400 microscope with an acceleration voltage of 20 kV.

For optical microscopy, a Digital Optical Miscoscope of VHX-1000 type was used to screen the sample surfaces at 250's magnification. It was equipped with a camera coupled with an activate tool to offer a pixel displacement allowing a very high resolution (up to 54 milion

pixels). A progressive scanning method without sparkling allowed the reproduction of the texture and color likely to eye view.

d) Compressive strength

The compressive strength of the samples was measured with an Instron 1195 Compression machine equipped with a computer program for compressive strength calculation and a displacement of 1mm/min. The dry compressive strength was obtained after curing the products at 90°C for 7 days. For wet compressive strength, these specimens were immersed in water overnight and measured wet while the wet-dry compressive strength is for immersed specimens dried overnight at 60°C.

e) Thermogravimetric /Differential Thermal analyses

TGA/DTA analyses were performed with a Netzsch STA409 PC/PG instrument in helium flowing at 60 mL/min. The samples were heated to 1000°C at 10°C/min.

f) Mössbauer Spectroscopy analyses

The Mössbauer spectroscopy of iron was used to find out changes occurring in this nucleus during the geopolymerisation process in order to highlight the possible implication of this element in the geopolymerisation reactions. ^{57}Fe Mössbauer spectra of ash before and after treatment with sodium hydroxide were measured at 295 K with a magnetic field of 47 mT applied parallel to the γ-rays.

II-5-2: Effect of the activating solution composition on the stability and thermomechanical properties of geopolymers from Va1

All the analyses performed in this section were carried out at VUB.

NaOH, KOH and silicate solutions with low modulus were tested. The reactivity of the systems was studied with Differential Scanning Calorimetry. The resulting products were characterized by Scanning electron microscopy (SEM), Infrared spectroscopy (IR) and X-ray diffraction (XRD). The products stability was assessed by dry, wet and wet-dry compressive strength measurements. The pH of the immersed products was also controlled. Thermogravimetric Analysis (TGA), Thermomechanical Analysis (TMA) and Dynamic Mechanical Analysis (DMA) were used to investigate the high temperature behavior of the different compositions.

Some methods and equipments (XRD, DSC, SEM, Compressive strength) used in this section were similar to the previous one. The new equipments or methods used are presented below:

a) pH of the solution of immersed products

In order to have an idea on the amount of unreacted reagent, the groups of six synthetised samples were immersed in 334g of distilled water for each group and the pH of the solution was taken. This was done using a Didital pH-metter of type Inolab WTW.

b) Thermal analyses

- **Thermogravimetric Analysis**

TGA analyses were performed with a TGA Q5000 instrument in nitrogen flowing at 25mL/min. The samples were heated to 1000°C at 5°C/min and then cooled to 50°C at 50°C/ min.

- **Dynamic Mechanichal Analysis**

For our study, a DMA 7 of Perkin Elmer was used with a quartz expansion probe (3 mm diameter). The purge gas was air at 50 mL/min. A static force of 250 mN and a dynamic force of 200 mN with an applied frequency of 1 Hz were used. The samples were cycled twice between 25°C and 1000°C, while equilibrating for five min at the minimum and maximum temperature. The heating and cooling rate was 5°C/min. Cylindrical samples of about 4 mm diameter and 10 mm height obtained from geopolymer paste moulded and cured at 90°C for 7 days in small cylindrical tubes were used and placed between a platinum cup and lid for measurement.

II-5-3: Impact of processing conditons and thermal behavior of geopolymers from Va1

All the analyses carried out in this session were performed at VUW.

NaOH was used as the sole alkaline activator. The structure of the polymers was studied by XRD and FTIR and the influence of the Na_2O/SiO_2 molar composition and curing conditions

on the compressive strength of the geopolymer cement was determined, as were the mechanical and physical properties of the corresponding mortar containing various proportions of standard mortar sand. The thermal properties of these materials were also determined by TGA/ DSC and dilatometry, to assess their suitability as refractories.

a) Fourier Transform Infrared Spectroscopy

Powdered samples were mixed with KBr for FTIR analysis using a Perkin Elmer FTIR. For each spectrum, 32 scans with a resolution of 8 cm^{-1} were used in transmission mode on KBr pellets made with about 2 mg sample and 200 mg KBr.

b) Percentage of water absorption and apparent density

The determination of these parameters was made according to ASTM C 20-00. The dried specimens were kept in plastic bags to prevent the fixation of atmospheric air. Subsequently, mass Md is determined and they were introduced into a beaker containing distilled water. The mixture was boiled for two hours, ensuring that the specimens are immersed. After letting the mixture cool for 24 hours, the wet mass (Mw) and the mass suspended in water (Ms) were determined.

i) The water absorption ab (%) expresses in percentage the quotient of the weight of water absorbed to the weight of the dry specimen. It is given by the equation:

$$ab = \frac{Mw - Md}{Md} \times 100$$

ii) The bulk density ρ (g/cm^3) is defined as the quotient of the dry mass of the sample by the volume occupied by solid matter, including the voids contained in the grains (bulk volume). It is given by the equation:

$$\rho_a = \frac{Md}{Mw - Ms}$$

c) Compressive strength

The compressive strength was obtained by calculation after measuring the compressive load that the specimens can withstand before it breaks. This was done with an ELE ADR-Auto 2000 KN Compression machine equipped with a computer program for compressive strength calculation and pace rate of 0.9 KN/s. The material was placed between the two flat surfaces of the compression device, and compressed with a uniform speed. The result obtained is an average of at least three replicate specimens.

d) Scanning electron microscopy

Scanning electron micrographs of fractured samples coated with 16 nm of carbon for backscattered electron or second electron imaging were determined using a Joel JSM 6500F microscope. The accelerating voltage was fixed to 15.0 kV.

e) Thermal analyses

The thermal behavior of the sample of composition $Na_2O/SiO_2 = 0.25$ dry-cured at 90°C was determined by differential scanning calorimetry (DSC) and thermogravimetry (TG) using a TA instrument SDT Q600 V8.2 in flowing air (50ml/min) and a heating rate of 10°C.min^{-1}.
The dilatometric curve was obtained on a cylindrical sample 21.5 mm x 6 mm dia. using a modified Harrop Laboratories TDA-H1-CP6 dilatometer at a heating rate of 5°C.min^{-1} up to 1000°C, held at this temperature for 0.5 hr then cooled at 5°C.min^{-1} to about 100°C. The sample was subjected to two cycles.
The Figure 20 illustrates the production of geopolymer using Va1.

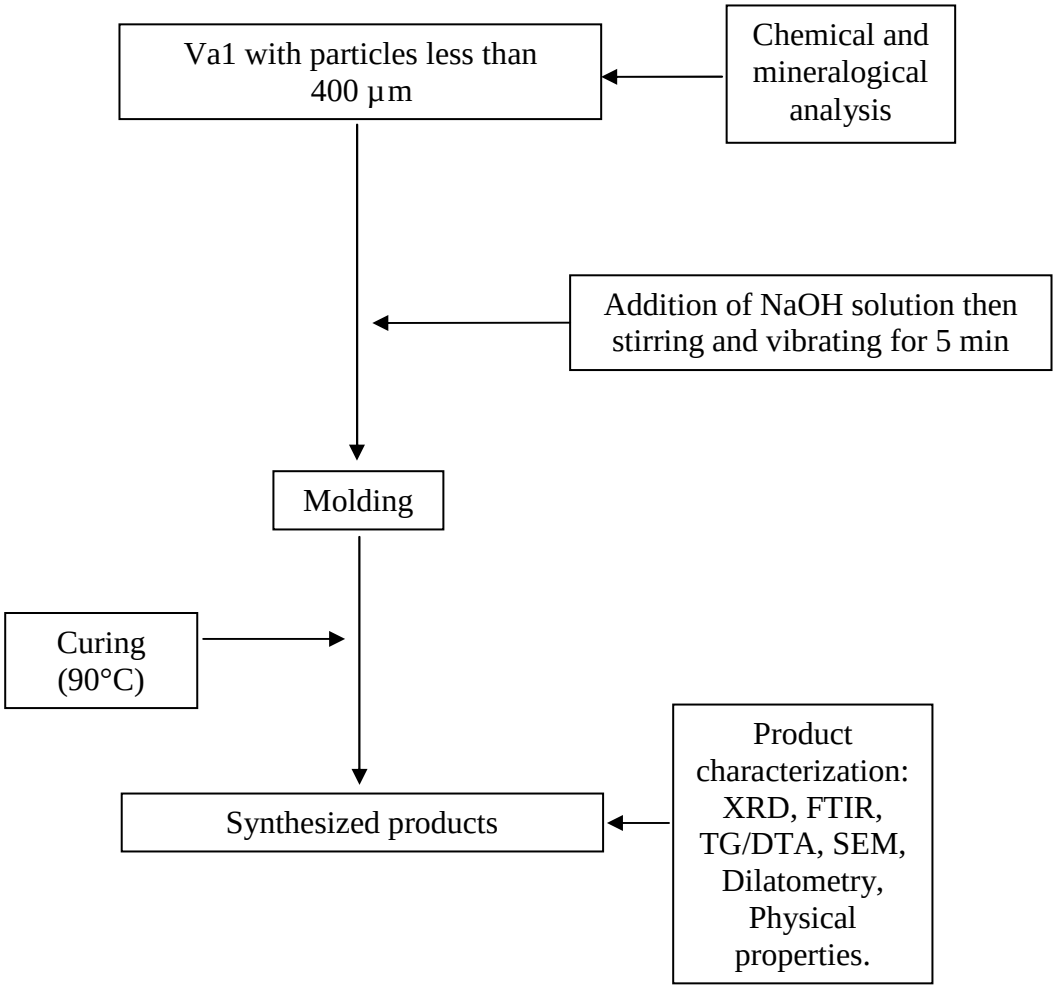

Figure 20: Production of geopolymer using Va1

II-6: Conclusion

Four samples of volcanic ashes were used, but the studies were extended only on the more reactive ash (from Foumbot's Petponoun site (Va1). NaOH, KOH, with or without silicate solution were used as alkaline activator medium.

Several techniques were used for raw materials and products characterization:

X-ray fluorescence, X-ray diffraction, Fourrier Transform Infrared Spectroscopy, Scaning Electron Miscroscopy, Digital Optical Microscopy, Mössbauer Spectroscopy, Differential Scaning Calorimetry, Thermogravimetry and Differential Thermal Analysis, Mechanic and Dynamic Mechanical Analyses.

CHAPTER III: RESULTS AND DISCUSSION

III-1: INFLUENCE OF CHEMICAL AND MINERALOGICAL COMPOSITION ON THE REACTIVITY OF THE FOUR VOLCANIC ASHES

In chapter I, volcanic ashes were described to be suitable for geopolymer synthesis due to their high content in silica and alumina. Geopolymerisation of volcanic ashes is however influenced by the difference in mineralogical and chemical composition of the ashes, which may greatly affect the reactivity of the materials as well as the final properties of the synthesized products.

The present section investigates the suitability of four different volcanic ashes (Va1, Va2, Va3 and Va4) for geopolymers synthesis, in order to highlight a possible correlation between the chemical and the mineralogical composition of the ashes and their reactivity or the final properties of the synthesized products.

NaOH was used as the sole alkaline activator. The reactivity of the systems was studied with Differential Scanning Calorimetry (DSC). The resulting products were characterized by Scanning Electron Microscopy (SEM), Infrared Spectroscopy (IR), X-ray diffraction (XRD), Mössbauer Spectroscopy, Differential Thermal Analysis and Thermogravimetry Analysis (DTA/TGA). The stability of the products was assessed by dry, wet and wet-dry compressive strength measurements.

III-1-1: Mineralogical composition of volcanic ashes and geopolymers

The X-ray spectra of the volcanic ashes showed a mixture of amorphous and crystalline phases (Figure 21) composed of Anorthite sodian disordered:$(Ca,Na)(Si,Al)_4O_8$, Augite: $(CaMg_{0.74}\ Fe_{0.25})Si_2O_6$, Forsterite ferroan: $(Mg_{0.9}\ Fe_{0.1})_2SiO_4$ for Va1; Quartz : SiO_2 Augite : $(CaMg_{0.74}\ Fe_{0.25})Si_2O_6$, Magnetite : Fe_3O_4, Anorthite sodian intermediate-$(CaNa)(SiAl)_4O_8$, Microline intermediate-KAlSi3O8 for Va2; Anorthite sodian disordered: $(Ca,Na)(Si,Al)_4O_8$, Augite: $(CaMg_{0.74}\ Fe_{0.25})Si_2O_6$, Forsterite ferroan: $(Mg_{0.9}\ Fe_{0.1})_2SiO_4$ for Va3 and Anorthite sodian disordered: ($Ca,Na)(Si,Al)_4O_8$, Augite: $(CaMg_{0.74}\ Fe_{0.25})Si_2O_6$, Nepheline: NaAlSiO4, Forsterite: Mg2SiO4, Hematite: Fe_2O_3 for Va4. The main difference observable by XRD between the spectra of pure ashes and those treated with sodium hydroxide were the appearance of Sodium Aluminosilicate Hydroxide Hydrate- $Na_8(AlSiO_4)_6(OH)_2.4H_2O$ on the spectra of activated ashes. The presence of initial minerals in the final products is also suggesting incomplete dissolution of the crystalline phases present in the starting materials.

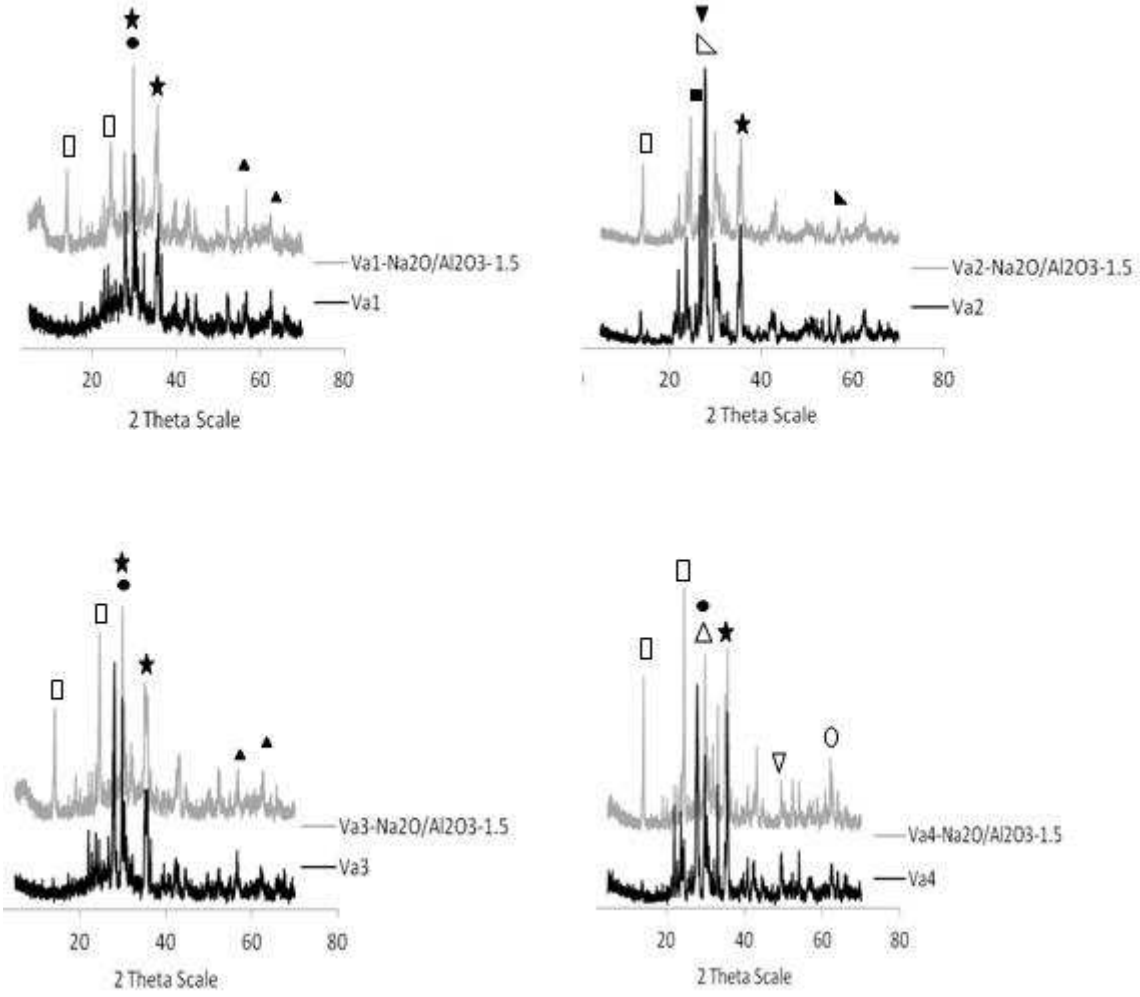

Figure 21: XRD spectra of pure (bottom) and reacted ashes at Na_2O/Al_2O_3 of 1.50

- ● = Anorthite sodian disordered:$(Ca,Na)(Si,Al)_4O_8$,
- ★ =Augite: $(CaMg_{0.74}\ Fe_{0.25})Si_2O_6$,
- ▲ =Forsterite ferroan: $(Mg_{0.9}\ Fe_{0.1})_2SiO_4$
- ■ = Quartz : SiO_2
- ◣ = Magnetite : Fe_3O_4,
- ▼ = Microline intermediate-$KAlSi_3O_8$
- ◺ =Anorthite sodian intermediate-$(CaNa)(SiAl)_4O_8$
- ○ = Forsterite: Mg_2SiO_4
- △ =Nepheline: $NaAlSiO_4$,
- ▽ =Hematite: Fe_2O_3
- ▯ =Sodium Aluminosilicate Hydroxide Hydrate- $Na_8(AlSiO_4)_6(OH)_2$-$4H_2O$

Conventional geopolymers resulting from the dissolution of aluminosilicate in a strongly alkaline medium are expected to be amorphous (Barbosa et al., 2000; Rahier et al., 1996; Bell et al., 2009b). However, the presence of a new crystalline phase not originating from the starting material has been previously reported for geopolymers resulting from volcanic ash, fly ash as well as metakaolinite especially after reaction with silicates with a low modulus (Verdolotti et al. 2008; Rahier et al., 1997; Lemougna et al., 2011, Bell et al, 2009b).

By treating an amorphous pozzolana with sodium hydroxide or sodium hydroxide plus sodium aluminate, Verdolotti et al., (2008) obtained a product with crystalline diffraction peaks, possibly from a zeolite, overlapping the amorphous baseline. For the current volcanic ashes, it is likely that the reactions that took place in alkaline medium may involve the transformation of the major part of the initial amorphous phases of the ash into the amorphous to semi crystalline geopolymer phase, but also a crystalline phase of sodium aluminosilicate hydroxide hydrate. The alteration or transformation of part of the initial crystalline phase is also likely and will be evidenced in the Mössbauer spectroscopy section.

The amount of amorphous phase was estimated with the analysis software by the method of subtracting the crystalline surface area on the XRD spectra. The results obtained were 58% for Va1, 6% for Va2, 33% for Va3 and 9% for Va4. After reaction, the amount of amorphous phase in the products was estimated at a Na_2O/Al_2O_3 molar ratio of 1.50 to be 44%, 27%, 37% and 29% respectively in the specimens resulting from Va1, Va2, Va3, and Va4 (Figure 22).

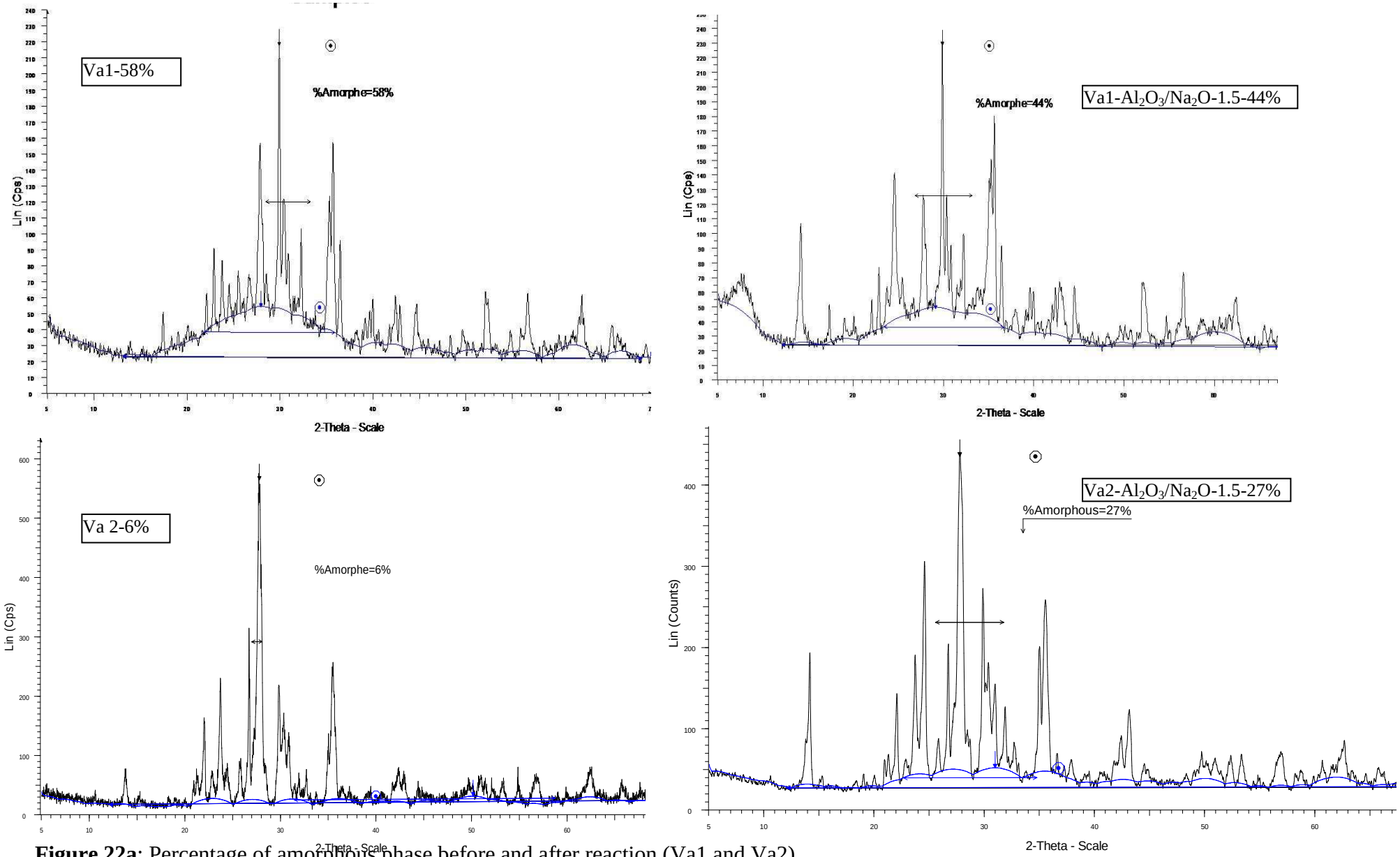

Figure 22a: Percentage of amorphous phase before and after reaction (Va1 and Va2)

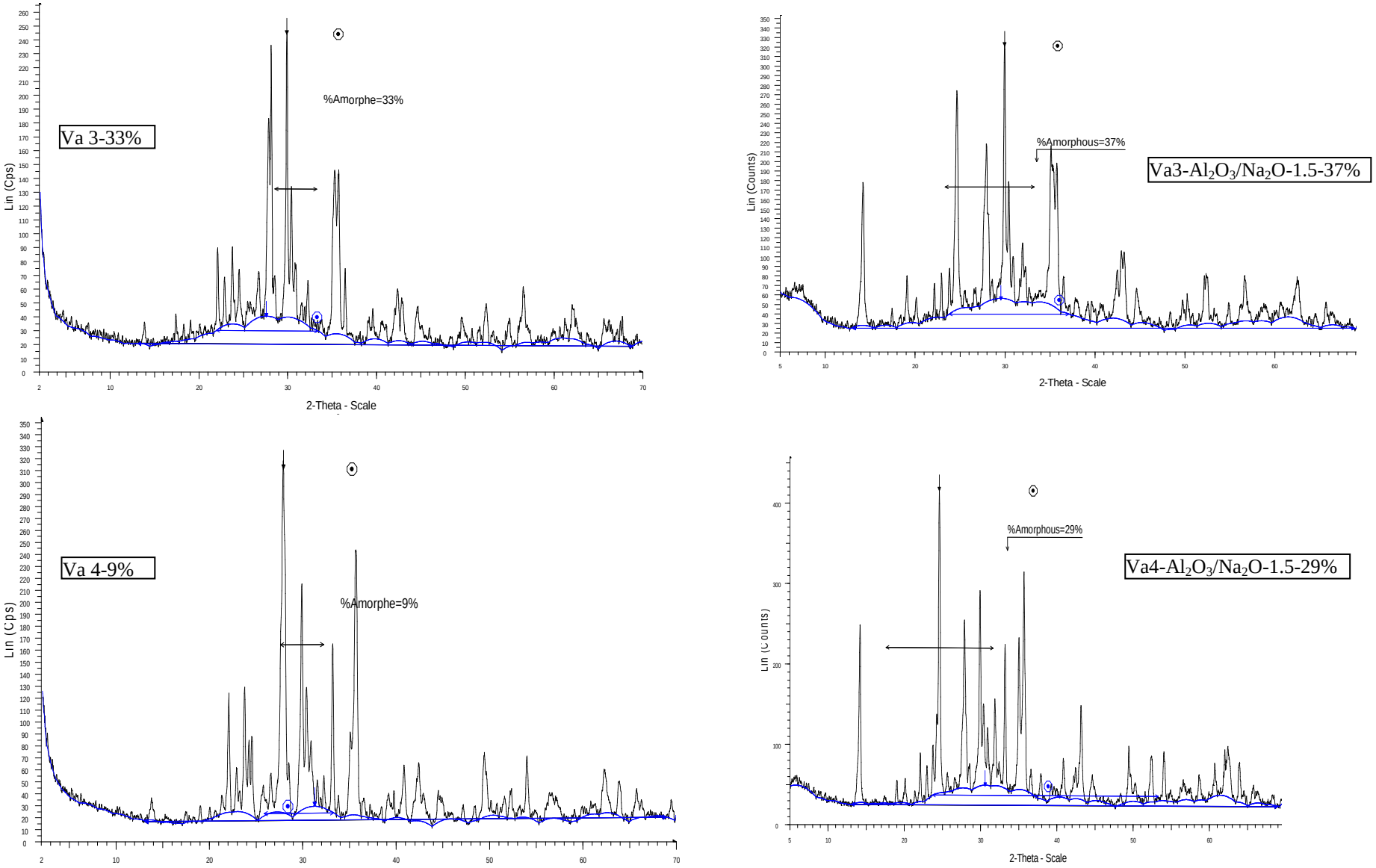

Figure 22b: Percentage of amorphous phase before and after reaction (Va3 and Va4)

A positive correlation was found between the amount of these phases and the heats of reaction (Figure 23). This trend was also observable on the DSC curves (Figure 24 and 27) showing higher reaction heat and reactivity for the more amorphous materials. An extrapolation of the curve (Figure 23) shows that there is still some reactivity remaining at 0% of amorphous material, suggesting that part of the crystalline phases also reacted. This can explain the increase of the amount of amorphous fraction after reaction for Va2, Va3 and Va4.

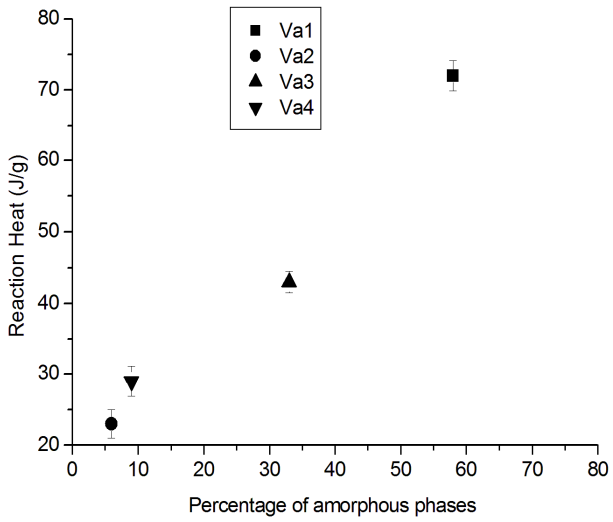

Figure 23: Influence of the percentage of the amorphous phase in the starting ashes on the reaction heat at Na_2O/Al_2O_3 of 1.00

III-1-2: Reactivity of the mixtures

The heat flow measured in a DSC experiment is proportional to the reaction rate. The DSC thermograms of the fresh geopolymer mixtures from the different ashes at Na_2O/Al_2O_3 molar ratio of 1.5 are presented in Figure 24.

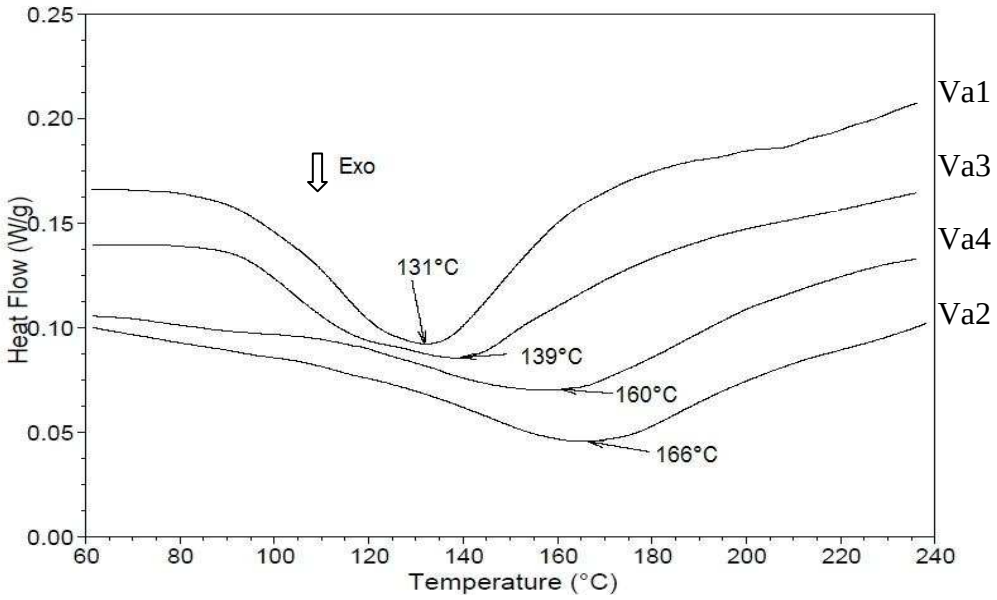

Figure 24: DSC curves of reacted ashes at Na_2O/Al_2O_3 of 1.50

It is observed that the peak maxima varies between 131 and 166°C, appearing in the order Va1<Va3<Va4<Va2. The reaction heat of all the fresh geopolymer mixtures from the four ashes with different Na_2O/Al_2O_3 molar ratio (1.00 to 1.75) are presented in Figure 25.

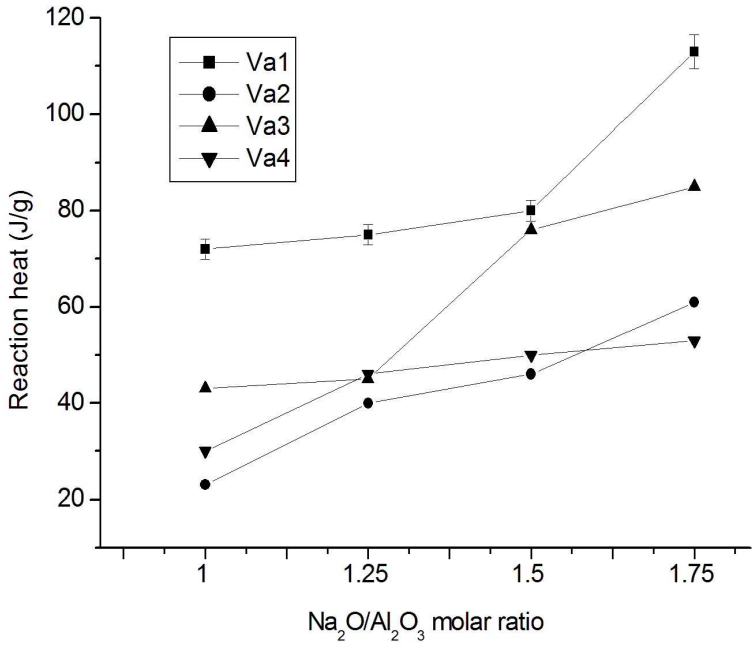

Figure 25: Reaction heat of freshly mixed mixtures

Globally, it appeared that the reaction heat increases with the amount of NaOH added to the mixture. The trend observed is different to previous studies reported on metakaolin-based geopolymer where the reaction heat was observed to increase with the addition of silicate solution in the fresh mixture, reaching a maximum value at the Na/Al ratio of 1 (Rahier et al, 1996b). This difference could be linked to the mineralogical composition of the ashes, the presence of some crystalline phases dissolving only slowly before reacting, and the rate of dissolution increasing with the addition of sodium hydroxide in the mixture. Another reason is that the crystalline reaction product formed has a Na/Al ratio of 8/6 as shown in previous work (Lemougna et al., 2011). One could thus expect a maximum at a ratio of 1.33 if the amorphous phase has the same composition. The temperatures of the maximum reaction rate for all the mixtures are higher while the reaction heats are smaller than those reported (Rahier et al., 1996b; Rahier et al., 1997) for inorganic polymer glasses resulting from alkaline activation of metakaolin. Most of those compositions react between 60-120°C and the reaction heats reaching 580 J/g with metakaolinite. The present volcanic ashes are therefore considered to be less reactive than thermally activated kaolinite.

In the following part it will be tried to find explanations for the differences in reactivity between the different volcanic ashes. It has been reported that particle size does influence the reactivity, finer particles increasing the reaction rate, the heat flow signal being larger and reaching the baseline earlier (Rahier et al., 2003). Based on particle size analysis (Figure 26), the fineness of the ashes were in the range Va1>Va2>Va4>Va3, but this does not correspond to the trend observed on the reaction heats ($|\Delta H|$ Va1> $|\Delta H|$ Va3> $|\Delta H|$ Va4>$|\Delta H|$ Va2) suggesting that other factors such as the chemical or the mineralogical composition of the ashes went into play.

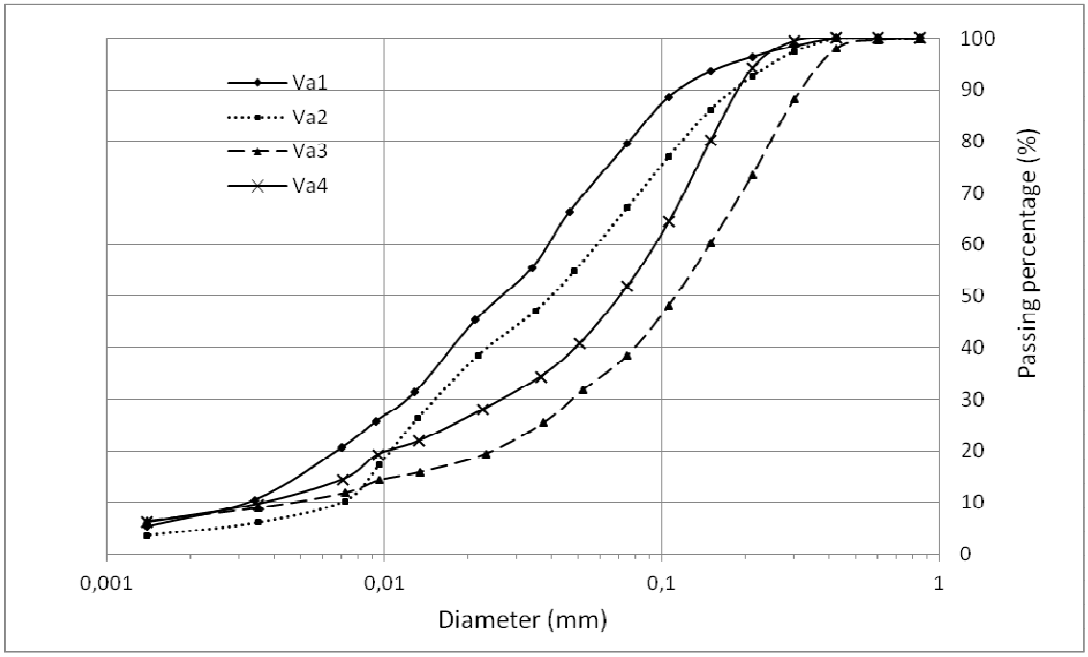

Figure 26: Particle size distribution of pure ashes

The isothermal DSC measurement at 90°C of the different ashes (Figure 27) also shows that the reactivity (height of the signal at the beginning of the measurement) of the ashes are in the order Va1> Va3> Va2> Va4, similarly to the trend observed for the temperatures of appearance of the peak max (Figure 24) for non isothermal measurements. As the chemical composition of all the ashes (mostly for Va1, Va3, and Va4) were very similar (Table 6), it is likely that factors that influenced the reactivity should be more linked to the mineralogical composition and crystallinity. Figure 27 also shows that the main part of the reaction is finished after about 5 hours at 90°C.

Table 6: Chemical composition of the different ashes (mass %)

Oxide	Fe_2O_3	MnO	TiO_2	CaO	K_2O	P_2O_5	SiO_2	Al_2O_3	MgO	Na_2O	SUM
Va1	12	0.19	2.9	11	1.7	0.9	43	15	6.8	4.6	99.39
Va2	8.5	0.16	1.8	6.1	3.1	0.9	55	15	2.9	5.3	99.62
Va3	14	0.19	3.3	11	1.7	0.8	43	15	5.8	4.1	99.51
Va4	13	0.17	2.9	10	1.5	0.8	44	16	5.5	4.4	99.57

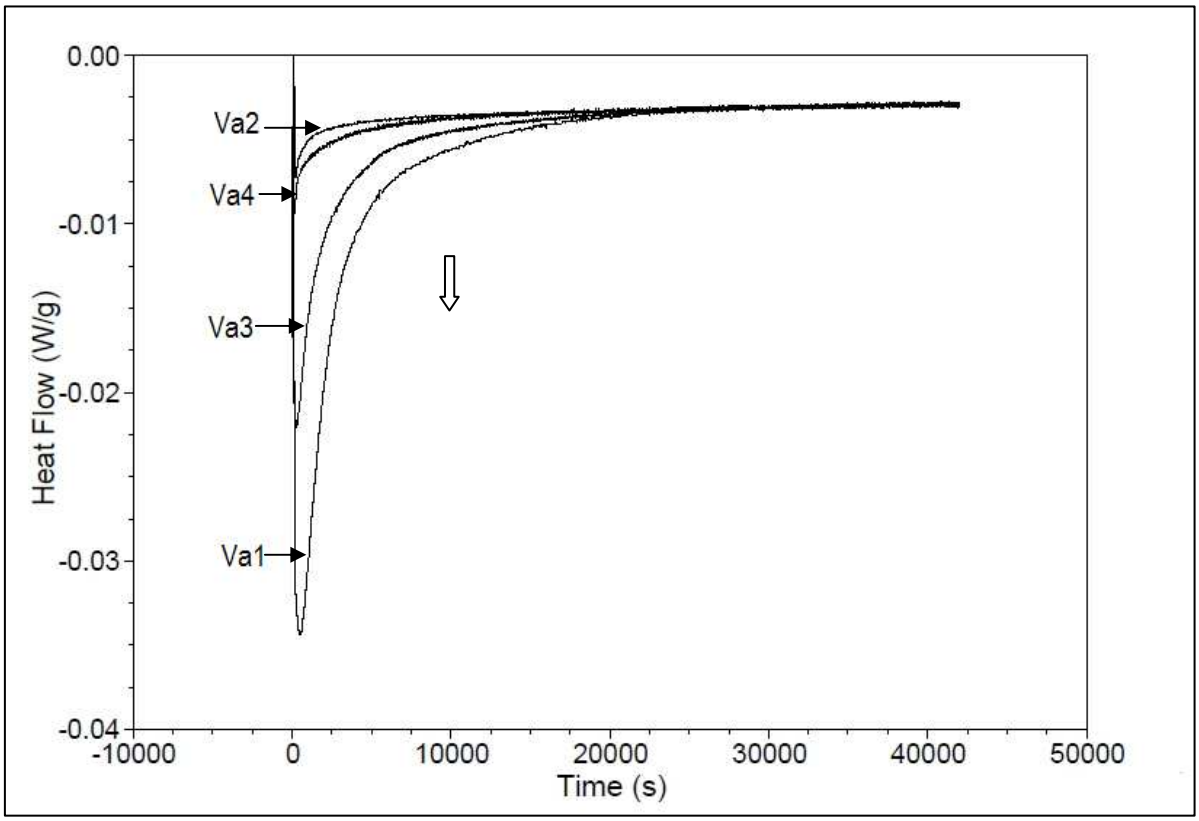

Figure 27: Isothermal (90°C) DSC curves of the different ashes at Na_2O/Al_2O_3 of 1.50

After isothermal (90°C) measurements, the samples were heated at 240°C and some residual reaction heats were found upon heating. The values of these reaction heats were 3J/ g for Va1 and Va3 versus 9 and 21 J/g for Va4 and Va2 respectively, following the trend of more residual reaction heat for the less amorphous materials.

It is also worth pointing out that the lowest NaOH concentration resulted in the lowest peak temperature for all the samples (Figure 28) in contrast to what would have been expected for a completely amorphous metakaolinite material (Rahier et al., 1997). This trend is also likely to arise from the amorphous to semicrystalline character of the ashes, increasing NaOH concentration leading to an increase of the crystalline part of the ash taking part to the reactions. Therefore, the shift of the peacks max to higher temperatures is suggested to be linked to the slower dissolution of the crystallines phases in the reaction mixture, only limited amount of these phases being involved in the reactions when NaOH concentration is low.

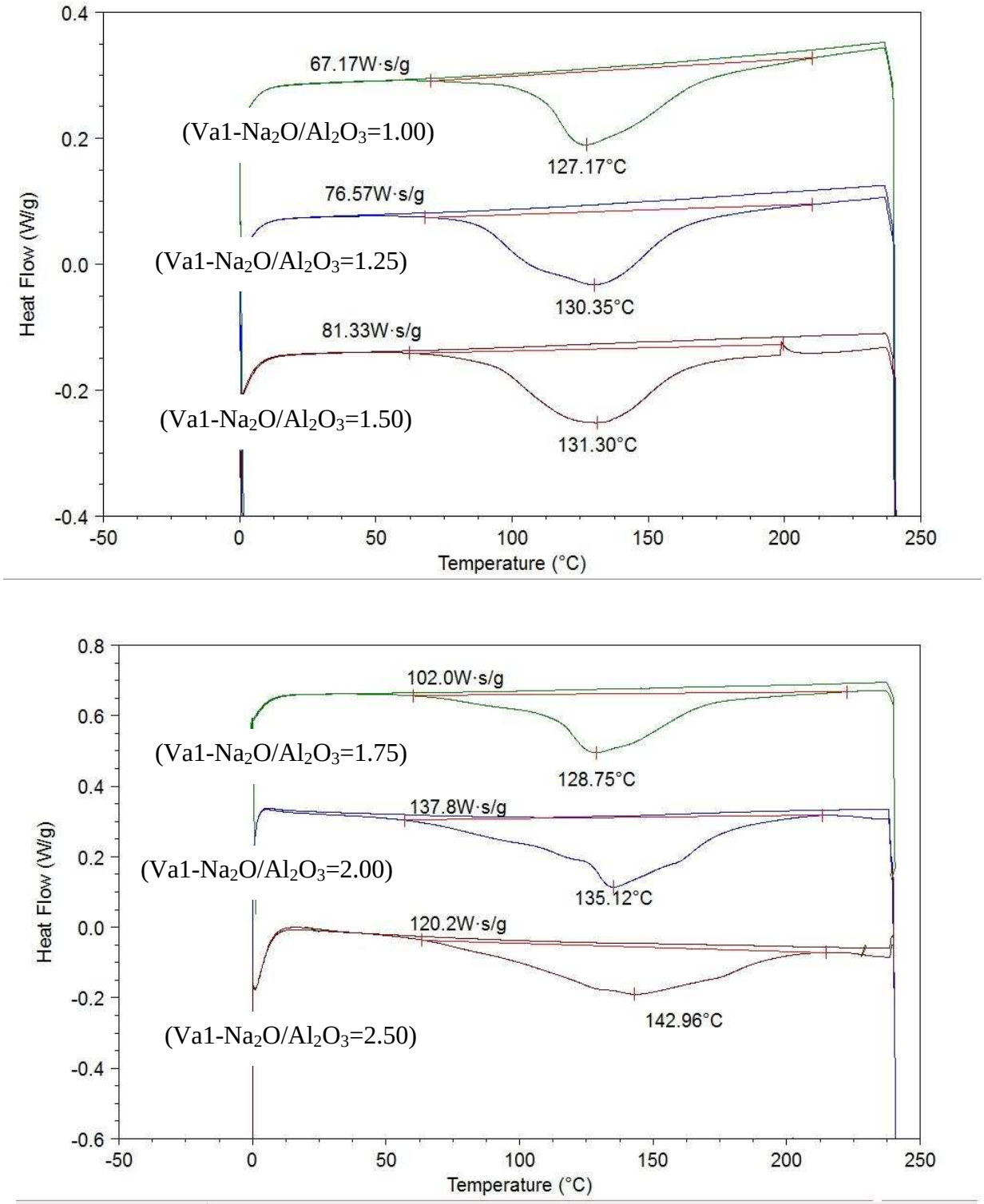

Figure 28: DSC thermograms showing the trend on reaction heats and the shift of peak max while increasing the concentration of the activating solution (Va1 sample)

III-1-3 : Infrared spectra

The infrared spectra presented in Figure 29 showed a broad absorbance at 820 -1250 $cm^{-1}$and 480-600 cm^{-1} assigned to internal vibration of Si-O-Si and Si-O-Al (Davidovits, 2008) in both raw volcanic ash and resulting inorganic polymer samples. The appearance of some sharp bands indicates the formation of crystalline phases. The band around 1640 cm-1 arises from water molecules, which are surface absorbed or entrapped in the large cavities of the polymeric framework, while the band around 1430 cm-1 is attributed to stretching vibrations of the O–C–O bond resulting from the atmospheric carbonation of the unreacted high alkaline aqueous phase, which is diffused on the geopolymeric materials surface (Dimitrios et al. 2007). These two later bands were not present in the pure ash and were the main difference between its spectra and those of synthesized products.

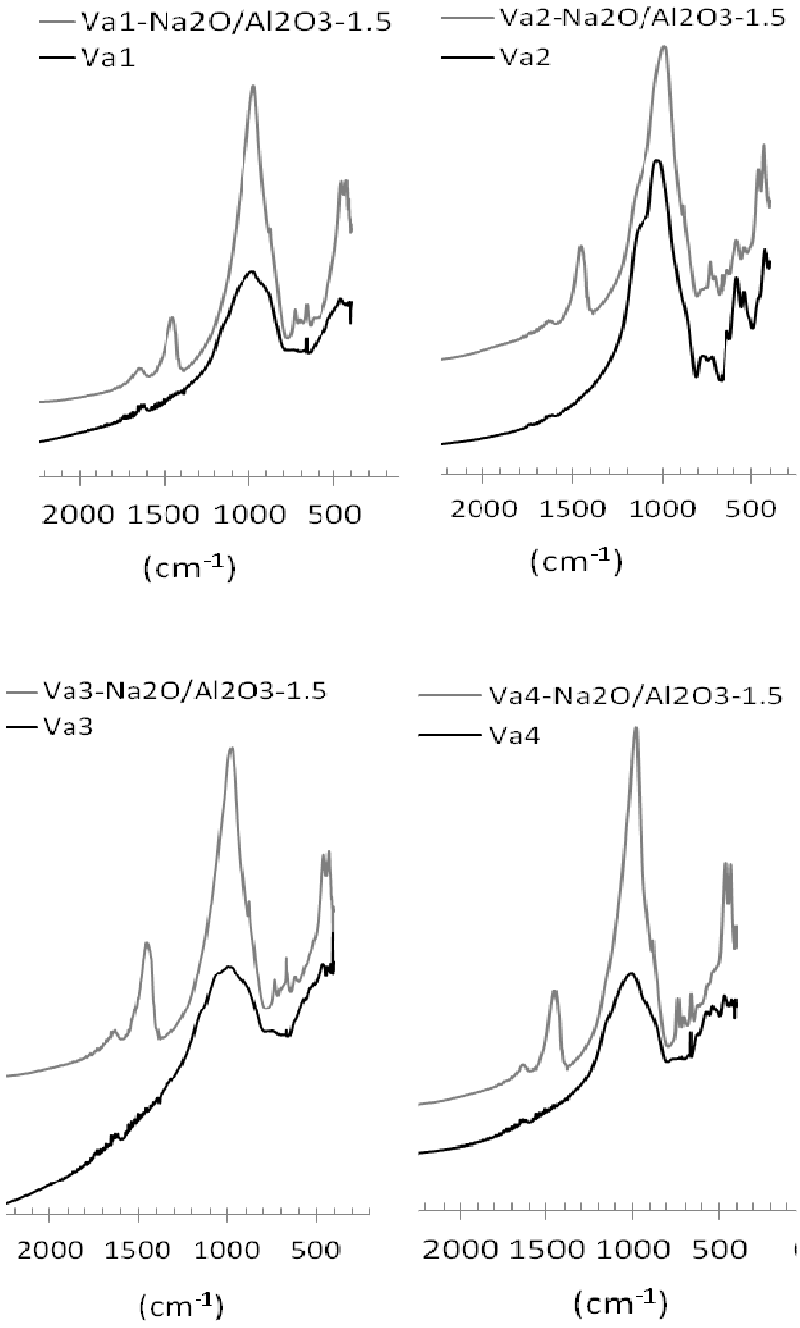

Figure 29: IR spectra of pure (bottom) and reacted ashes at Na_2O/Al_2O_3 of 1.50

III-1-4 : Microstructure

The microstructural analysis of polished products shows that the particle dissolution is not completed during the reaction (Figure 30).

A)

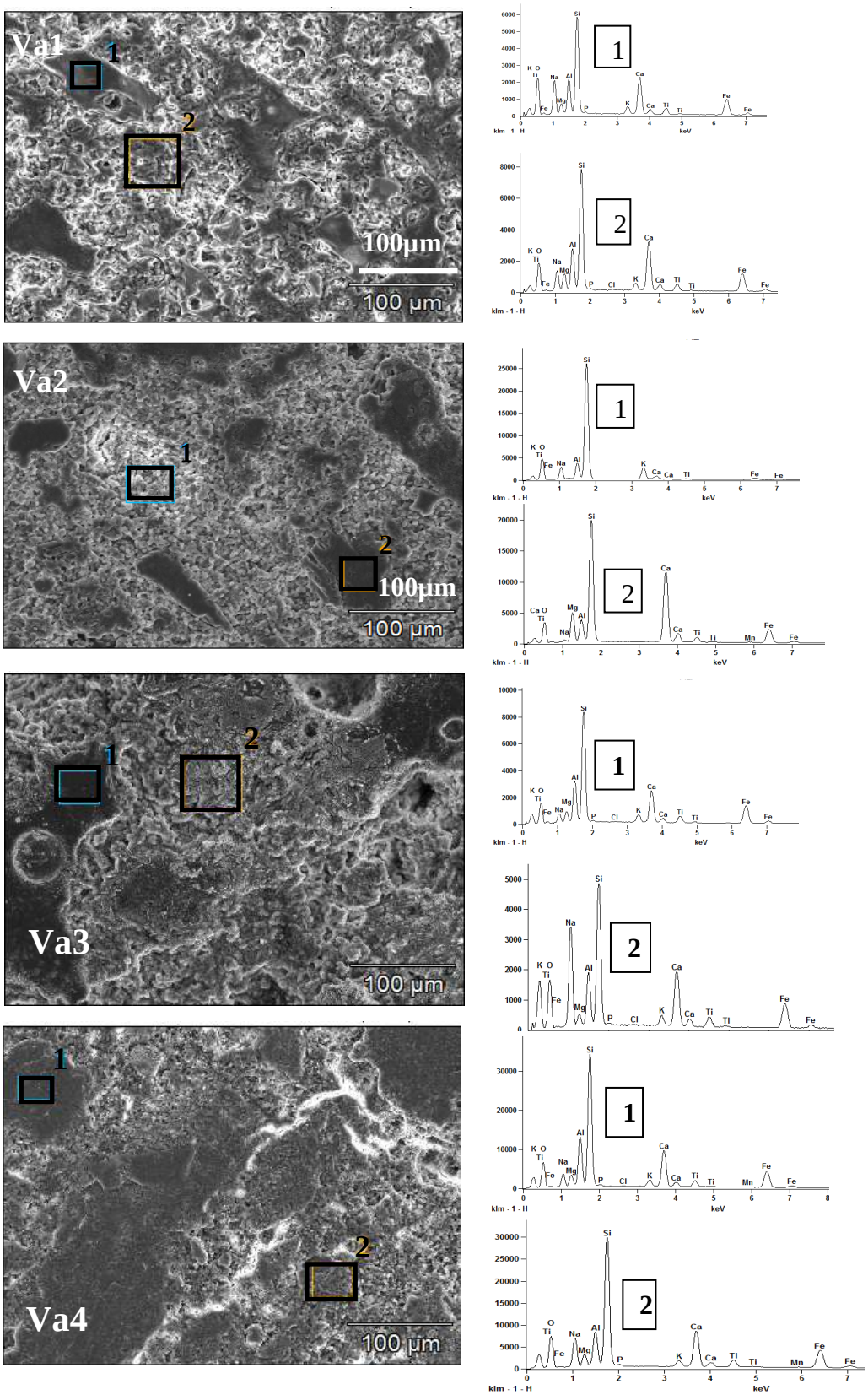

B)

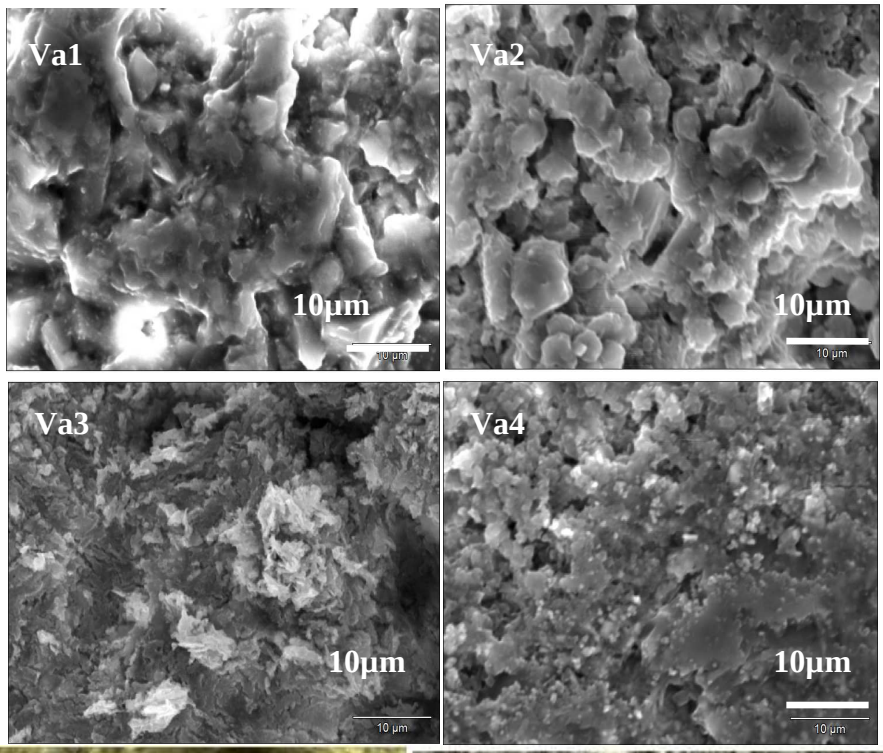

C)

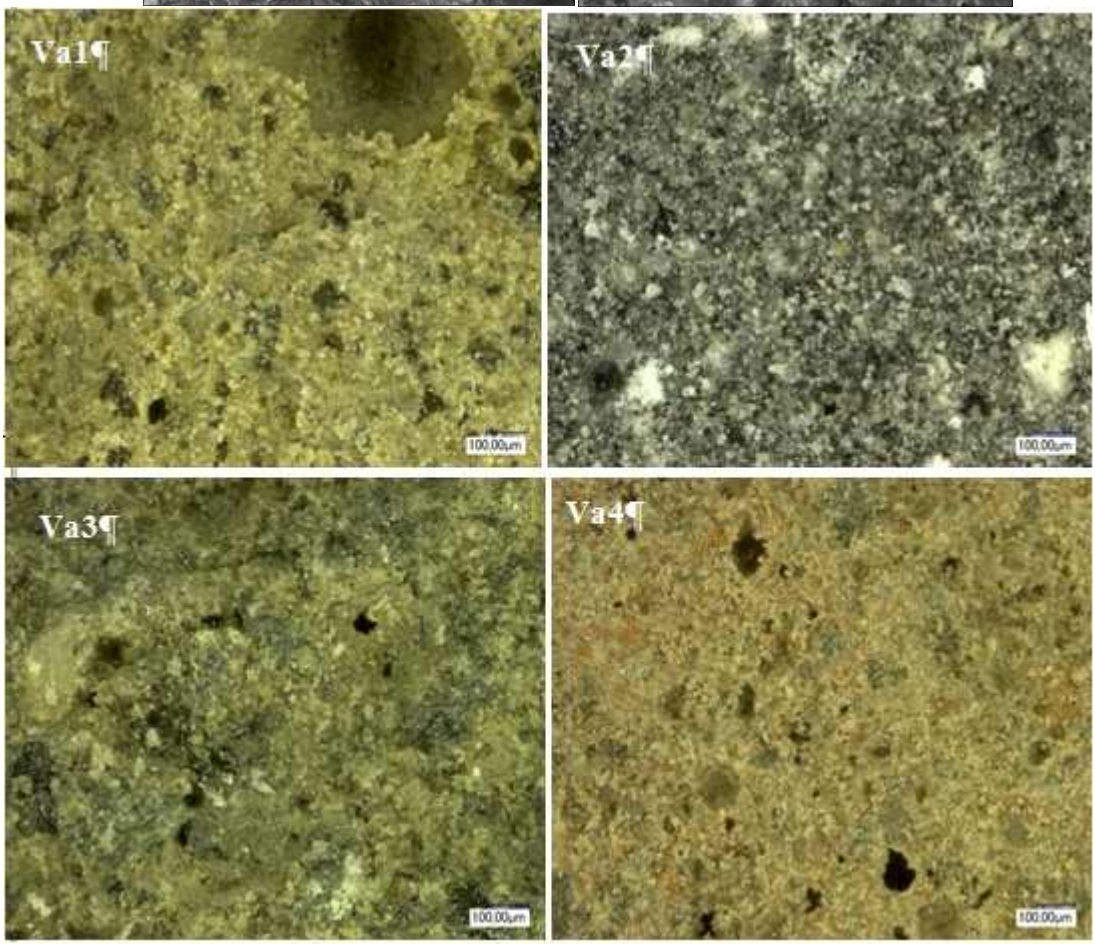

Figure 30: Microstructure of synthesized products at Na_2O/Al_2O_3 of 1.5: *A) 250 magnification, showing area of geopolymer matrix and undisolved particles; B) 2000 magnification; C) 250 magnification viewed with optical microscope*

Relicts of ash particles were found to be surrounded by the geopolymer matrix. The morphologies of all the samples were similar at lower magnification. However, higher magnification presented a mixture of lath shaped and agglomerate morphology with a great tendency for agglomeration for Va2 and Va4, possibly suggesting a more crystalline character. Geopolymers are known to contain amounts of unreacted solid aluminosilicate source (Duxson et al., 2005a; Schmucker and MacKenzie, 2005). However, there is no definitive and accurate method for quantitatively determining the amount of unreacted materials in a particular specimen. The unreacted material is also expected to affect the mechanical properties (Duxson et al., 2005a). The geopolymer matrix was the only part of the sample to contain added sodium, and was found by EDS in the area selected to correspond to the atomic composition of Al _ 5 at.%, Si _ 13 at.%, Na _13 at.% for Va1; Al _ 3 at.%, Si _ 25 at.%, Na _8 at.% for Va2; Al _ 5 at.%, Si _ 15 at.%, Na _25 at.% for Va3; Al _ 5 at.%, Si _ 18 at.%, Na _12 at.% for Va4. The high atomic concentration of sodium in the geopolymer matrix on the area selected for specimen Va3 could arise from its migration due to atmospheric conditions. The fluctuations observed in the geoplymer matrix compositions may be due to the presence of some small residual undisolved particles with different chemical composition. However, the composition of the matrix may be different as the.composition of the reactive part of the volcanic ash can be different.

Optical microscopy showed a typical difference in color on the samples from the different ashes. Some isolated pores of few microns were also observed on all the samples. Specimens of synthesized samples from all the ashes at Na_2O/Al_2O_3 of 1.5 are presented in photo 7, showing not great change in color between the pure ashes and their resulting products.

Photo 7: Specimens of synthesized samples from all the ashes at Na_2O/Al_2O_3 of 1.5

III-1-5 : Thermal behavior (TG/DTA)

The thermal behavior of synthesized products assessed by thermogravymetry analysis and differential thermal analysis are presented in Figure 31. The pure ashes show almost no weight loss up to 1000°C (less than 1 w%) (Figure 31_A). Some baseline fluctuations are observed in the curves.

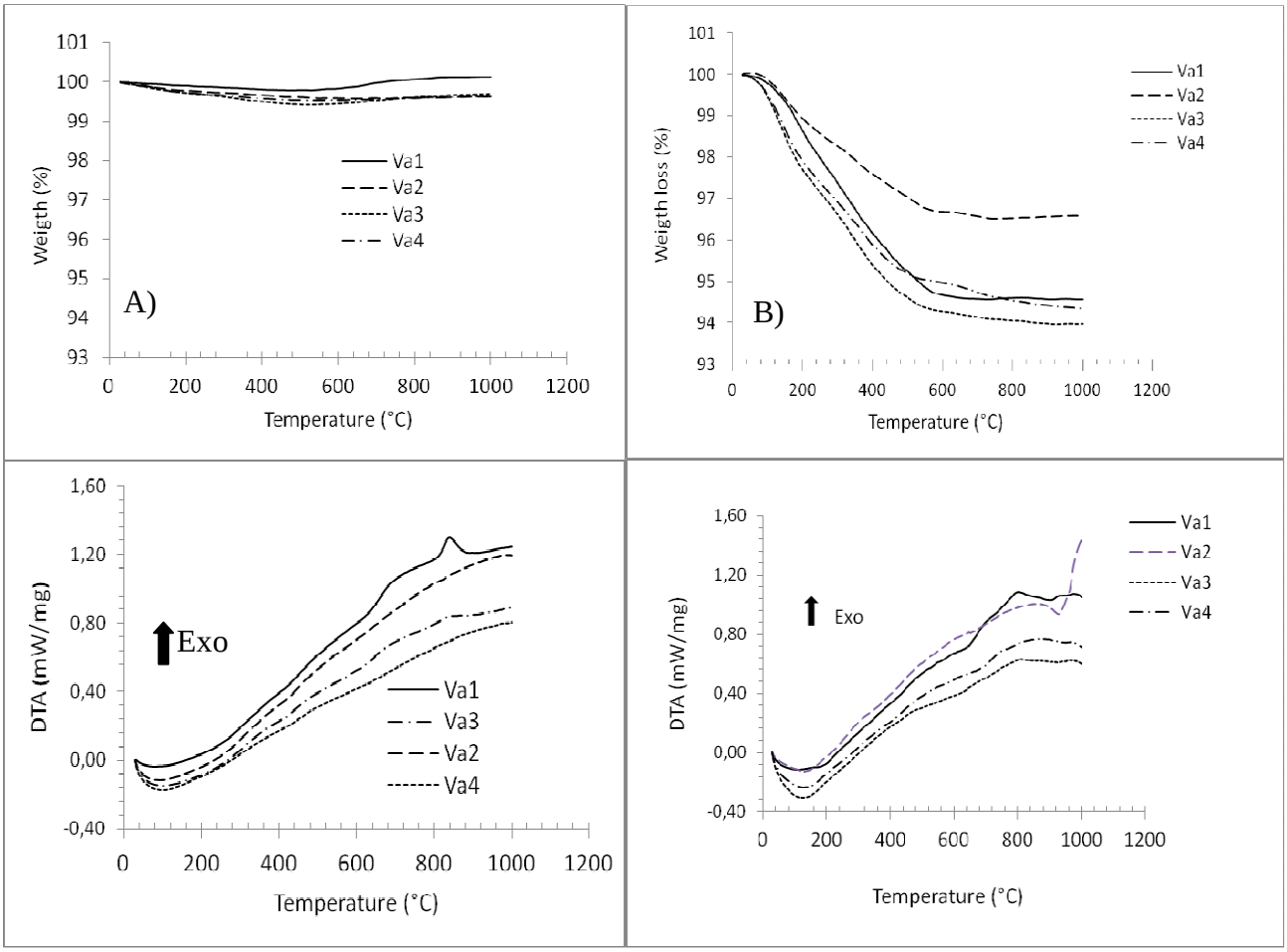

Figure 31: TG/DTA curves of A) the volcanic ashes, B) the geopolymers

For all the geopolymers, the DTA and the TGA curves are more or less similar. It is observed that the weight losses are between 3.5 and 6 %. Sample Va2 presented the lowest weight loss (around 3.5%), possibly in consistence with its small reactivity observed in the DSC analysis, those of the other ashes being between 5.5 and 6%. On the DTA curves, the endothermic reaction observed below 200°C is attributed to the loss of residual water after the curing

period. After this temperature, no clear endothermic reaction is observed up to 1000°C either in pure ashes or synthesized products. After 200°C, all the samples were found to lose weight at a more or less constant rate up to 600°C, above which the weight loss becomes negligible up to 1000°C. Between 200°C and 600°C, the weight loss is likely to arise from the destruction of some OH groups in the products matrix since the loss on ignition was negligible for all the pure ashes. The weight losses of all the synthesized specimens are about four times smaller than those reported (about 25%) for metakaolin based geopolymer (Bell et al., 2009b, Rahier et al., 1996b) after heating up to 1000°C, suggesting somewhat a higher thermal stability of the synthesized materials. However, these products were already dried in the furnace at 90°C during the curing, with a residual synthesis water of about 3% of the specimen mass (see drying curve in annexe 1) while the products from metakaolin resulted from a curing at 50°C (Bell et al., 2009b) or at room temperature (Rahier et al., 1996b).

III-1-6: ^{57}Fe Mössbauer analyses

Va1 and Va3 were selected for Mössbauer spectroscopy analyses. The data has been fitted to three quadrupole doublets consistent with Hyperfine Splitting Fe(II) (red lines) and Fe(III) (blue lines) (Figure 32). The interest of studying iron behavior in ceramic or geopolymerisation processes relies on the fact that this element is commonly found as impurities at various percentages in natural aluminosilicate materials and even some industrials by-products such as fly ashes which can be used as raw materials for the processes above-mentioned (J.Y.Y. Andji et al., 2009; E.I. Diaz et al., 2010). The role of iron in geopolymerisation has been subjected to some controversies, probably linked to the nature of the initial components in the geopolymer mixtures. Iron was suggested to be able to inhibit geopolymerisation reaction (Provis, 2006) but was also suggested to possibly contribute to geopolymer formation by integrating the network (Perera et al., 2007). In our case, the weight percentages of iron assimilated to Fe_2O_3 during chemical analysis by X-ray fluorescence are 12 and 14% for Va1 and Va3 respectively.

The ^{57}Fe Mössbauer spectra of the two ashes, before and after alkali activation, are shown in Figure 32 and the corresponding Mössbauer parameters (quadrupole splitting (ΔEQ), isomer shift (δ) and line width (ΓL=R) are tabulated in Table 7. The spectra of both ashes before reaction with alkali are remarkably similar, and can be fitted to two Fe^{2+} quadrupole doublets and one Fe^{3+} doublet. Since both these ashes were shown by XRD to contain the two

crystalline iron-bearing minerals ferroan forsterite and augite, the Mössbauer spectra should also reflect their presence. Ferroan forsterite is a member of the olivine group in which the Fe^{2+} is in octahedral coordination in two sites that are not always distinguished by Mössbauer spectroscopy (Greenwood and Gibb, 1971) . The quadrupole splitting ΔEQ of site A in the present spectra is within the range of reported values for the olivines (2.80-3.02 $mm.s^{-1}$) (Bancroft et al., 1967) and this assignment is also supported by the isomer shift δ which is close to the reported range (1.16-1.18 $mm.s^{-1}$). By contrast, augite is a member of the pyroxene group, in which the single-stranded silicate chains are cross-linked by 6-fold coordinated cations (Greenwood and Gibb, 1971).

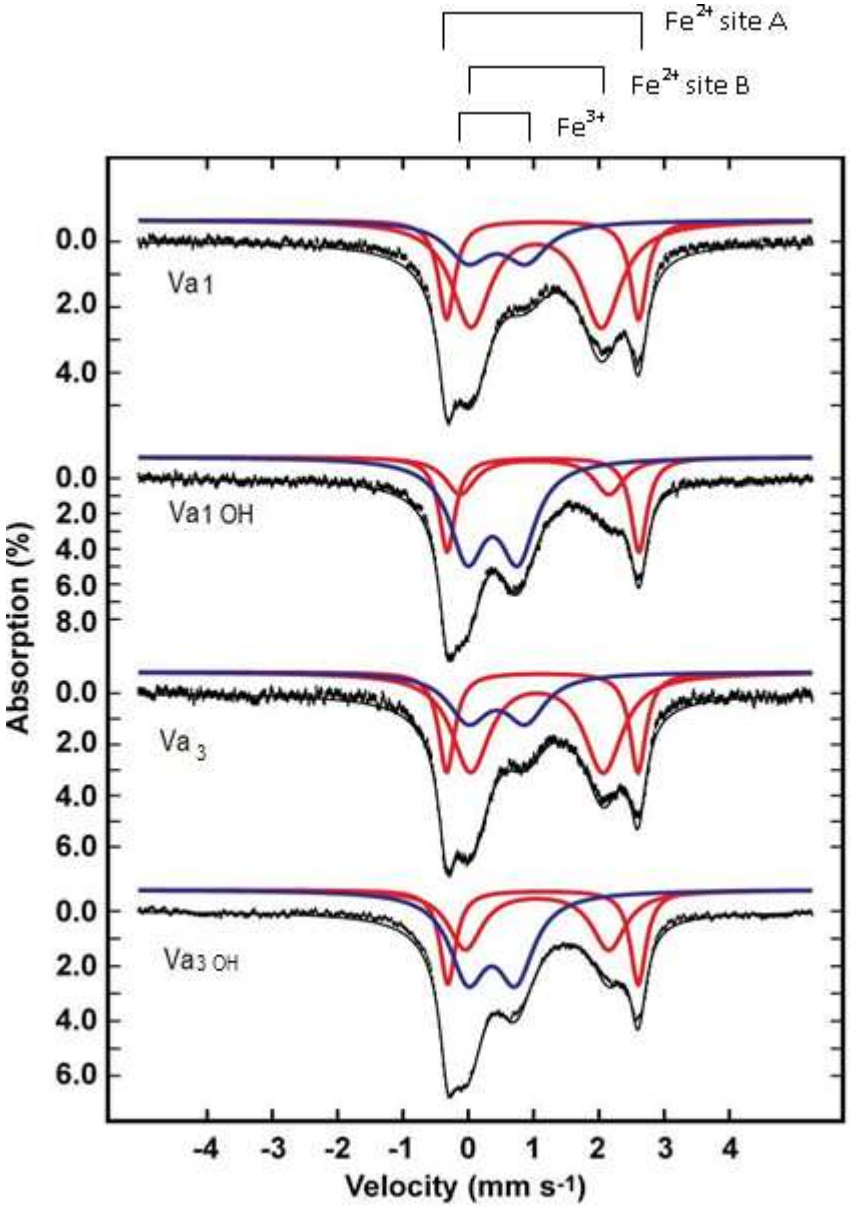

Figure 32: ^{57}Fe Mössbauer spectra of ashes (Va1 and Va3) before and after treatment with sodium hydroxide.

Table 7: ^{57}Fe Mössbauer parameters of ashes (Va1 and Va3) before and after treatment with sodium hydroxide.

Sample	Species	δ / mm s^{-1}	ΔE_Q / mm s^{-1}	$\Gamma_{L=R}$ / mm s^{-1}	I / %
Va1	Fe(II) A	1.14	2.94	0.31	23
	Fe(II) B	1.04	2.00	0.73	55
	Fe(III)	0.44	0.89	0.79	22
Va1 OH	Fe(II) A	1.15	2.94	0.30	24
	Fe(II) B	1.08	2.28	0.56	17
	Fe(III)	0.37	0.77	0.66	52
Va3	Fe(II) A	1.13	2.93	0.30	22
	Fe(II) B	1.05	2.03	0.71	50
	Fe(III)	0.44	0.88	0.74	25
Va3 OH	Fe(II) A	1.15	2.92	0.30	22
	Fe(II) B	1.05	2.20	0.63	29
	Fe(III)	0.36	0.73	0.68	44

Since the quadrupole splitting is sensitive to the degree of distortion from octahedral symmetry, less distorted sites, as in forsterite, showing larger quadrupole splittings (Bancroft et al., 1967), the more distorted octahedral Fe^{2+} site with the smaller quadrupole splitting is assigned to augite; this is also consistent with the reported Mössbauer parameters for this group of minerals (ΔEQ = 1.91-2.69 mm.s^{-1}, δ = 1.12-1.18 mm.s^{-1}) (Bancroft et al., 1967) . The Fe^{2+} doublet B assigned to augite is also significantly broader than that of the ferroan forsterite doublet A (Table 7). Augite contains two 6-fold coordinated Fe^{2+} sites which can however only be visually distinguished at much higher iron contents than in the present ashes (Greenwood and Gibb, 1971) and the overlap of these two sites could explain the broadness of this doublet. The intensity ratios of these doublets are also very similar in unreacted Va1 and Va3 (Table 7), but the intensity of doublet B (augite) is more than twice that of doublet A (forsterite), suggesting that the former is the principal iron-containing species in these ashes.

Both ashes contain a third doublet with Mössbauer parameters consistent with Fe^{3+} (ΔEQ = 0.89 mm.s^{-1}, δ = 0.44 mm.s^{-1}). Assignment of the ferric site to a particular phase is somewhat problematical. Ferric sites are known to exist in the silicate minerals of the garnet and epidote groups, but neither of these minerals was seen in the XRD traces, and their reported Mössbauer parameters (Greenwood and Gibb, 1971) are significantly different from the present parameters. Recalculation of the precise formula of the present augite suggests it contains a small amount of Fe(III), the resulting formula being $CaMg_{0.74}Fe(II)_{0.23}$ $Fe(III)_{0.02}$,

giving an atomic ratio FeIII/FeII of 0.086. This ratio is too small to explain the Fe(III) in the present Mössbauer spectra as arising from the augite. A further possibility is that the ferric iron resides in the amorphous phase shown to be present by the bulge in the background of the XRD traces. The absence of magnetic sextets in all of the spectra rules out most of the iron oxides and oxyhydroxides, although this is dependent on the size of the particles and temperature at which they were formed (Rossano et al., 2008; Spiering and Seifert 1985). A quadrupole doublet with reasonably similar parameters ($\Delta EQ = 0.69$ mm $.s^{-1}$, $\delta = 0.35$ mm $.s^{-1}$) reported for a metakaolinite based geopolymer treated with ferric nitrate solution (Perera et al., 2007) was suggested to be associated with some unspecified poorly crystalline ferric oxyhydroxide. Ferric doublets have been reported for nanophase ferric oxide particles, poorly crystalline ferric oxyhydroxides, Fe-bearing glasses, pyroxenes, orthopyroxenes and clinopyroxenes (Perera et al., 2007; Bancroft et al., 1967, 1968; Rossano et al., 2008; Mysen, 2006, Spiering and Seifert 1985; Van Cromphaut et al., 2007; Akasaka, 1983; Thompson et al., 2011), although the parameters of none of these species conform exactly to the present ferric doublet. The poorly crystalline character of the Fe(III) and Fe(II) site B is evidenced by the relatively broader linewidths of these doublets by comparison with Fe(II) site A (Table 7), supporting the association of the ferric sites with the amorphous component of the ashes and a relative poor crystalline character of augite comparatively to ferroan forsterite.

Upon conversion of the ashes to geopolymers by alkali activation, the Mössbauer parameters of Fe(II) site A, assigned to ferroan forsterite, remain unchanged in both ashes, indicating that this mineral is a spectator phase and takes no part in the in geopolymer-forming reaction. By contrast, a significant proportion of the Fe(II) site B, corresponding to augite, is oxidized to Fe(III) (Figure 32 and Table 7), shown by the 38% decrease in the intensity of the Fe(II) site B of sample Va1 with a concomitant 30% increase in Fe(III). A similar phenomenon is observed in sample Va3 in which the Fe(II) site B decreases by 21% while the Fe(III) site intensity increases by 19%.

These results, and the changes in the Mössbauer parameters of the Fe(II) site B and Fe(III) sites upon reaction with alkali indicate that some of the octahedral ferrous sites in the augite phase of the original ashes are taking part in geopolymer formation, but although the parameters of the Fe(II) sites in augite are slightly changed after reaction with the alkali, they are still consistent with ferrous iron in octahedral sites (Spiering and Seifert 1985; Bancroft et al., 1968), albeit less distorted than in the unreacted ash. By contrast, the Mössbauer parameters of the newly-formed Fe(III) sites are somewhat different from those of the ferric sites in the original ashes, showing a decrease in the isomer shifts and an increase in the

quadrupole splitting (Table 7). The room temperature isomer shifts of tetrahedral Fe^{3+} are reported to fall near or below 0.3 mm $.s^{-1}$, whereas the isomer shifts of octahedral Fe^{3+} occur above about 0.4 mm $.s^{-1}$ (Bancroft et al., 1967; Mysen, 2006). Thus, after alkali activation, the isomer shifts suggest a change in the Fe^{3+} coordination from 6- fold to distorted sites approaching tetrahedral coordination. These distorted sites are also similar to 5-fold coordinated sites, the reported parameters of which ($\Delta EQ = 0.74$ mm.s^{-1}, $\delta = 0.36$ mm.s^{-1}) (Rossano et al., 2008) are very similar to the present Fe(III) sites.

To summarize the Mössbauer results, one of the two crystalline Fe^{2+} -bearing mineral phases present in the original ashes, ferroan forsterite, does not participate in or interfere with the geopolymer-forming reaction, but a significant proportion of the augite present reacts with alkali to form new ferric sites with Mössbauer parameters similar to distorted tetrahedral or 5-fold coordinated sites which are most likely to be located in an X-ray amorphous noncrystalline phase. This suggests the possible inclusion of iron in the tetrahedral network of the geopolymer product. However, in the case of effective inclusion of iron in the amorphous geopolymer network, its tetrahedral coordination would be more likely for a simplistic chemical charge-balancing point of view. This possible inclusion could also explain the development of strength beyond the NaO_2/Al_2O_3 ratio of 1. On the other hand, the fact that iron site B (from forsterite ferroan) remained unaffected by alkali-activation of the ashes means that the behavior of iron during alkali activation of aluminosilicates relies on its chemical and mineralogical state in the starting materials.

III-1-7: Compressive strength

All the formulations developed strength during the curing period, but still some efflorescence was observable on specimens with high Na content on all the ashes and mostly for Va2 and Va3. The seven days' compressive strengths are presented on Figure 33. The values of dry compressive strength were between 42-61 MPa and 27-63 MPa for products resulting from Va1 and Va2 respectively. For specimens resulting from Va3 and Va4, these values were in the range of 16-32 MPa and 14-37 MPa respectively. It was observed that these values decreased after immersion of the samples overnight in water (wet compressive strength) but the strength was partly or totally recovered when the samples were dried overnight at 90°C.

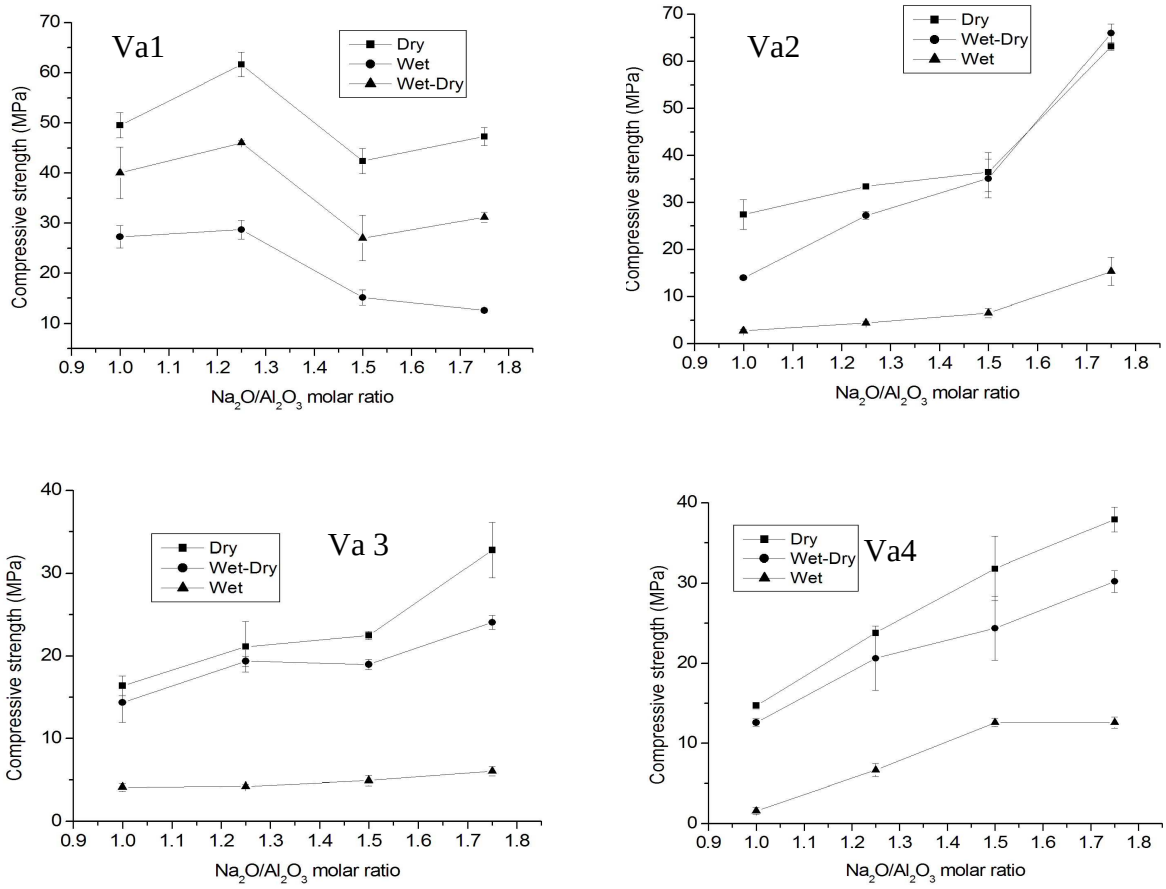

Figure 33: Compressive strength of reacted ashes cured for 7 days at 90°C

The decrease from the dry to the wet strength were about 50% for the Va1, but were much more significant for the other samples (about 75% for Va3, moving to 89% for Va2 and Va4 at lowest NaOH concentration). It is well known that this behavior is linked to the hydration of some Si-O-Si bonds to Si-OH bonds in the geopolymer matrix, leading to weakening the structure. It is also possible that some soluble components are formed such as sodium silicate, giving a good dry strength but a very low wet strength. Specimens from sample Va1 presented the best wet strengths, with values in the range of 12-28 MPa. The other specimens presented values of wet strength in the range of 1-15MPa, suggesting their possible higher content in soluble silicate compounds compared with specimens resulting from Va1. For all the specimens, the wet-dry compressive strengths were in the range 12-65 MPa.

Looking at the chemical composition of the different ashes, it is observed that the ratio Al_2O_3/SiO_2 is between 4.57 and 4.86 for Va1, Va3 and Va4, versus 5.97 for Va2. The optimum value of SiO_2/Al_2O_3 for geopolymer was reported to vary from 3.3-4.5 (Komnitsas

and Zaharaki, 2007), with some possible fluctuation since the amount of Si and Al available for geopolymer formation can be very different depending on the composition and especially the reactivity of the starting raw materials (De Silva et al., 2007). Considering the lower reaction heat and lower reactivity (the highest temperature of peak max on DSC curves (Figure 24) observed for sample Va2, it is likely that this sample presented some excess of SiO_2.

Increasing the amount of NaOH to the system leads to an increase of the final strength up to a maximum value with Na_2O/Al_2O_3 of 1.25 for Va1, following the trend observed in a previous report on metakaolin and volcanic ash based geopolymer (Lemougna et al., 2011; Ruscher et al., 2010). It was also observed on the specimens resulting from this particular ash (Va1) that excess NaOH leads to crack formation on the specimens, the size of cracks increasing with NaOH addition. Such an optimum is not observed for the other ashes that show an increase of the strength with added NaOH in the range of our study (Na_2O/Al_2O_3 of 1.00-1.75). For the highest amounts added, an excess of unreacted NaOH materialized by white efflorescence was visible on samples resulting from Na_2O/Al_2O_3 of 1.75. This means that the reaction was not completed.

The difference in reactivity and mechanical behavior of the present ashes could be linked to the type and amount of crystalline phases over the amorphous phase in the starting materials as will be done in the next part. For Va1 ash, we have more amorphous reactive phase that dissolves quickly in alkaline medium and is free to react; the effect of excess NaOH on the strength reduction being observable from Na_2O/Al_2O_3 of 1.50 on. That is different for the other ashes where we have a smaller amorphous fraction, and where increasing the NaOH content probably also has as major effect on the dissolution of the amount of crystalline phases, increasing the amount of reacting materials and the final strength. Therefore, the higher value of dry strength observed for Va2 is much more linked to its mineralogical composition since the reaction heat remains very low.

The trend observed on the values of wet strength at lowest NaOH concentration are in line with the amount of amorphous phase in the starting materials and the sample that globally presented the best strengths also resulted from the more amorphous starting material (Va1). For the higher concentrations of sodium hydroxide the correlation between the amount of amorphous phase in the starting materials and the final strength after 7 days curing is less obvious.

Looking at the percentage of iron on the samples analysed by Mössbauer spectroscopy (12 wt % and 14 wt % in Va1 and Va3 respectively) (Table 7), we can say that these percentages are qualitatively consistent with the view that the presence of iron interferes with the development of strength, but the difference in iron content between Va1 and Va3 is insufficient to explain the much greater strength developed by the latter at all alkali concentrations. This suggests the operation of other factors such as the chemical and mineralogical form of the iron, the particle size distribution and proportion of amorphous phases in the ashes which influence their reactivity. These results indicate that although the effect of iron on the geopolymer forming reaction is not very well understood at this stage, its presence in these concentrations does not mitigate against the development of adequate compressive strength.

In summary one can state that Va1 ash has the largest amount of amorphous reactive phase dissolving quickly, giving the largest reaction heat and best compressive strength. The effect of excess NaOH on the strength reduction is observable from Na_2O/Al_2O_3 of 1.50 on. All other ashes have a much smaller amorphous fraction, and increasing the NaOH content probably also increases the amount of crystalline phases dissolved, increasing the amount of reacting materials and thus the reaction heat and the final strength. It is however supposed that an excess of NaOH is needed to dissolve the crystals. Therefore, the relatively high value of dry strength observed for Va2 is probably more linked to its mineralogical composition since the reaction heat remains very low. The fact that the wet strength is very low indicates the formation of soluble reaction products.

III-I-8: Conclusion

The four ashes subjected to analysis were found to have great similarities in chemical compositions. However, the properties of geopolymers produced from these ashes are rather different. One parameter which greatly influenced the reactivity was found to be the amount of amorphous phase. The reactivity and the reaction heat of the systems increase with the amount of these amorphous phases in the starting ashes. The compressive strength was found to decrease after immersion of the specimens overnight in water, but was partly or totally recovered after overnight drying at 90°C. The dry compressive strength of synthesized products from all the ashes were in the range of 14-63 MPa suggesting their possible utilization as building materials.

Specimens from the most amorphous sample Va1 presented the best wet strengths, with values in the range of 12-28 MPa. The other specimens presented values of wet strength in the range of 1-15MPa. For all the specimens, the wet-dry compressive strengths were in the range 12-65 MPa. The wet strength at lowest NaOH concentration also increases with the amount of amorphous phase in the volcanic ashes and the sample that globally presented the best strengths also resulted from the more amorphous starting material (Va1). For the high NaOH concentrations no correlation between the amount of amorphous phase in the starting materials and the final strength could be established.

The Mossbauer spectroscopy analyses revealed that the behavior of iron during alkali activation of aluminosilicates relies on its chemical and mineralogical state in the starting materials.

The suitability of volcanic ashes for geopolymerization thus does not only depend on the chemical composition but mostly on the fraction of amorphous phase.

Due to the high content of iron in all the ashes (> 5%), it was not possible to check by NMR the coordination of Si and Al in the raw materials and the final products.

III-2: EFFECT OF THE ACTIVATING SOLUTION COMPOSITION ON THE STABILITY AND THERMOMECHANICAL PROPERTIES OF GEOPOLYMERS FROM Va1

Over the past two decades, extended works have been done on the influence of the composition of the activating solution on the reaction kinetics and product's properties of metakaolin and fly ash-based geopolymers (Rahier et al., 1997; Barbosa et al., 2000; Duxson et al., 2007, Nugteren, 2010). Very few studies have been reported on these parameters for volcanic ash based geopolymers, despite the huge potential availability of this raw material in several countries with past or present volcanism (Kamseu et al., 2007, Verdolotti, 2008; Kamseu et al., 2009).

The aim of this section was to investigate the influence of the activating solution's composition on the stability and thermomechanical properties of geopolymers made from Foumbot Petponoun's volcanic ash.

NaOH, KOH solutions and silicate solutions with low modulus were tested. The reactivity of the systems was studied with Differential Scanning Calorimetry. The resulting products were characterized by Scanning Electron Microscopy (SEM), Infrared spectroscopy (IR) and X-ray diffraction (XRD). The products stability was assessed by dry, wet and wet-dry compressive strength measurements. Thermogravimetric Analysis (TGA), Thermomechanical Analysis (TMA) and Dynamic Mechanical Analysis (DMA) were used to investigate the high temperature behavior of the different compositions.

III-2-1 : Reactivity of the mixtures

The chemical composition of the ash is presented in Table 8. The temperature of maximum reaction rate of all the mixtures and their DSC curves are presented in Table 9, Figure 34 and Figure 35.

Table 8: Chemical composition of volcanic ash (major elements)

Oxide	Fe_2O_3	MnO	TiO_2	CaO	K_2O	P_2O_5	SiO_2	Al_2O_3	MgO	Na_2O	SUM
Volcanic ash	12.7	0.2	2.9	11.3	1.7	0.9	43.2	15.1	6.8	4.5	99.3

Table 9: Temperature of maximum reaction rate and reaction heat of the different mixtures

Formulations	Va(<125 µm)-Na	Va-Na	Va-NaSil	Va-Na+K	Va-(Na+K)Sil	Va-K0.l8	Va-K	Va-KSil
Temperature of maximum reaction rate (°C)	131	134	146	145	175	187	190	178
Reaction enthalpy (W.s /g)	83	62	68	56	72	57	47	38

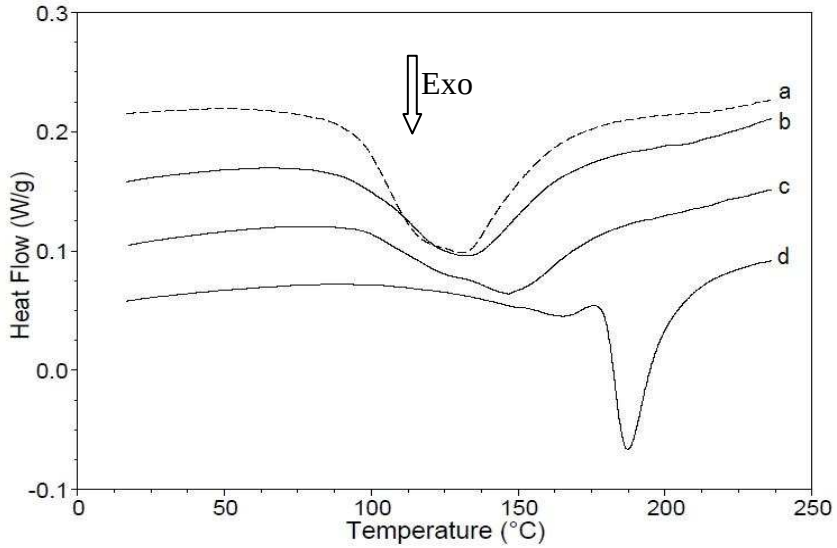

Figure 34 : DSC curves of mixtures without amorphous silica
c) Va(<125µm)-Na, b) Va-Na, c) Va-Na+K, d) Va-K. Curves are shifted for clearity.

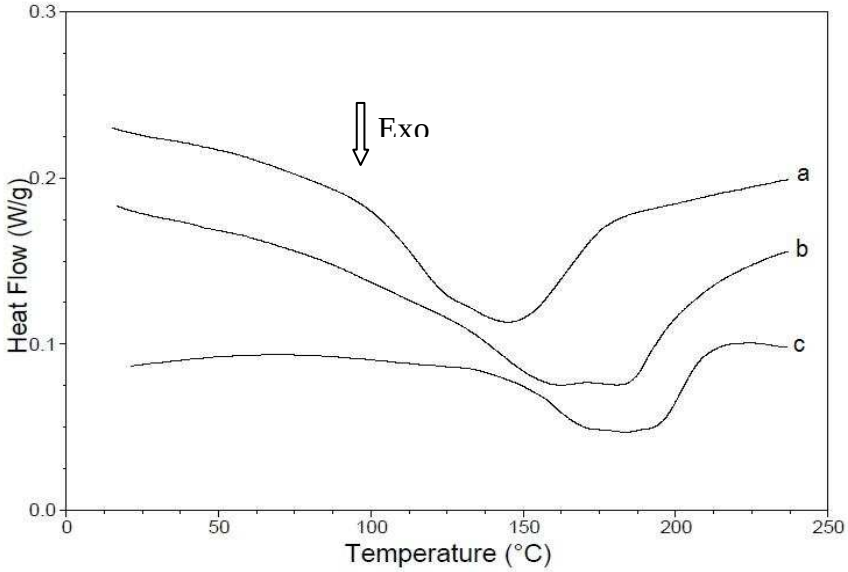

Figure 35: DSC curves of mixture with amorphous silica Va-NaSil b) Va-(Na+K)Sil, c) Va-KSil

The reaction occurs in several steps whichs becomes more clear if K is used as activator. It appears that NaOH solutions react faster than KOH with a maximum reaction rate at around 134°C versus 187°C for KOH for the same molar composition. This trend is in accordance with previous reports on inorganic polymers from metakaolin and silicate solutions (Rahier et al., 1997; 2007).The addition of amorphous silica in the mixture leaded to little delay of the reaction rate and broadens the DSC curves. Removing coarse particles (40 wt% of ash particle above 125µm) leads to an increase of reaction heat of about 30%, with a reduction of the temperature of maximum reaction rate with a couple of degrees while using sodium hydroxide as the alkaline activator (Figure 34 and Table 9). Reduction of 14% of water from the mixture also leaded to an increase of about 19 % of reaction heat, with a reduction of the temperature of maximum reaction rate for a couple of degrees while using potassium hydroxide as the alkaline activator (Table 9).The temperatures of the maximum reaction rate for all the mixtures are higher while the heats of reaction are smaller than those reported (Rahier et al., 1997; 2003) for inorganic polymer glasses resulting from alkaline activation of metakaolin. However the trends observed for water content and particle size influence are similar. Higher water content leading to lower viscosity was reported to increase the temperature of maximum reaction rate and favor sedimentation in the mixture, resulting to inhomogeneous sample of inorganic polymers from metakaolin (Rahier et al.,1997); meanwhile the reaction rate was found to increase with decreasing particle sizes, the heat flow signal being larger for smaller particles and reaching the baseline earlier (Rahier et al., 2003).

III-2-2 : Compressive strength

All the formulations developed strength during the curing period, but still some efflorescence was observable mostly on specimens with NaOH after a few days of exposure to the atmosphere. The seven and twenty one days' compressive strength are presented on Figure III-2-3 and Figure 36.

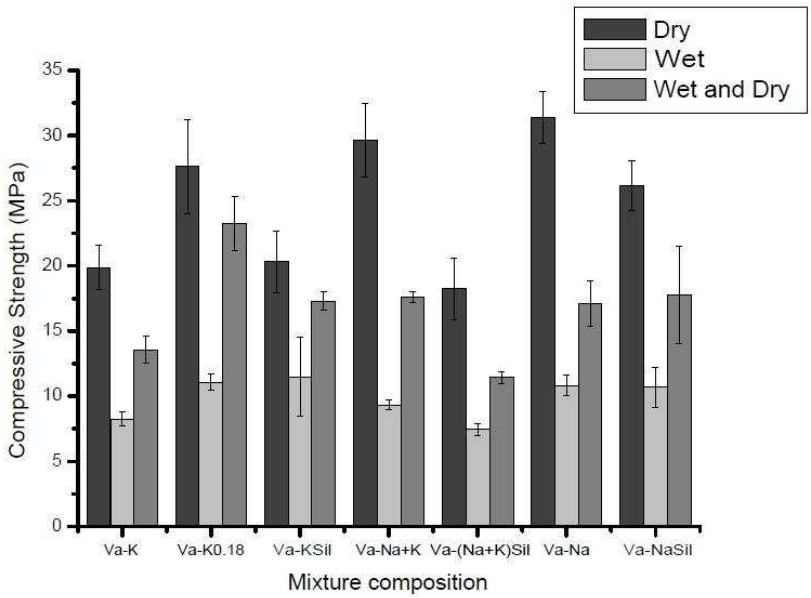

Figure 36: 7 days compressive strength of different compositions (Va-K, Va-K0.18, Va-KSil, Va-Na+K, Va-(Na+K)Sil, Va-Na, Va-NaSil) cured at 90°C

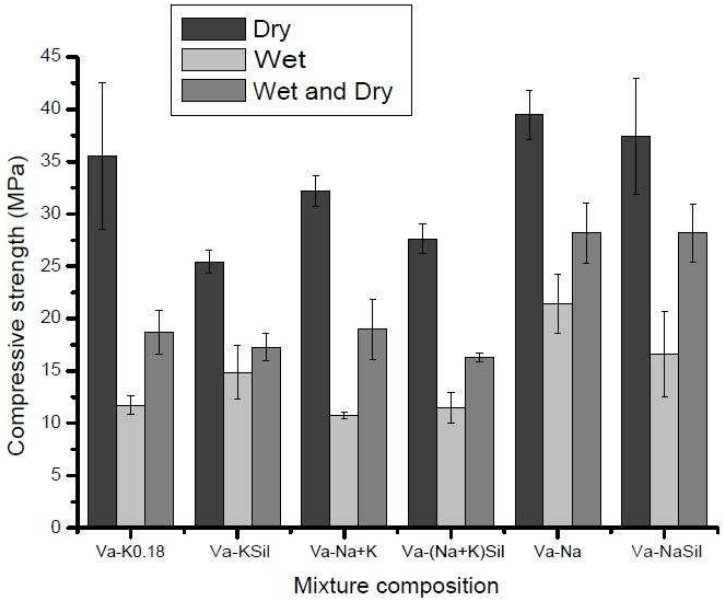

Figure 37: 21 days compressive strength of different compositions (Va-K, Va-K0.18, Va-KSil, Va-Na+K, Va-(Na+K)Sil, Va-Na, Va-NaSil) cured at 90°C

The values of dry compressive strength vary from about 20 to 30 MPa for seven days and 25 to 40 MPa for 21 days of curing. These values decrease after immersion of the samples over night (wet compressive strength) but the strength is partly recovered when the samples are dried at 40°C. It is well known that this behavior is linked to the hydration of some Si-O-Si bonds to Si-OH bonds in the geopolymer matrix, leading to weakening the structure. The values of wet compressive strength are around 10 MPa after seven days of curing, but increase with curing time up to about 20 MPa at 21 days for samples resulting from the best formulation (Va-Na). A long curing period leads to an increased strength development for all the mixtures, with an increase of about 25% for Va-Na (Figure 38) and 29% for Va-K0.18 (Figure 36 and Figure 37) .

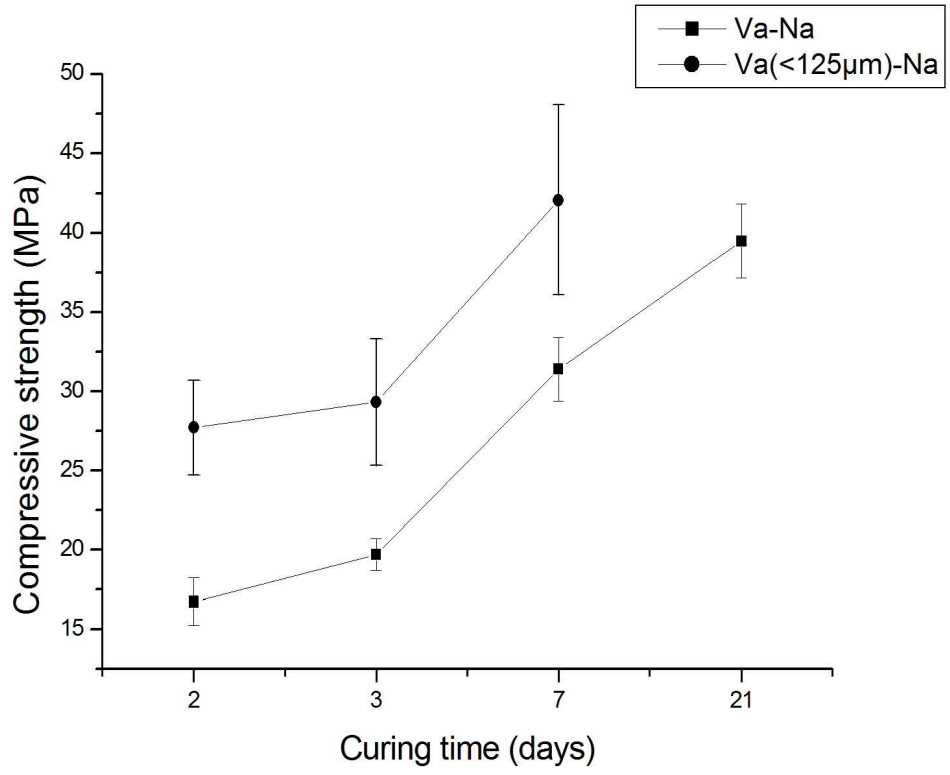

Figure 38: Influence of particle size on compressive strength development

The values of 7 days compressive strength for Va-Na specimens are below the maximum value of 55 MPa, reported in (Lemougna et al., 2011) for a similar sample (same deposit) with a molar composition NaO_2/SiO_2 of 0.3. As no significant change was observed on the chemical and mineralogical composition, it may be likely that the change on compressive strength could arise from the mould size effect, small cylindrical moulds used in the present

study being more sensitive to structural defects than bigger cubic moulds used in previous work (Lemougna et al., 2011). Some microcracks were also observable on specimens with potassium hydroxide suggesting the presence of some internal tensions during the curing period of these specimens. The origin of these cracks may be linked to incomplete reaction for K specimens (weaker structure, thus faster crack formation). Since the cure is not hermetically, these cracks may arise from the fact that during the curing period, the amount of water necessary for reaction became insufficient at a moment where there was still an important proportion of none reacted KOH and volcanic ash, This does not only hinder the mobility of ions in the matrix but also creates internal tensions.

Based on the mechanical tests only small differences between potassium, sodium and silicate solutions are observed. Taking into account the faster reaction with NaOH, a larger difference would be expected after 7 days. However, no great difference was observed up to 21 days. On the other hand the influence of particle size and water on specimens made with sodium and potassium hydroxide is much more obvious.

Improving the rheology of the mixture by reducing the water content as was done for the mixture with potassium hydroxide was found to increase reactivity and favor compressive strength development. This trend is in accordance with previous reports on the role of water in geopolymerisation (Rahier et al., 1996b; Barbosa et al.,2000; Zuhua et al., 2009). Excess water hinders the polycondensation reactions resulting in smaller reactivity (Rahier et al., 1996b; Zuhua et al., 2009) and may also dilute the reaction mixture or leach out the more soluble ions, transporting them away from the reaction zone (Barbosa et al., 2000). However, insufficient water leads to a bad wetting of the starting material resulting again in small reactivity (Rahier et al., 1996b). Water is therefore critical even in the final stages of geopolymerisation because it is needed as the transport medium and the polycondensation processes occur concomitantly with dissolution (Zuhua et al., 2009).

Reducing the amount of coarse particles in the starting ash has favored the development of compressive strength with an increase of about 33% after seven days curing of specimens made with NaOH (Figure 38). This is probably due to the relative increase of finer particles in the remaining ash leading to higher reactivity as was found by DSC measurements. The relatively smaller reactivity of un-sieved ash may be due to the limited mass transport of the coarser particles (smaller reactive surface) during the break down phase before the polymerization (Rahier et al., 2003).

Globaly, the NaOH solution seemed to lead to a better strength while adding amorphous silica in the system slightly reduced strength for most of the mixture. Theoretically, Si-O-Si

linkages are stronger than Si-O-Al and Al-O-Al bonds meaning that the strength of geopolymers should increase with Si/Al ratio since the density of Si-O-Si bonds increases with Si/Al ratio (Duxson et al., 2007). However, the coexistence of an aluminosilicate network and silicate chains in the right proportion and spatial distribution was found to maximize the mechanical strength of the geopolymer matrix (Ruscher et al., 2010). The optimum value of SiO_2/Al_2O_3 for geopolymer was reported to vary from 3.3-4.5 (Komnitsas and Zaharaki, 2007), but could still fluctuate since the amount of Si and Al available for geopolymer formation can be very different depending on the composition and especially the reactivity of the starting raw materials (De Silva et al., 2007). Some details on the atomic composition of the reacted and unreacted phase of the synthetised materials are presented in the microstructural analysis section presented below. Another reason for the lower mechanical strength could be the lower reaction rate, as illustrated before by DSC analysis.

There are some divergences with previous reports regarding the influence of alkaline ions, mostly potassium and sodium on the development of compressive strength (Duxson et al., 2007; Komnitsas and Zaharaki, 2007). Potassium ions appear to be responsible for a greater degree of condensation compared to sodium ions under the same conditions, being more basic, and promoting greater dissolution of silicates for a better strength (Komnitsas and Zaharaki, 2007). However, some authors also observed that the mechanical properties of geopolymers cured for 7 days are not seriously affected when specimens with different alkali (potassium or sodium) composition were used (Duxson et al., 2007).

For the current volcanic ash, considering the lower reaction rate and micro cracks developed on specimens containing potassium hydroxide, a better comparison of its influence versus sodium hydroxide on the final strength would request further investigation, taking into account various curing conditions and water/solid ratios. The photo 8 presents the specimens in immersion prior to wet compressive strength measurement.

Photo 8: Specimens (Va-K, Va-K0.18, Va-KSil, Va-Na+K, Va-(Na+K)Sil, Va-Na, Va-NaSil) in immersion prior to wet compressive strength measurement.

III-2-3 : X-Ray spectra

The X-ray spectra of the volcanic ash show a mixture of amorphous and crystalline phases made with Augite – (CaMg 0.74 Fe 0.25) Si_2O_6 , Anorthite sodian disordered, (Ca, Na)(Si, Al)$_4O_8$ and Forsterite, Mg_2SiO_4. These minerals did not completely dissolve during the reaction and were also observable in the reaction products. Some new crystalline phases were also found in the products: Sodalite, $Na_8Al_6Si_6O_{24}$ $(OH)_2(H_2O)_2$ and Natrite, Na_2CO_3 in the sample based on NaOH, and Potassium Aluminum Silicate Hydrate, $KAlSiO_4$-$1.5H_2O$ in the sample based on KOH (Figure 39).

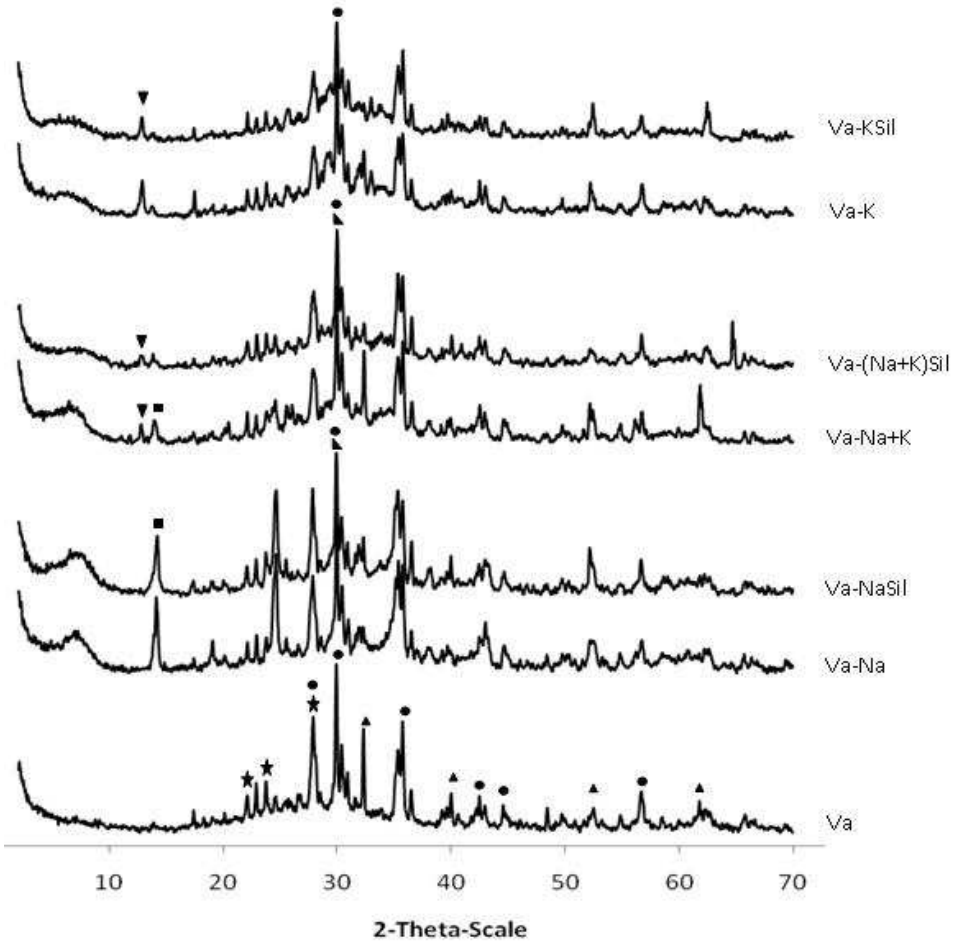

Figure 39: X-ray powder diffraction patterns of the volcanic ash starting material and resulting geopolymers composition (smoothed).
Key:
● = Augite – (CaMg 0.74 Fe 0.25) Si_2O_6
★ = Anorthite sodian disordered, (Ca, Na)(Si, Al)$_4O_8$
▲ = Forsterite ferroan: (Mg0.9Fe0.1)2SiO4
■ = Sodalite, $Na_8Al_6Si_6O_{24}$ $(OH)_2(H_2O)_2$
◣ = Natrite, Na_2CO_3
▼ = Potassium Aluminum Silicate Hydrate, KAlSiO4-1.5H_2O

Conventional geopolymers resulting from the dissolution of aluminosilicate in a strongly alkaline medium are expected to be amorphous (Rahier et al., 1996; Barbosa et al., 2000; Bell et al., 2009b). However, the presence of new crystalline phases not originating from the starting material have been previously reported for geopolymers resulting from volcanic ash, fly ash as well as metakaolinite especially after reaction with silicates with a low modulus (Rahier et al., 1997; Lemougna et al., 2011; Dimitrios et al., 2007; Verdolotti L., 2008).

III-2-4 : Infrared Spectra

The infrared spectra presented in Figure 40 show a broad absorbance at 820-1250 $cm^{-1}$and 480-600 cm^{-1} assigned to internal vibration of Si-O-Si and Si-O-Al (Davidovits, 2008) in both raw volcanic ash and resulting inorganic polymers samples.

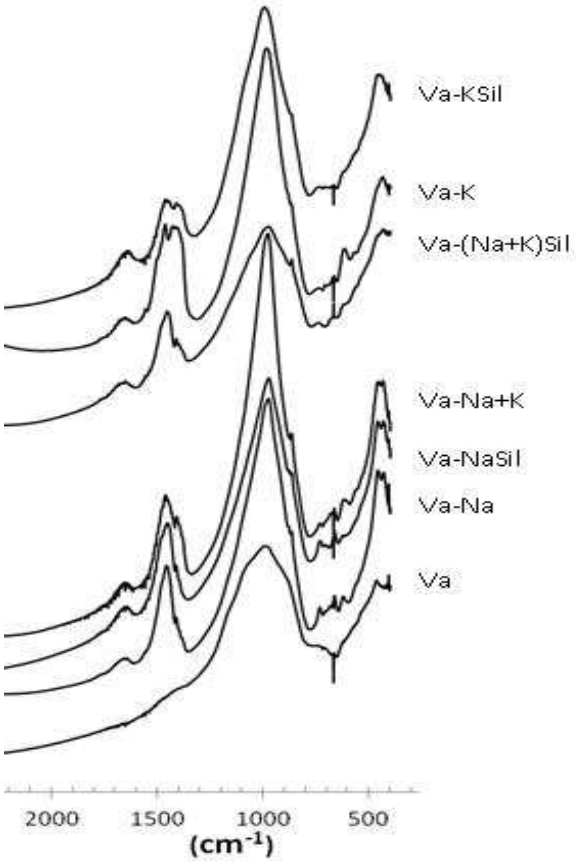

Figure 40: Infrared spectra of the volcanic ash (starting material) and resulting geopolymers

The band around 1640 cm^{-1} arises from water molecules, which are surface absorbed or entrapped in the large cavities of the polymeric framework, while the band around 1430 cm^{-1} is attributed to stretching vibrations of the O–C–O bond resulting from the atmospheric carbonation of the high alkaline aqueous phase, which is diffused on the geopolymeric materials surface (Dimitrios et al., 2007). These two later bands were not present in the pure ash and are the most obvious differences compared to the synthesized products. No sharp peaks from the crystalline hydrated phases in the OH-stretch region are observed suggesting the poorly crystallised and largely amorphous character of both pure ash and synthetised products. Additional peaks with low intensity observed on product spectra in the region 750-450 cm^{-1} are ascribed to the trace of sodalite (Ballirano et al., 1991) also observed on X-Ray spectra.

III-2-5 : Microstructure

The microstructural analysis of polished products show that the particles dissolution is not completed during the reaction as was observed in the SEM micrographs (Figure 41). Relicts of ash particles were found to be surrounded by the geopolymer matrix as can be seen on quantitative analysis of some areas. Specimens with NaOH were found to be more compact displaying no cracks, contrary to those based on KOH.

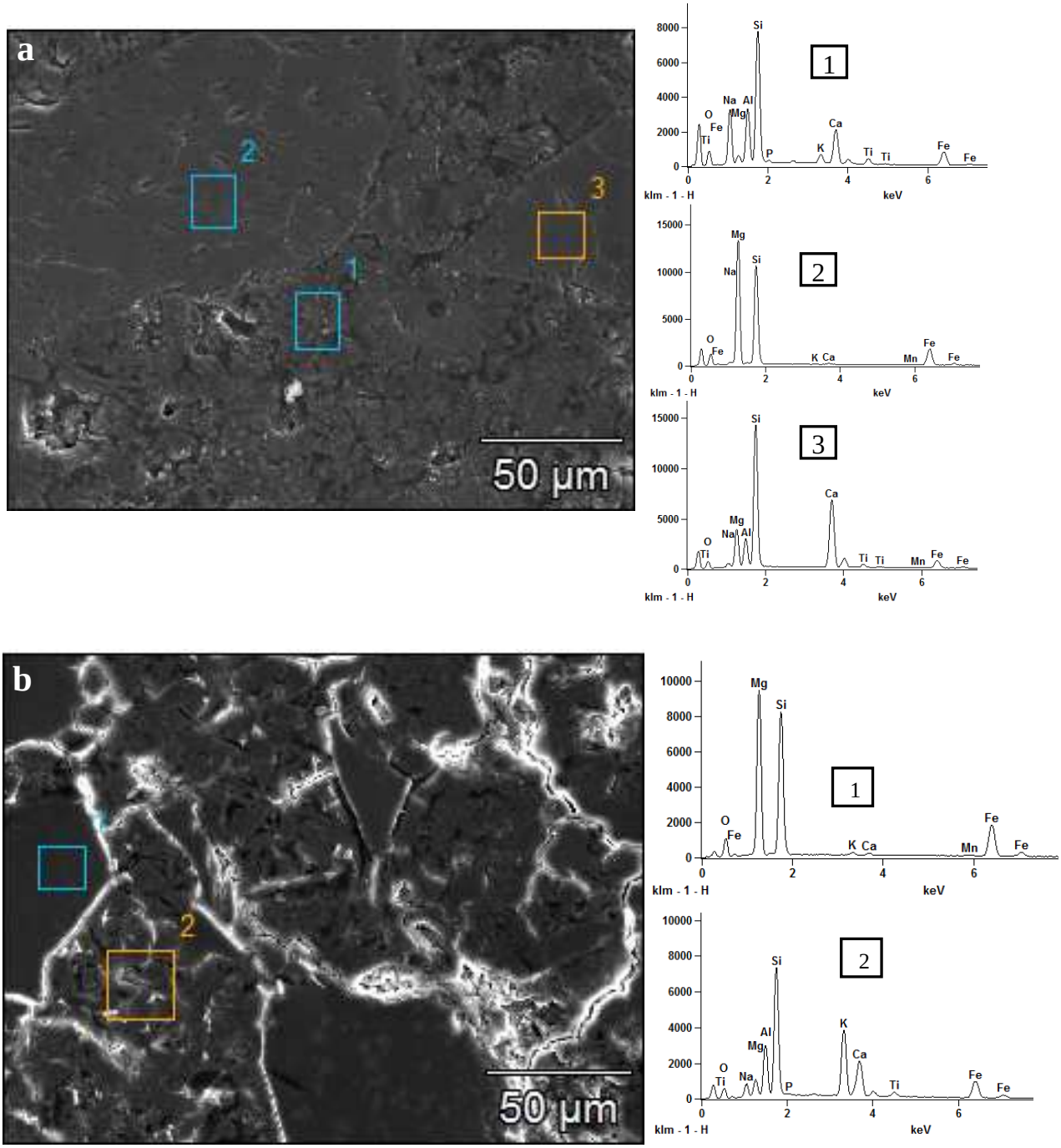

Figure 41: SEM micrographs. a) Va-Na, b) Va-K

On Figure 41.a, area 2 and 3 are undisolved particles. Their compositions do not contain the alkaline reagent. Their atomic composition are: 20% O, 38% Mg, 32% Si, 9% Fe for area 2 and 30% O, 9% Mg, 6% Al, 30% Si, 17% Ca, 3% Fe for area 3. Considering the mineralogical composition of the starting ash, area 2 and 3 should be rich in forsterite ferroan and augite mineral respectively. Area 1 is the reacted phase. It is atomically composed of 32% O, 20% Na, 1% Mg, 9% Al, 23%Si, 1% K, 6% Ca, 1% Ti, 4 % Fe. On Figure 8.b, we also have an undisolved particle in area 1 and the reacted phase in area 2 is atomically composed of 32% O, 5% Na, 3% Mg, 9% Al, 22% Si, 12% K, 8% Ca and 6% Fe. If we suppose that the Si and Al atoms in the reacted phases are fully oxydised, the SiO_2/Al_2O_3 ratio of these phases will be 5.1 and 4.9 in the areas selected for Na and K specimens respectively. These values are slightly above the maximum optimum value of 4.5 for SiO_2/Al_2O_3 in geopolymers (Komnitsas and Zaharaki, 2007) and could somewhat explain the absence of strength improvement while adding amorphous silica in the mixture composition.

Considering the wide spread distribution of calcium and somewhat iron on the EDS maps (Figure 42) these elements may have taken part to the reaction, contrary to magnesium which the presence on the maps were only concentred in some points. Based on microstructure investigation, no major difference was observed between K and Na volcanic ash based geopolymer, apart from the difference in atomic composition of the geopolymer matrix induced by the alkaline introduction during the preparation.

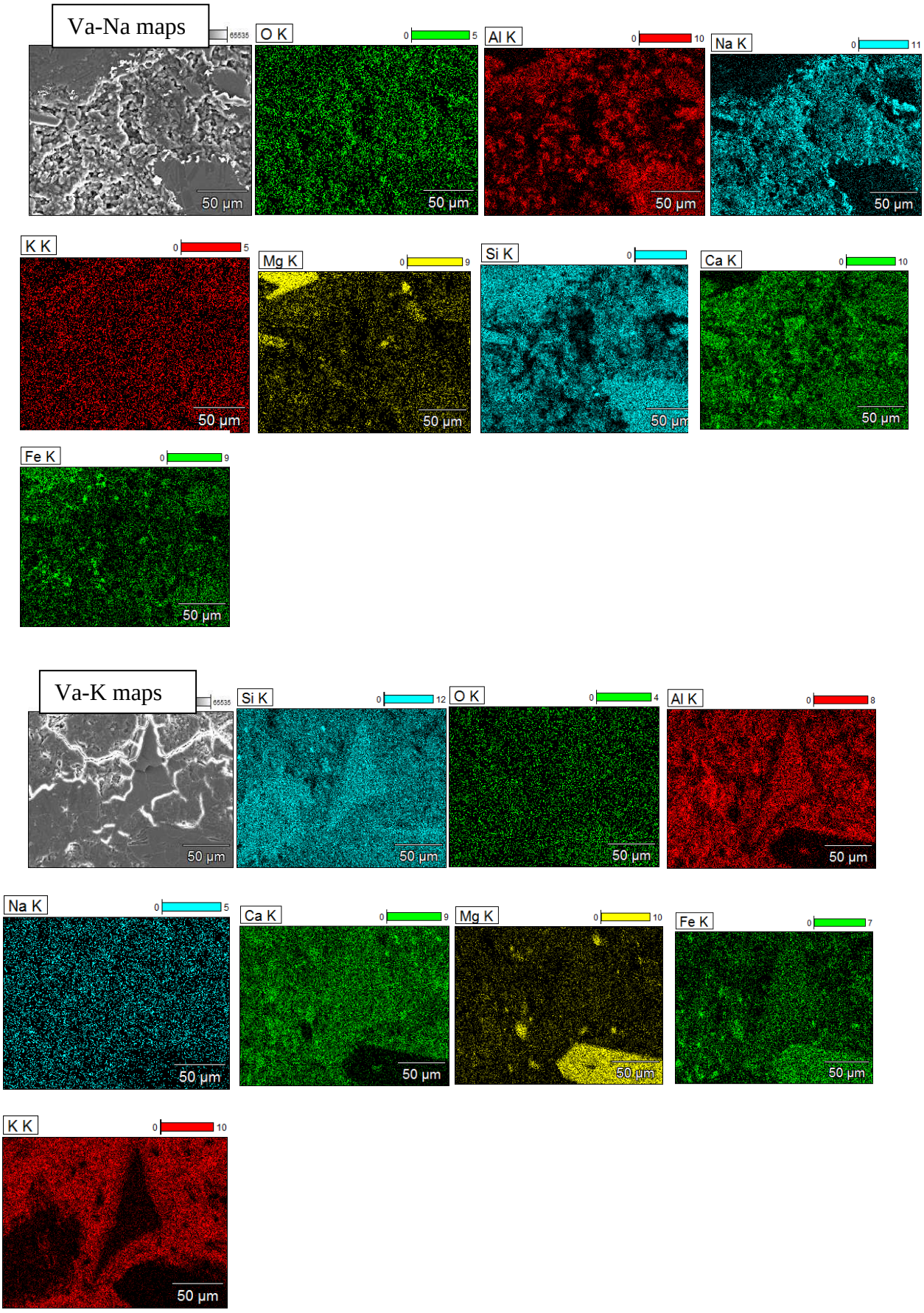

Figure 42: EDS maps of Va-Na and Va-K

III-2-6 : Thermal behavior (TMA-DMA and TGA)

The TMA thermograms of the different mixtures are presented in Figure 43.

The behavior of all the mixtures upon heating to 1000°C were more or less similar. A small shrinkage is observed below 200°C, probably due to the loss of residual water from the drying process. The material is then stable up to about 600°C where the slight expansion observed is associated with the change of the slope of the weight loss curves (Figure 43).

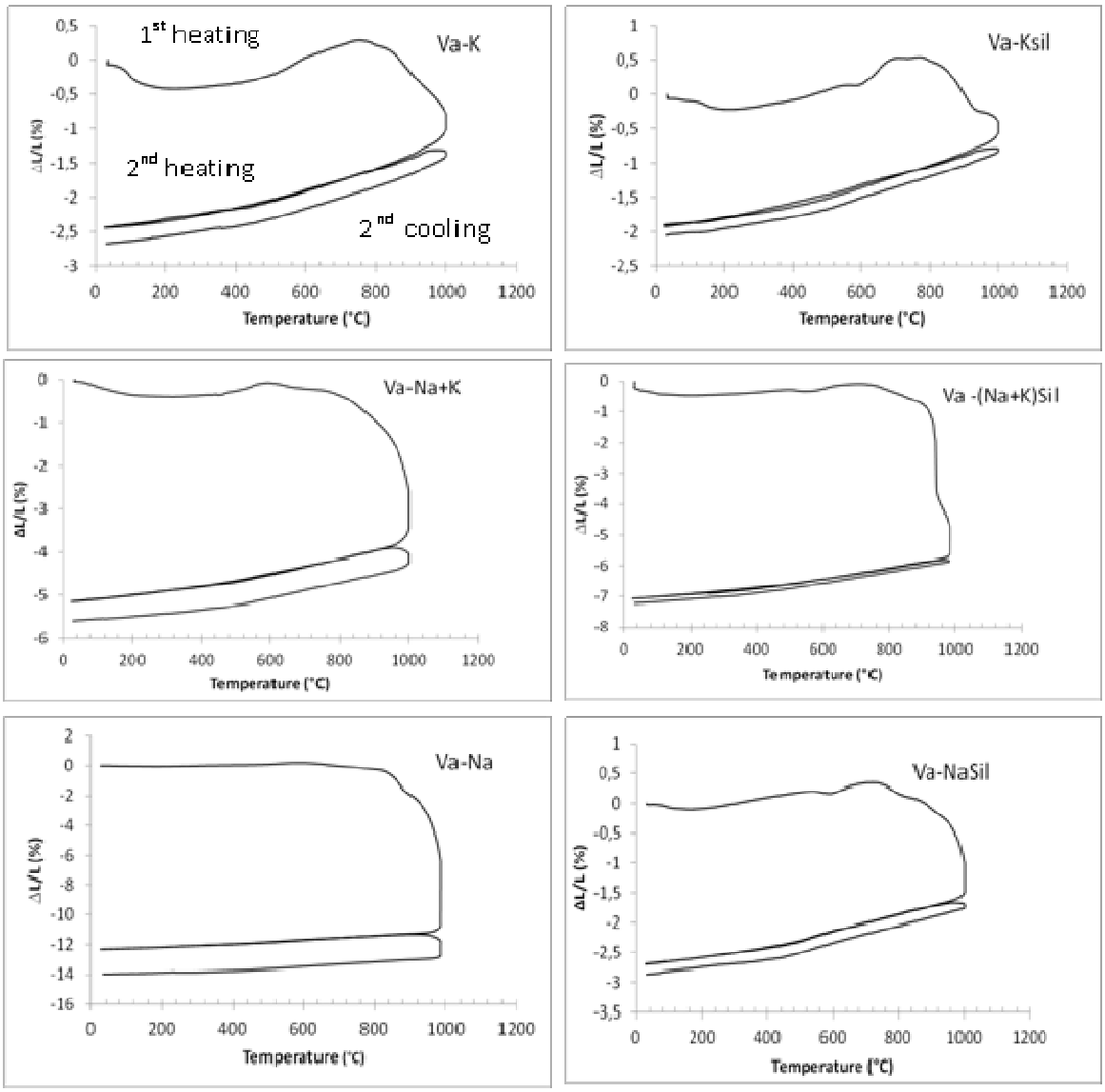

Figure 43: Thermograms of the different mixtures

Above 800°C the material starts to flow due to the onset of sintering reactions from which the major part of the change of sample's length comes from. During the cooling cycle the fired materials shrink more or less linearly and the coefficients of thermal expansion of the different samples are all between 8 $x10^{-6}C^{-1}$ and $16x10^{-6}C^{-1}$ (Table 10).

Table 10: Coefficient of thermal expansion of different compositions

Mixture composition	**Coefficient of thermal expantion ($x10^{-6}$°C)**	
	Between 200-300C	Between 600-700°C
Va-Na	10	12
Va-NaSil	8	13
Va-K	9	14
Va-KSil	10	14
Va-Na+K	10	16
Va-(Na+K)Sil	10	16

During the second heating cycle, the samples expanded linearly only up to about 900°C before starting to flow between this temperature and 1000°C. The second cooling produced a coefficient of thermal expansion similar to the first cooling and the flowing occurs only >950°C. Thus, when the sample cools below 950°C, the remaining change of length is due to the recovery of the thermal expansion. Globally, the overall shrinkage is very small (below 1%) up to 800°C, compared to an ideal geopolymer from metakaolin presenting about 6 to 8% of shrinkage at this temperature (Rahier et al., 1996b; Bell et al., 2009b). The final reductions of samples lenght vary between 2 and 7%. The K samples are more thermally stable than the Na samples. The Na sample little deformed and presented an overall length reduction of 14%. There is a slight difference around 600°C on the slopes of the curves after the first heating, resulting in little change of the values of thermal expansion coefficients which are almost similar at lower temperature (200-300°C), but slightly differ at higher temperature (600-700°C). The values of the coefficients of thermal expansion obtained are in the same order with those reported from metakaolin-based inorganic polymer glass and are in agreement with literature values for ceramic materials (Rahier et al., 1996).

The themogravimetry analyses curves are presented in Figure 44.

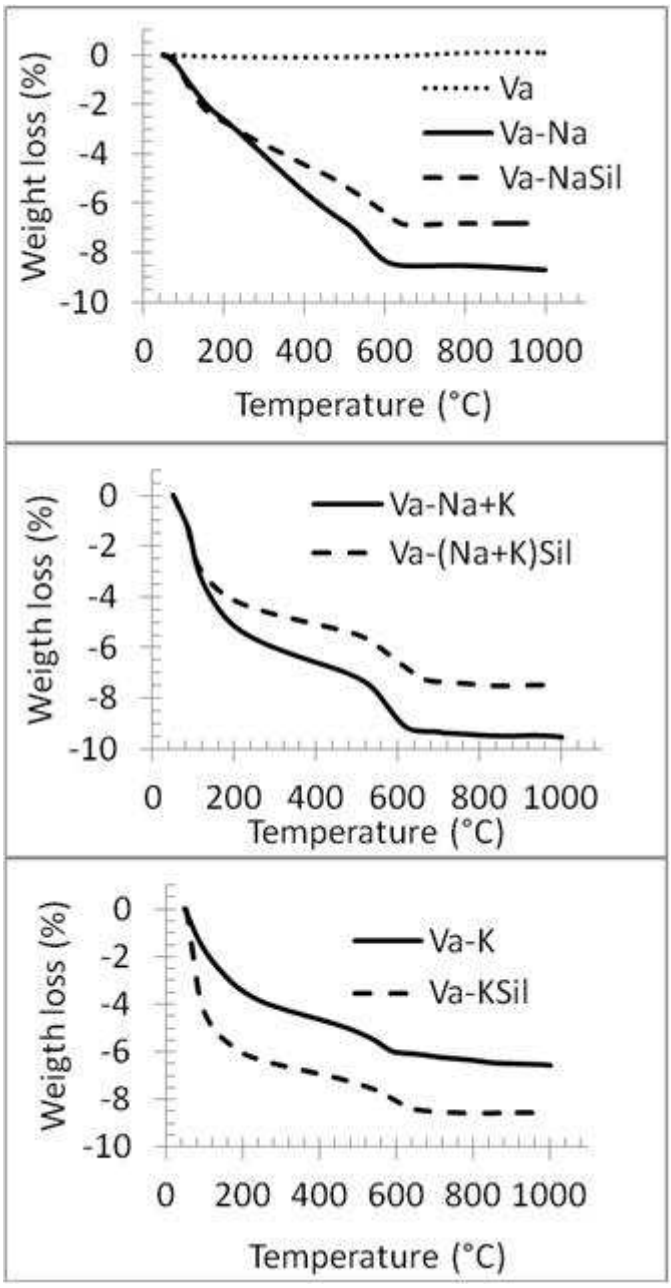

Figure 44: Themogravimetry curves

It is observed that the weight loss of the pure ash is below 0.5% during the heating and cooling cycle at 1000°C while those of synthesized specimens are between 6 and 10 %. Considering the residual added water after seven days curing at 90°C obtained after weighting the specimen before and after curing (The mass of water represents about 16% (210g/1330g) of the total mass of the initial geopolymer mixture for Va-Na specimen and about 15 % (210g/1378g) for K specimen. After seven days curing, the remaining water is about 3% of

the specimen mass for Va-Na versus about 1.5% for Va-K (Annexe 1)). Part of weight loss during the samples' heating up to 1000°C should be attributed to the destruction of some structured OH in the matrix coming from added sodium or potassium hydroxide. The total weight loss of specimens containing only sodium occurs below 640°C while the mass of specimens with potassium continue to decrease slightly up to 840°C. The weight loss of all the synthesized specimens remains smaller than those reported (about 25%) for metakaolin based geopolymer (Rahier et al., 1996b; Bell et al., 2009b) after heating up to 1000°C.

The results from dynamic mechanical analysis (tanδ versus heating temperature) are presented in Figure 45.

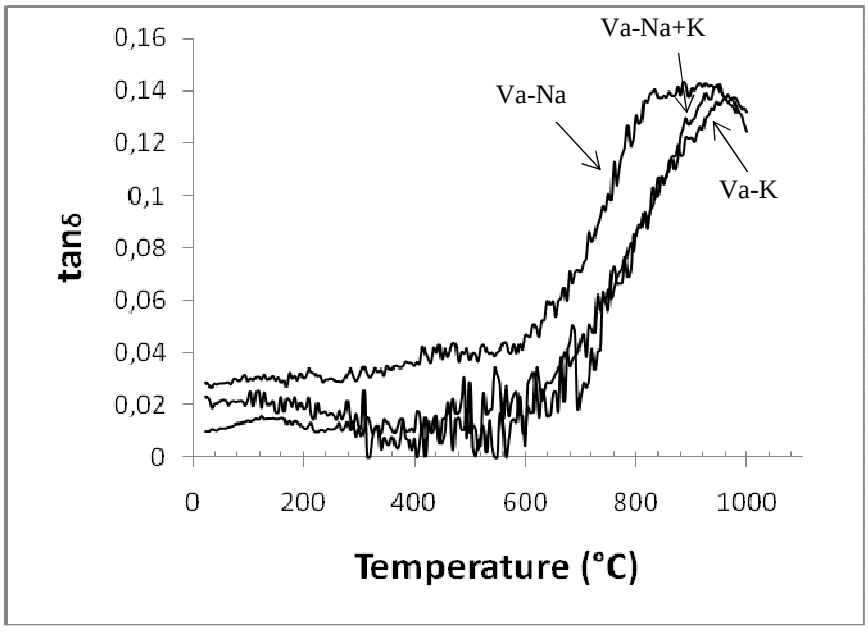

Figure 45: Dynamic Mechanical Analysis curves

These results are for the second heating; data from the first heating being less helpful due to the surface of specimen which was not perfectly flat, reducing the contact quality with the probe. The data presented are for Va-Na, Va-K and Va-Na+K specimens. The glass transition starts at about 600°C for all the specimens, but end at different temperatures, since the maximum values of tanδ is also observed at different temperatures, lowest for Va-Na

specimen (about 850°C) versus about 875°C and 900°C for Va-Na+K and for Va-K specimens respectively. The results obtained are close to those reported (Tg=700-800°C) on inorganic polymer glasses made from metakaolin (Rahier et al., 1996b). The glass transition temperature is linked to the chemical composition of the material. Constituent such as Si, Al and alkaline ions play a different role in the thermorheological behavior of the glass. Alkalines are network modifiers and lower Tg, while SiO_2 is network former and is in fact the basis of the glass network (Rahier et al., 1996b). It is commonly known that the Tg of Na glasses is lower than that of K glasses and this was also observed in the current volcanic ash based materials.

III-2-7: Efflorescence test and pH of the solution of the immersed samples.

In order to get an idea on the stability of the materials, six cylindrical samples were immersed in distilled water (334g) and the pH was monitored. The results show that some amount of unreacted alkaline is present in the samples and is free to migrate into water when the samples are immersed, leading to an increase of the pH of the solution from 7.5 to 11 or 12 following the type of the samples. The extent of increase is presented in the Table 11.

Table 11: pH of the immersed solution after two days of samples immersion

pH of the initial solution: 7.5	
Samples formulations	**pH of the immersed solution**
Va-Na	11.01
Va-Na+K	12.01
Va-K210	12.25
Va-K180	12.33
Va-NaSil	11.15
Va-(Na+K)Sil	11.73
Va-KSil	11.95

The efflorescence test was also carried out on individual specimens from different compositions. It appeared that Potassium based specimens are less sensitive to efflorescence. Photo 9 present specimens for efflorescence test after 2 and 14 days.

(A)

(B)

Photo 9: Specimens for efflorescence test after 2 days (A) and 14 days (B)

It was observed that some effluorescence started to appear on specimen containg NaOH only after 2 days when ¼ of the sample (the bottom) is immersed in water (Photo 9_A). After 14 days, specimens containing NaOH are completely covered with white effluorescence while specimens containing KOH are still free of effluorescence (Photo 9_B).

III-2-8 : Conclusion

The present section investigated the influence of the composition of the activating solution on the compressive strength and thermo mechanical properties of inorganic polymers made from Foumbot Petponun volcanic ash. No significant change was observed on varying the composition of the alkaline solution on the 7 and 21 days compressive strength. However KOH promoted more thermally stable materials while NaOH was found to promote faster reaction rate and better strength, with about 40 MPa and 20 MPa as dry and wet compressive strength respectively at 21 days. The material strengths are found to decrease after immersion in water for 24 hours, but the strength is partly recovered after drying the immersed specimens at 40°C. Some minerals remained unaffected in the alkaline solution. This complicates the calculation of the obtained Si/Al ratio as not all Si and Al present in the original material is used in the geopolymer. The largest particles only act as reactive filler while smaller particles dissolve in the activating solution, forming the inorganic polymer matrices. Reducing the amount of coarse particles promoted higher reactivity and better compressive strength development for specimens made with NaOH.

The geopolymer products were found to be relatively stable to heat, presenting a glass transition between 600-900°C and shrinking only slowly up to 800°C. The results obtained suggest the possible use of the synthesized materials for building applications and low temperature refractory up to about 700-800°C.

III-3: IMPACT OF PROCESSING CONDITIONS AND THERMAL BEHAVIOR OF GEOPOLYMERS FROM Va1

Processing conditions have been proven to influence physical properties of geopolymers (Rahier et al., 1997, Komnitsas and Zaharaki, 2007; Tailby and MacKenzie, 2010; Izquierdo et al., 2010; Elimbi et al., 2011). To improve these properties (particularly mechanical ones), several studies have been carried out on varying curing temperature or alkaline metal on metakaolinite and fly ash based geopolymer (Xu and van Deventer , 2000; Rahier at al., 2007, Komnitsas and Zaharaki, 2007, Bell et al., 2009a, 2009b; MacKenzie et al., 2010; Nugteren, 2010, Ruscher et al., 2011). Very few studies have been carried out on volcanic ash based geopolymer (Verdolotti, 2008; Kamseu et al., 2009; Elimbi et al.,).

The aim of this section is to investigate the influence of curing temperature and Na content on the development of compressive strength of volcanic ash-based geopolymer from Foumbot's Petponoun ash. For this purpose, several compositions of various molar ratios were prepared and polymerized with NaOH as the sole alkaline reagent. The structure of polymerized products as well as phase transformation up to 1000°C was studied by XRD, Fourier transform infrared spectroscopy (FTIR), TGA/DSC, dilatometry and compressive strength measurements on products heated at 250°C, 500°C, 750°C and 900°C.

Natural sand was used as filler for the preparation of geopolymer motar and the changes induced on the properties were observed by scanning electron microscopy, compressive strength, bulk density and open porosity by the water absorption method.

III-3-1: Effect of processing conditions on the mechanical properties and structure of geopolymer pastes

The particle size distribution and the chemical composition of the sand are presented in Table 12 and Figure 46.

Table 12: Chemical composition of sand and volcanic ash

Sample	Fe_2O_3	MnO	TiO_2	CaO	K_2O	P_2O_5	SiO_2	Al_2O_3	MgO	Na_2O	LOI	SUM
Volcanic ash	13.22	0.18	2.74	10.38	1.53	0.61	44.19	14.06	9.73	3.69	-0.62	99.71
Sand	3.22	0.10	0.27	3.98	1.33	0.08	68.54	15.93	1.04	4.30	0.93	99.71

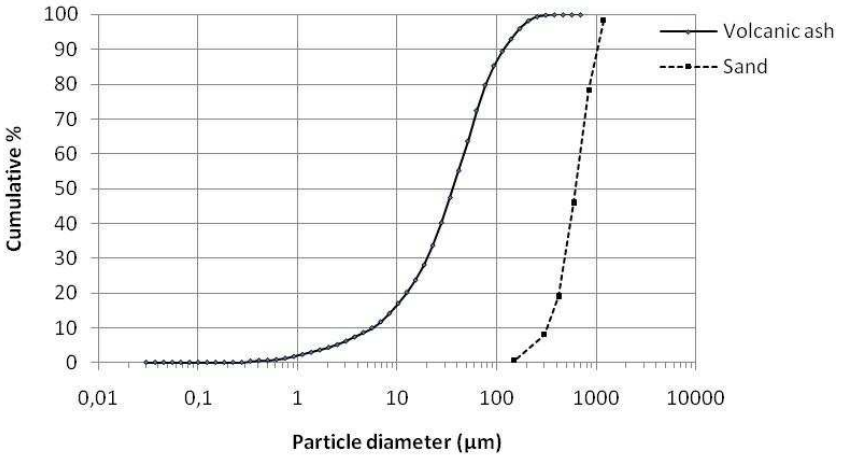

Figure 46: Volcanic ash and sand granulometric curves

All the sample formulations developed strength after curing period, but the strength of the sample with Na_2O/SiO_2 = 0.15 was too low to be determined by the compressive test machine. All the dry-cured samples showed some efflorescence, particularly in the sample with Na_2O/SiO_2 = 0.35, which also displayed major cracking.

The seven-day compressive strengths of the sample of composition Na_2O/SiO_2 = 0.25 subjected to various curing temperatures, dry or immersed in water, are shown in Figure 47.

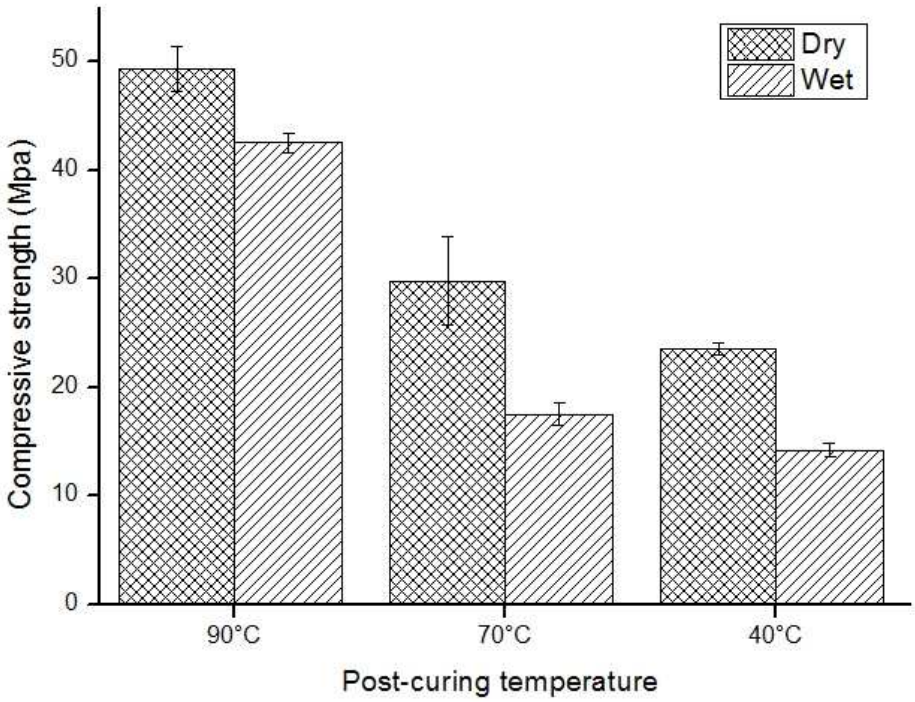

Figure 47**:** Effect of post-curing temperature under wet and dry conditions on the 7-day compressive strength of geopolymers of molar composition Na_2O/SiO_2 = 0.25.

The compressive strength increases significantly as the curing temperature is increased from 40 to 90°C, the samples post-cured in water (measured wet) showing consistently lower compressive strengths, unlike the behavior of conventional cementitious products. The compressive strengths (14-42 MPa and 23-49 MPa for wet and dry post-curing respectively) are similar to those reported for flyash/clay geopolymers by van Jaarsveld et al., (2002) who observed a substantial improvement of compressive strength when the curing temperature was increased from 30 to 70°C. Wet curing of volcanic ash-based geopolymer may have the effect of removing the unreacted sodium species, counteracting the formation of efflorescence in the final products.

The 7-days compressive strengths of all the samples subjected to dry post-curing at 90°C presented in Figure 48 shows that the strength reaches a maximum at the composition $Na_2O/SiO_2 = 0.3$ before decreasing again at $Na_2O/SiO_2 = 0.35$.

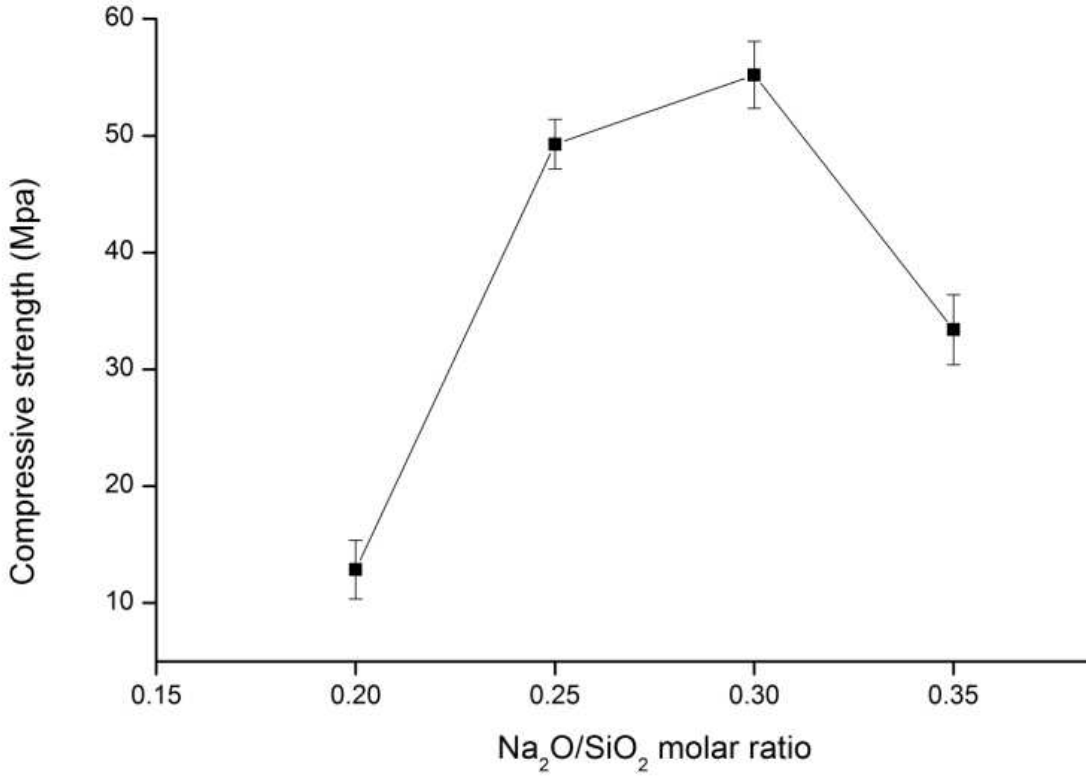

Figure 48: Influence of the Na_2O/SiO_2 oxide molar ratio on the 7-days compressive strength of geopolymers cured at 90°C under dry conditions.

These results indicate that sufficient alkali must be present for dissolution of the reactive part of the starting materials, giving an increased amount of geopolymer and thus higher compressive strength. A similar dependence of the geopolymerisation reaction on the sodium hydroxide concentration was also reported by Temuujin et al., (2009) who also observed a reduction in compressive strength when additional water was used in the synthesis. To better understand the trends observed, the water absorption and bulk density have been measured (Table 13).

Table 13: Water absorption and bulk density of the geopolymer paste and mortar samples

Sample	paste	paste	paste	paste	mortar, 10% sand	mortar, 25% sand	mortar, 40% sand
Na_2O/SiO_2 molar ratio	0.20	0.25	0.30	0.35	0.30	0.30	0.30
Water absorption (%)	16.95 (0.40)	14.08 (0.28)	14.24 (0.73)	14.80 (0.37)	14.61 (0.71)	12.55 (0.13)	11.34 (0.10)
Bulk density ($g.cm^{-3}$)	1.86 (0.03)	1.91 (0.03)	1.91 (0.02)	1.86 (0.03)	1.91 (0.02)	1.92 (0.02)	1.97 (0.02)

(Figures in parenthesis are the standard deviation of three measurements).

The sample of composition Na_2O/SiO_2 = 0.2 showed the lowest density and the highest water absorption, probably because it contains less of the reaction product than in the other compositions. The bulk density increases for higher Na_2O/SiO_2 ratios but decreases again for the highest ratio studied. This is in line with the compressive strength. The samples with sand have a decreasing water absorption capacity and increasing density as was expected. The water absorption values are all <15% apart those of the sample with Na_2O/SiO_2 = 0.2, satisfying the requirement of these products for building applications according to ASTM standards C216 (SW). The reduction of strength at the highest Na_2O/SiO_2 molar ratio can thus be related to its lower density. It was also observed that those samples showed a significant formation of efflorescence and cracks.

The X-ray patterns of both the volcanic ash and resulting geopolymers **(**Figure 49**)** show a large amount of amorphous material, in addition to initially present the crystalline minerals augite/diopside ($Ca(Mg, Fe,Al)(Si,Al)_2O_6$), ordered anorthite, ($(Ca, Na)(Al,Si)_2Si_2O_8$) and ferroan forsterite ($(Mg,Fe)2SiO_4$) next to a new phase.

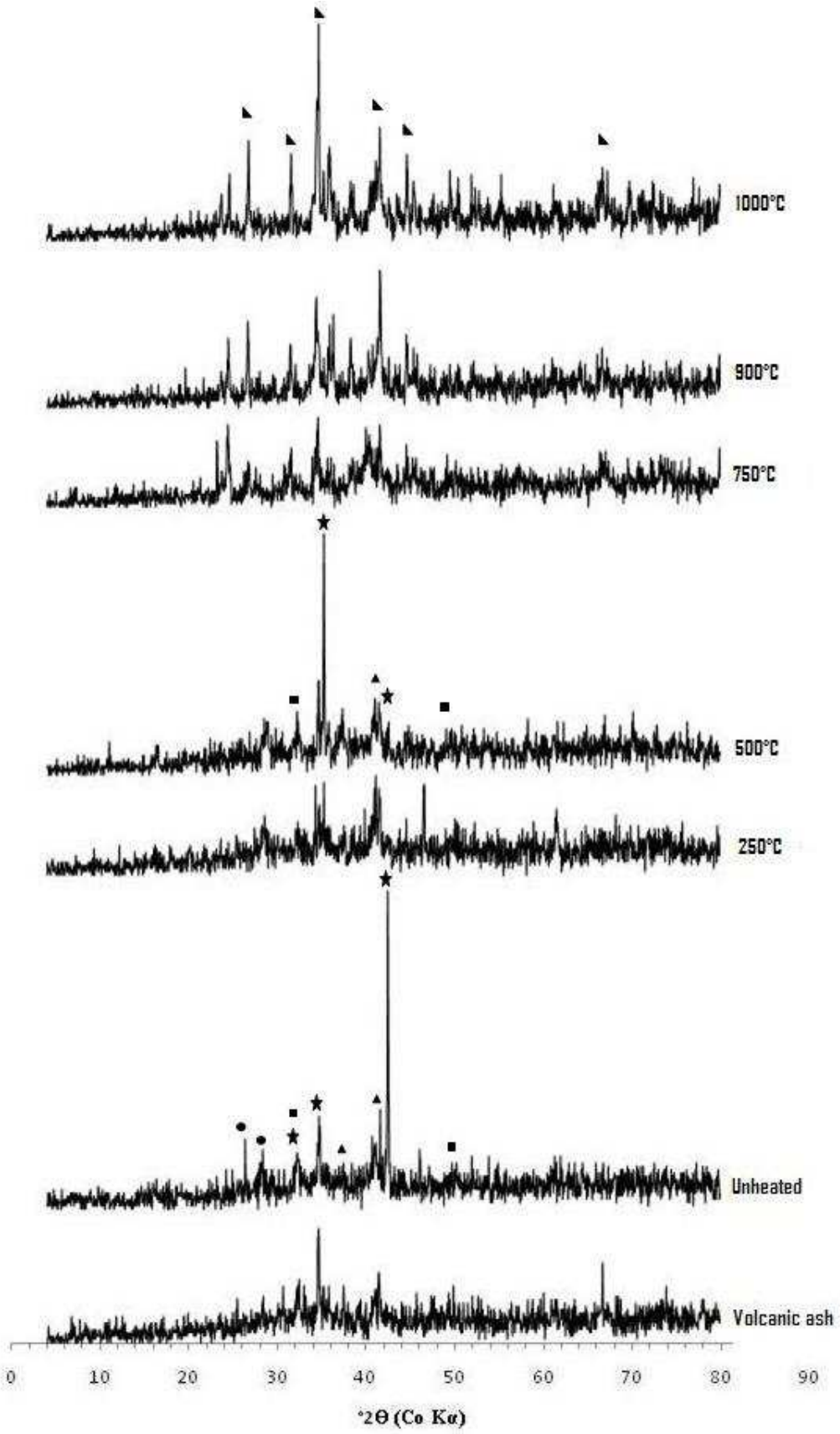

Figure 49: X-Ray diffractograms of volcanic ash, geopolymer (at Na_2O/SiO_2 = 0.25) and heated geopolymers (temperatures mentioned)

The intensities of some of the crystalline diffraction peaks are somewhat reduced in the geopolymer paste, possibly due to the formation of the new amorphous phase and the appearance of the new crystalline phase $Na_8(AlSiO_4)_6(OH)_2.4H_2O$ resulting from the reaction of the volcanic ash with NaOH. Although conventional geopolymers are X-ray amorphous (Rahier, 1996; Brew and MacKenzie; 2007MacKenzie, 2009), the presence of crystalline phases in geopolymers prepared from volcanic ash has previously been reported (Kamseu et al., 2009; Verdolotti et al., 2008). By treating an amorphous pozzolan with sodium hydroxide or sodium hydroxide plus sodium aluminate, Verdolotti et al. (2008) obtained a product with crystalline diffraction peaks, possibly from a zeolite, overlapping the amorphous baseline. Since the initial volcanic ash contains calcium, iron and magnesium, these elements may have taken part in the formation of the geopolymer structure, either by integrating in the network or acting as crystalline fillers. Previous studies (Komnitsas and Zaharaki, 2007; van Jaarsveld et al., 2003) reported that the presence of calcium in the geopolymer raw material improves the mechanical properties due to the possible reduction of microstructural porosity resulting from the formation of amorphous Ca–Al–Si gel. The influence of different calcium compounds on metakaolin based-geopolymers showed XRD features of conventional geopolymer composites containing additional crystalline fillers, suggesting that calcium may either act as a filler, or integrate with the geopolymer network, depending on the chemical form of the additive (MacKenzie et al., 2007). The behavior of magnesium and iron may be similar to that of calcium. Iron has been suggested to be detrimental to geopolymer network formation by removing OH^-, thereby slowing down the dissolution of residual aluminosilicate (Provis, 2006), but this is at variance with (Perera et al., 2007), who reported that iron resides in octahedral sites in metakaolin-based geopolymers, either as isolated ions in the geopolymer matrix or as oxyhydroxide aggregates which have not reacted with the geopolymer components. Thus, in the present geopolymers, some of the ferrous iron remains in the various microcrystalline phases present in the original volcanic ash, but some probably also occupies specific geopolymer sites instead of forming $Fe(OH)_2$, imparting a homogeneous color to the samples, and a homogeneous iron distribution, as revealed by EDS maps (Figure 50).

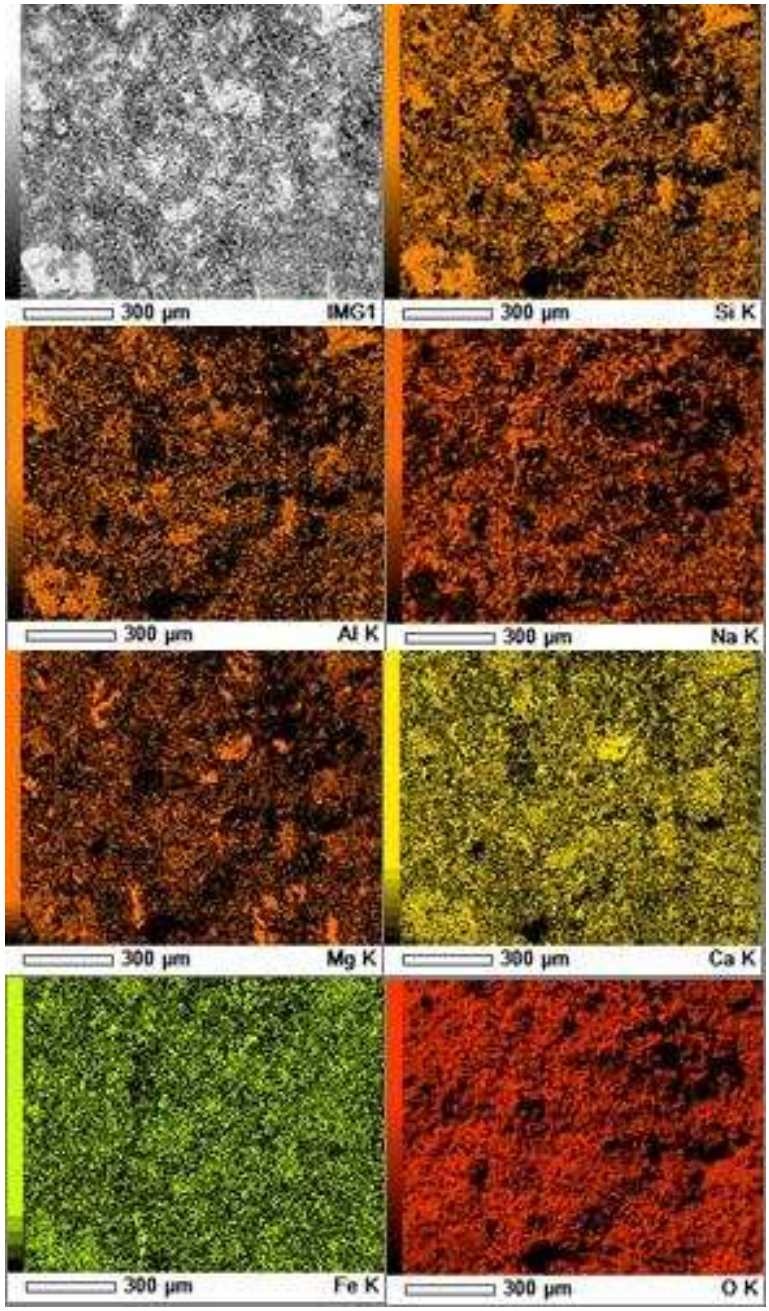

Figure 50: EDS Maps of fractured sample at $Na_2O/SiO_2 = 0.25$

SEM/EDS examination of the fracture surface of the sample with $Na_2O/SiO_2 = 0.25$ showed a more or less homogeneous distribution of Si, Al, Fe, Na, Ca and O in the geopolymer matrix. Areas of high Si concentration were associated with high Al concentration, indicating the presence of undissolved aluminosilicate particles in the geopolymer matrix. Mg was less homogeneously distributed in the matrix, suggesting that this element probably does not participate in the geopolymer formation reaction. Higher magnification revealed a mixture of lath-shaped and agglomerated morphologies (Figure 51) which persisted in samples heated up

to 900°C (Figure 51 d). However, above 750°C, a slight increase in the lath lengths is seen, accentuated at 1000°C (Figure 51 e), possibly due to the onset of some solid state reactions.

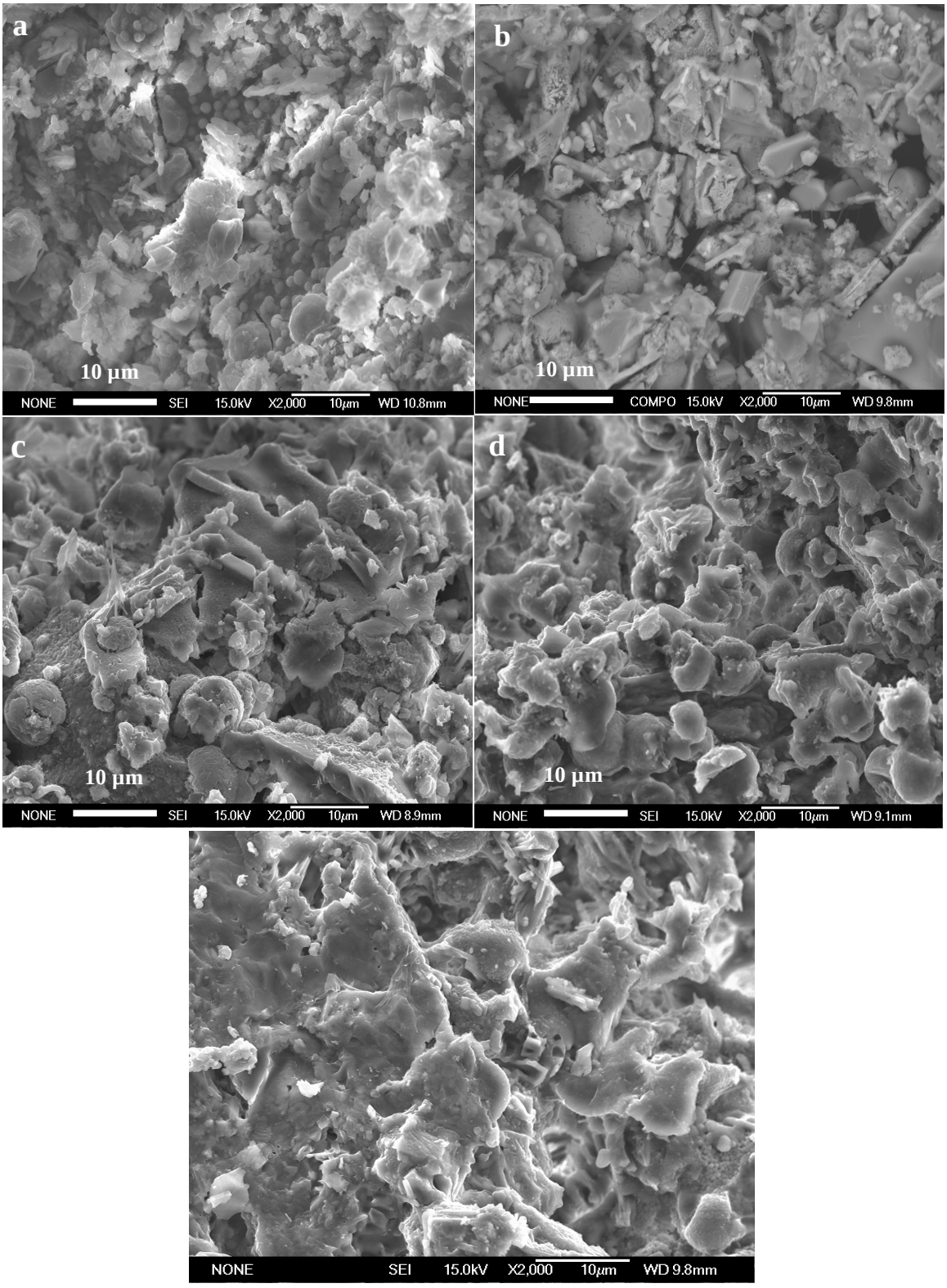

Figure 51: Microstructure of products: *a) as synthetised; b) heated at 500°C; c) heated at 750°C; d) heated at 900°C; e) heated at 1000°C.*

An important conclusion is that not all the Si and Al present in the volcanic ash is available for the geopolymerisation. Some of the crystalline phases remain and it is not possible to check if the complete amorphous phase is dissolved by the alkaline solution.

The FTIR spectra of the initial volcanic ash and resulting geopolymers, both unheated and heated to various temperatures (Figure 52) show two broad absorbance bands, at 820-1250 cm^{-1} and 450-730 cm^{-1} assigned to the internal vibrations of Si-O-Si, and Si-O-Al respectively. The main difference between the spectra of the initial volcanic ash and the NaOH-activated geopolymer is a shoulder at about 1500 cm^{-1} arising from sodium carbonate. The bands at 1700 cm^{-1} and 3500 cm^{-1} arise from the presence of structural water remaining in the geopolymer matrix after dry post-curing at 90°C. The FTIR spectra of the volcanic ash and resulting geopolymer are very similar to those reported by Verdolotti et al., (2008) in materials synthesized from Italian pozzolans with sodium hydroxide and sodium aluminate. These authors suggest that the broadness of the absorbance band at 820-1250 cm-1 reflects the variability of the bond angles and bond lengths of the tetrahedral structures around the silicon atoms, and the absorbance peak at 730 cm-1 arises from the stretching vibration of Al^{VI}–O–Si bonds. The coordination of Al and Si in the present geopolymers could not be confirmed by solid-state MAS NMR spectroscopy because of the content of iron present.

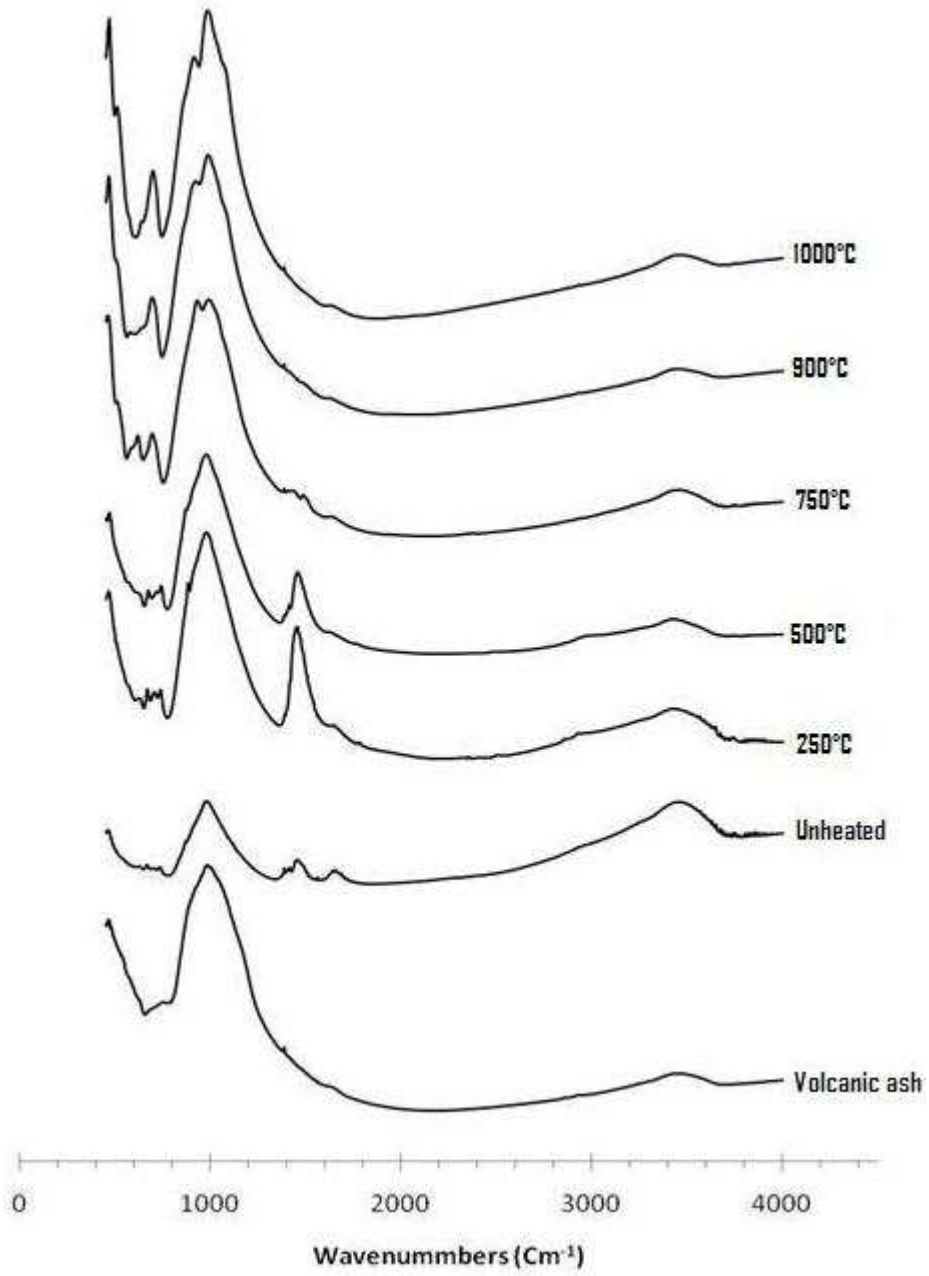

Figure 52: FTIR spectra of the initial volcanic ash and geopolymer sample of molar composition $Na_2O/SiO_2 = 0.25$, unheated and thermally treated at the indicated temperatures.

III-3-2 : Properties of mortar from geopolymer paste

The effect of adding varying amounts of mortar sand to the geopolymer paste of composition $Na_2O/SiO_2 = 0.3$ is shown in Figure 53.

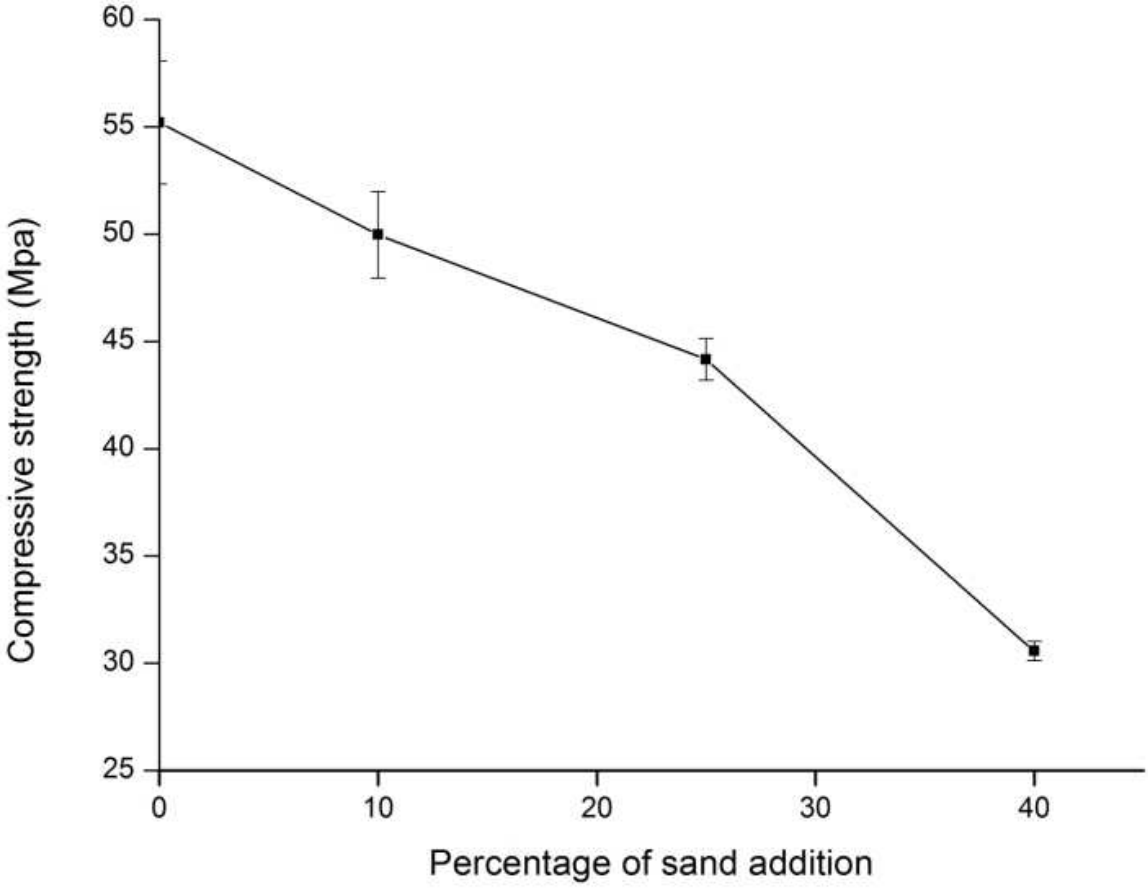

Figure 53: Influence of the addition of mortar sand on the compressive strength of a mortar of molar composition $Na_2O/SiO_2 = 0.3$.

Although the addition of sand reduces the porosity and increases the bulk density of the geopolymer mortar, the resulting compressive strength is less than for the geopolymer matrix, and decreases as the proportion of sand increases. This strength decrease may be the result of diluting the geopolymer by the sand without contributing any significant strength of its own. These results are similar to those obtained for a metakaolin-based geopolymer by Barbosa and MacKenzie, (2003) who reported a reduction of compressive strength upon adding 10-20 vol% of various granular inorganic fillers. By contrast, different behavior was reported (Temuujin et al., 2010) in fly ash-based geopolymer, in which no significant change in

strength was obtained by the addition of up to 50% sand, suggesting a partial dissolution of the aggregate surface in the geopolymer matrix giving increased interfacial bonding. Thus, the present volcanic ash geopolymer more closely resembles the behavior of metakaolin-based geopolymer than fly ash geopolymer. Strength development of geopolymer mortars may therefore vary from case to case depending on the strength of the geopolymer gel, the interfacial bonding between the geopolymeric gel, the aggregate itself (Temuujin et al., 2010) and even the aggregate particle size distribution. In any case, the addition of sand filler can reduce manufacturing costs provided it is not added in proportions greater than required to maintain the physical properties appropriate to the proposed application. The compressive strength of 30 MPa obtained with 40% sand addition is still within the requirements of ASTM C216 (SW) for building materials.

III-3-3 : Effect of heat on the geopolymers

The effect on the compressive strength of heating the sample with Na_2O/SiO_2 = 0.25 to various temperatures is shown in Figure 54.

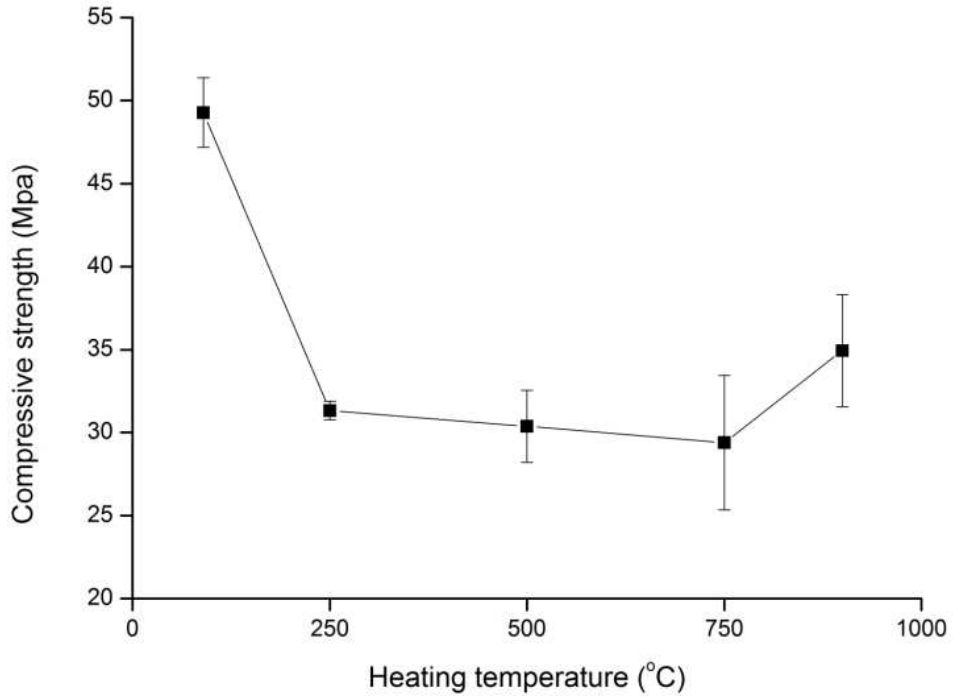

Figure 54: Effect of thermal treatment temperature on the compressive strength of a geopolymer paste of molar composition Na_2O/SiO_2 = 0.25.

Heating to 250°C results in a significant strength reduction to 30MPa, which is then maintained to 750°C, when the strength increases to about 35 MPa at 900°C. The reduction of strength upon initial heating is probably due to the loss of (structural) water from the geopolymer matrix, weakening the structure, and also to the possible concomitant development of micro cracks. The Photo 10 shows the specimens made and heated at different temperatures.

Photo 10 : Samples made and heated at different temperatures

The DSC/TG curves of the sample with Na_2O/SiO_2 = 0.25 (Figure 55) show about 70% of the mass loss occurs <250°C; this is attributed to the loss of structural water, since the negligible loss on ignition value for this volcanic ash indicates the absence of organic matter.

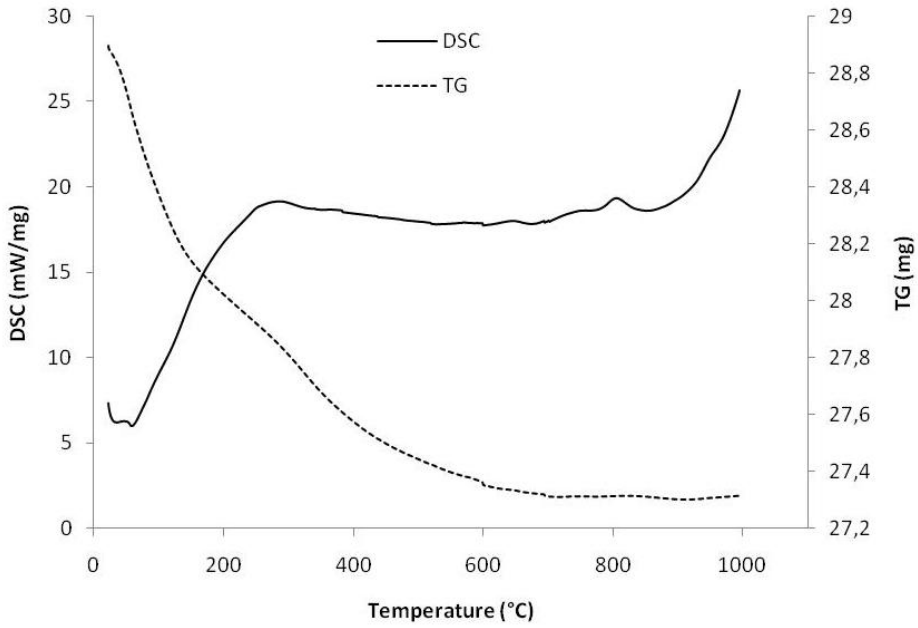

Figure 55: DSC/TG curves of a geopolymer paste of molar composition Na_2O/SiO_2 = 0.25.

The mass loss at about 250°-600°C is attributed to the removal of more tightly bound water. The decomposition of sodium carbonate formed by atmospheric carbonation of unreacted NaOH is seen above 600°C. Above 900°C, the DSC curve shows an exothermic reaction, due to the formation of new phases associated with the onset of sintering of the geopolymer matrix. Similar behavior was observed in the sample shrinkage during the first heating cycle (Figure 56). The sintering observed also explains the increase in strength as the cracks will be removed upon sintering.

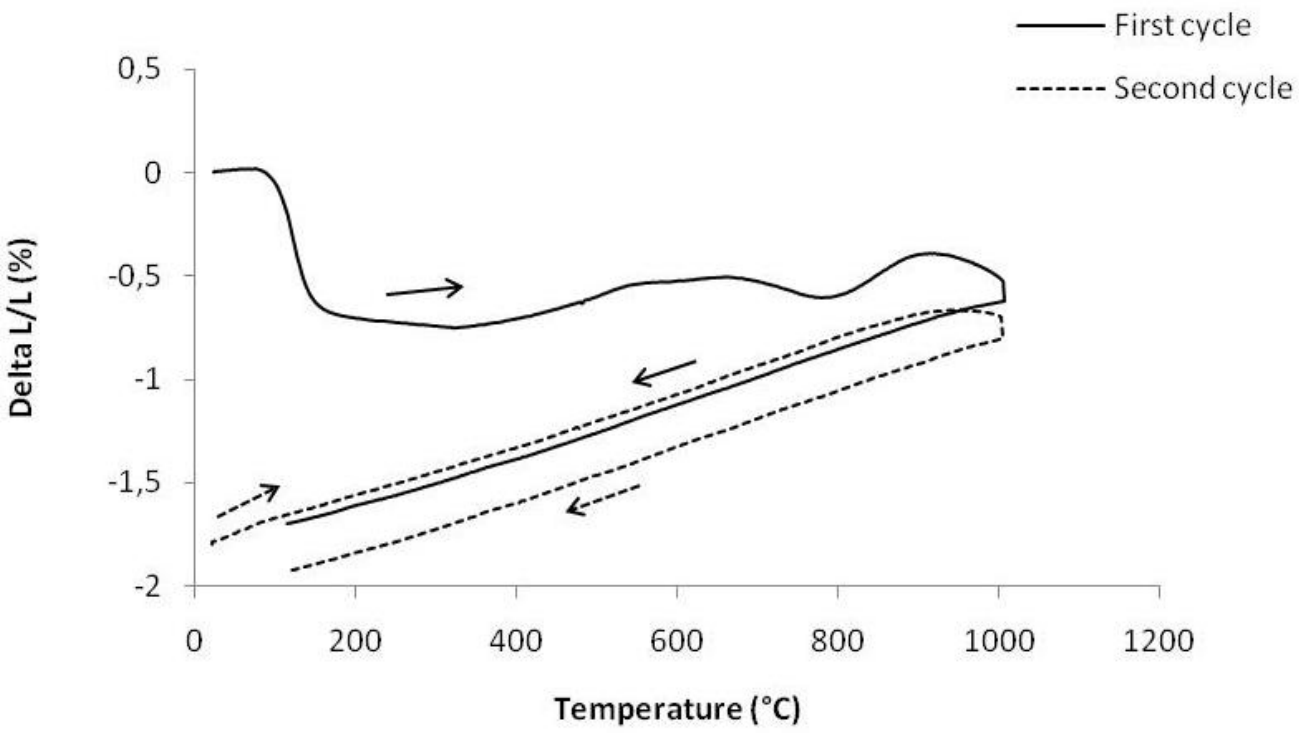

Figure 56: Dilatometer curves of a geopolymer paste of molar composition Na_2O/SiO_2 = 0.25.

Between room temperature and about 110°C, the 0.4% linear shrinkage is due to the removal of less tightly bound water as the drying process is completed.

Above this temperature the sample dimensions remain relatively constant up to 1000°C. Over the last hundred degrees the sample continued to shrink, reflecting a small degree of sintering. During the cooling cycle the fired material shrank more or less linearly with a coefficient of thermal expansion of about $12x10^{-6}$ $°C^{-1}$. The overall shrinkage of the sample after firing to 1000°C and cooling is 1.8%, confirmed by measuring with calipers before and after firing. During the second heating cycle, the sample expanded linearly only up to about 900°C before

starting to shrink between this temperature and 1000°C (Figure 56). Cooling produced a coefficient of thermal expansion similar to the first heating cycle and permanent shrinkage occurs only >900°C. Thus, when the sample cools below 900°C, permanent shrinkage stops and the remaining change of length is due to the recovery of the thermal expansion. The overall shrinkage after heating and cooling during the second cycle was about 0.25%. The physical evolution of materials during heating is a critical factor in determining their suitability for applications ranging from construction to refractories and adhesives (Duxson et al., 2006).

Compared to the overall shrinkage value of about 8% observed by Barbosa and MacKenzie (2003) or Duxson et al., (2006) for metakaolin based geopolymer heated to 800- 900°C, the shrinkage of the present volcanic ash-based geopolymer is about four times smaller, indicating a superior dimensional stability within this temperature range.

The FTIR spectra (Figure 52) show that there is no major phase transformation upon heating to 500°C, apart from the removal of structural water and possibly the migration of unreacted Na compounds due to thermal activation. Above 750°C there is no further evidence of sodium carbonate, which begins to decompose at 600°C. The appearance at 750°C of a new shoulder at about 1015 cm-1 is due to the formation of a new phase, the intensity of which increases with increasing temperature. Similarly, the XRD diffractograms of the heated samples (Figure 49) indicate no major phase transformation up to 500°C. Apart from the destruction of the sodium aluminum silicate hydroxide hydrate by the removal of structural water at 110°C, the major new crystalline phase formed is nepheline ($(Na,K)AlSiO_4$); this nepheline appears at about 750°C and is clearly observable by XRD at 900°C. The oxidation of ferrous iron upon heating is also likely, in view of the color change from grey to brown in samples heated at 750-1000°C. These high-temperature iron phases could not be identified by XRD because of their relatively small concentration. Neither can solid-state reactions leading to amorphous or glassy phases be ruled out, and are likely in view of the increase in the intensity of the amorphous characteristics of the X-ray traces at higher temperatures. Taking into account the thermal analysis results and the thermal evolution of the microstructure, phase transformation becomes significant only above 900°C. This may reflect the geological origin of the volcanic ash, and its previous high temperature thermal history.

III-3-4 : Conclusion

Volcanic ash from Foumbot Petponun site was used to produce inorganic polymers (geopolymers), using sodium hydroxide as the sole alkaline activator. The results show that this low-energy geopolymerisation process can synthesize this natural pozzolanic starting material into viable products with properties suitable for building and low-grade refractories applications.Both the curing conditions (temperature, wet or dry conditions) and the Na_2O/SiO_2 molar ratio were found to influence the development of the compressive strength. Dry curing gave products with superior compressive strength (about 50 MPa) compared to the same materials cured in water. The optimum compressive strength in this material (about 55 MPa) was obtained for samples with $Na_2O/SiO_2 = 0.30$, but higher Na_2O concentrations were found to be detrimental to the mechanical properties. The addition of sand to produce a mortar reduced the compressive strength, but the resulting samples were still within the ASTM recommendations for building materials. The geopolymer products were found to be relatively stable to heat, retaining about 60% of their initial compressive strength and shrinking only slowly up to 900°C. The compressive strengths of the heated materials and their thermal behavior suggest their suitability as low-grade refractories as well as in potential building applications.

III-4: Brief enquiry on environmental concerns and economic practicability

The international scientific community began to address the environmental problems associated with Portland cement manufacture sometime ago; consequently, scientists have been working on a design for new binders for many years now. At the same time, the gradually growing knowledge base on alkali– activated cements and concretes has cast light not only on their benefits in terms of low energy costs and environmental impact, but also their good mechanical performance and long durability (C. Shi et al., 2011).

In Cameroon these studies started after the years 2000 with the Laboratory of physico chemistry of mineral materials of the University of Yaoundé I and the laboratory of the materials analysis of the Local Materials Promotion Authority. Some achievements are highlighted in master theses and papers (Elimbi et al., 2011; Kamseu et al., 2009; Lemougna, 2008, Lemougna et al., 2011). If these studies were favored by the positive environmental impacts of alkaline activated binders reported by a huge number of papers (Davidovits and James, 1984; Rahier et al., 1997; Barbosa et al., 2000; Xu and Van Deventer, 2000; Davidovits, 2002; Barbosa and MacKenzie, 2002; Kamseu et al., 2009; Temuujin et al., 2010) and the positive impact that the possible use of these new binders made up with local aluminosilicates could have on the trade balance, the economic practicability of the experimental results remain a challenge.

III-4-1: Environmental impact

Globally, cement companies are producing nearly two billion tones per year of their product and emitting nearly two billion tones of CO_2 (or 6 to 7% of the planet's total CO_2 emissions) in the process. At this pace, by 2025 the cement industry will be emitting CO_2 at a rate of 3.5 billion tones per year, more or less equal to the total emissions in Europe today (including the transport and energy industries). In light of the foregoing facts, there would appear to be little doubt that alternative binders, less aggressive to the environment, must (at least partially) replace Portland cement (C. Shi et al., 2011). Due to the absence of a high temperature calcination step in geopolymer synthesis, the syntheses processes request less energy. Geopolymer from volcanic ashes present additional advantage as ashes deposits are generally readily accessible and have the advantage that they can be economically mined, with enormous benefits of low cost mining and limited negative environmental impact compared

with traditional open pit quarry-type clay mining (Kamseu et al., 2009). Furthermore, the absence of the need for their thermal activation (generally around 700°C) as required for the type 1/1 clay minerals presents additional advantage in terms of low energy consumption. The overall CO_2 reduction on the synthesis process of geopolymer from ashes and/or slags compared to OPC production is about 80% (Izquierdo et al., 2009; Tailby and MacKenzie, 2010). These indicators suggest that any projects leading to develop the practical use of volcanic ash geopolymers are in line with sustainable development and should be encouraged at every level.

III-4-2: Economic practicability

The main concern for the development of geopolymer materials in Cameroon probably relies on the use of sodium hydroxide which is still relatively expensive in the country, leading to a production cost relatively high for an artisanal scale of production compared to the Portland cement industrially produced locally. Cameroon presently has two industrial Portland cement plants, both for the Lafarge group. One of them located in the littoral Region is just a grinding plant for exported clinker while the second is a complete production unit using limestone and clay available in the northern part of the country (around the plant) to manufacture OPC. They follow the traditional dry process for Portland cement production, using a rotative kiln to make clinker at about 1450°C.

The price of a 50Kg bag of OPC (CPJ 35) in Cameroon is currently about XAF 6000 while a 25 Kg bag of sodium hydroxide is about XAF 15000. For their percentage in weight for soil stabilization, we generally need about two times more cement than sodium hydroxide for more or less the same properties (a 25 Kg bag of sodium hydroxide or a 50 Kg bag of cement will give approximately the same number of building blocks of a particular format).

It is likely that to make the geopolymers materials economically competitive versus OPC in Cameroon, the production need to be industrialized and also possibly various grades of materials should be manufactured and proposed based on the materials final properties (which are also linked to the amount of alkaline used) while considering building standards. However, it is obvious that if the OPC was to be produced in an artisanal scale (with a firing temperature of about 1450°C and two grinding steps of particles mostly below 80 µm), the price of the 50 Kg bag would have been far above XAF 6000. Another economic advantage more general as it plays on the trade balance will be to increase the offer of building materials (with geopolymers building materials) while reducing exported clinker and/or cement which

is also present in the local market (with a price more or less equivalent to the one produced locally). This option would deserve more attention if we have a look over the data of Portland cement importations or other building materials like ceramic tiles in Cameroon over the last decade (Figure 57 and 58):

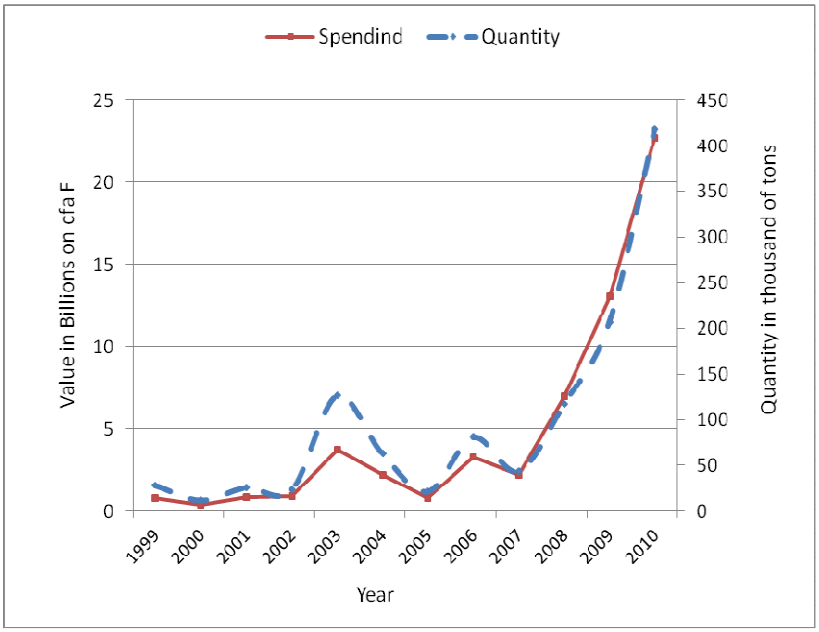

Figure 57: Portland cement importation in Cameroon

Source (National Statistic Institute, Cameroon)

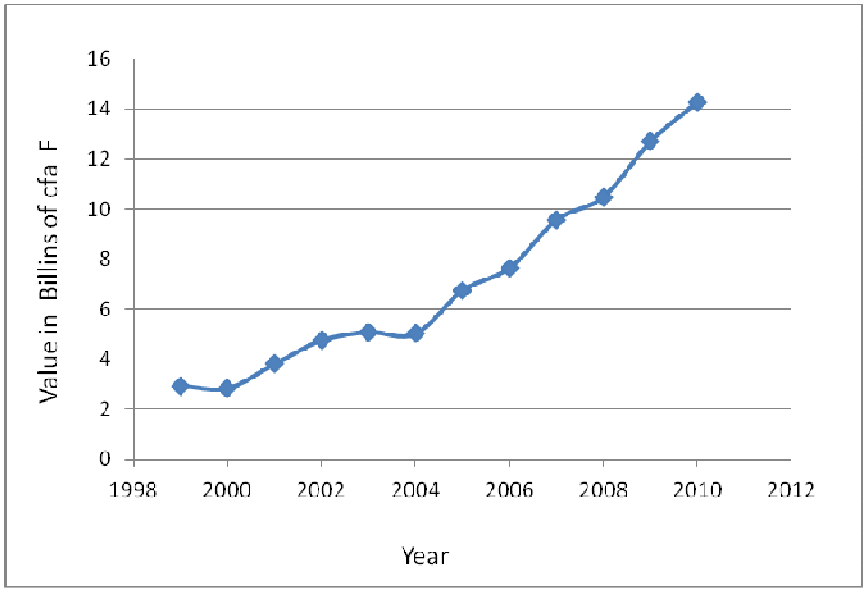

Figure 58: Ceramic tiles importation in Cameroon

Source (National Statistic Institute, Cameroon)

The Figure 57 and 58 show that the loss of currencies associated to building materials importations has considerably increased during the last decade, reaching 23 billions of CFA francs in 2010.

It is also worth pointing out that the cost of sodium hydroxide in Cameroon could be significantly reduced if there is a great need for an industrial process. The use of geopolymerisation for an industrial production of some building materials like ceramics tile was also described to be less time and energy comsuming (Davidovits, 2008) increasing the productivity by a factor of 2 to 5 over the traditional ceramic process. For the particular case of possible industrial production of geopolymer building materials from volcanic ash, the main performance indicators of the competitiveness of the process over traditional OPC production is the possible use of temperatures below 100°C and the need of only one grading step during the the overall production process. The Table 14 summarises the advantages and weaknesses of a possible industrial production of geopolymer versus OPC in Cameroon.

Table 14: Advantages and weaknesses of industrial production of geopolymers versus OPC in Cameroon.

	OPC	**GEOPOLYMERS**
Strengths	Good structural performance	Good structural performance Relatively low CO_2 emission Low energy required
Weakness	High CO_2 emission High temperature (energy) required	Need for chemical alkaline activator and curing environment

Consindering the great potential availability raw materials for geopolymer synthesis in Cameroon, the great loss of currencies due to building materials importation and the successful development of industrial pilot scale production of geopolymer building materials in Austrialia, the need to increase investigations and research projects for a pilot scale industrial production of geopolymer building materials in Cameroon appears to be obvious since its successful implementation can only have a positive impetus on the trade balance and the socioeconomic development.

III-5: Suggestions and Prospects

Previous sections have shown that volcanic ashes from Cameroon can be use to produce geopolymers with potential applications as building materials. For an industrial production, various grades of materials could be synthétised to favor accessibility of materials to a larger part of the population. Due to the need for a high NaOH solution to dissolve the amorphous to semi crystalline volcanic ash and the difficulty to react all the alkaline introduced in the system, its appears to be important to envisage in the possible production process a means to recuperate the non reacted NaOH by proceeding to a post curing in hot water. This will also contribute to reduce the possible effluorescence on the products under utilization while reducing the overall NaOH used for the process (See proposed schematic skech in Figure 59).

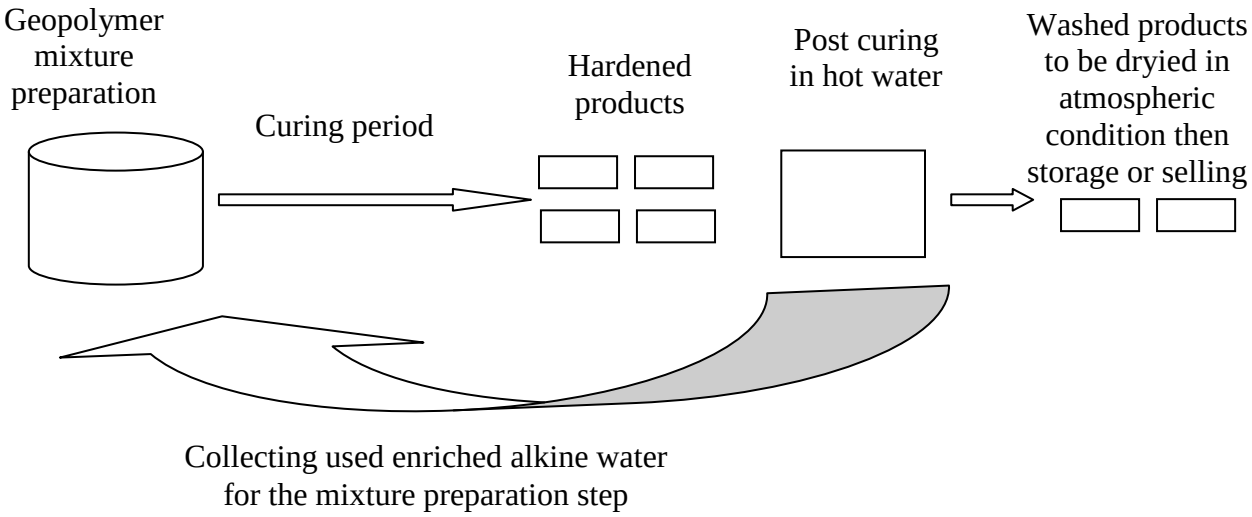

Figure 59: proposal schematic skech for geopolymer preparation from volcanic ash

It was observed that the reactivities of the volcanic ashes used were linked to the amount of amorphous phase, somehow related to the sites where the ashes originated. Consequently setting up in collaboration with the Department of Earth Science, University of Yaoundé I, a database for all unexplored Cameroon's volcanic ashes deposits and their suitability for geopolymer synthesis will contribute to increase the availability of data for a possible wide spread production of geopolymers in Cameroon. Trying to improve materials properties by mixing volcanic ash with other type of aluminosilicate materials such as clays also need to be envisaged meanwhile extending the studies on the durability and other type of natural aluminosilicates materials will also be of interest.

GENERAL CONCLUSION

GENERAL CONCLUSION

The broad aim of this work was to investigate and provide information on the possibilities to produce geopolymers for structural and high temperature applications from Cameroon's volcanic ashes. Four samples of volcanic ashes were used, but the studies were extended only on the more reactive ash (from Foumbot's Petponoun site (Va1)). NaOH, KOH, with or without silicate solution were used as alkaline activator medium.

The four ashes subjected to analysis were found to have great similarities in chemical compositions and the parameter which greatly influenced the reactivity was found to be the amount of amorphous phase, the reactivity of the systems increasing with the amount of these phases in the starting ashes. The compressive strength was found to decrease after immersion of the specimens overnight in water, but was partly or totally recovered after overnight drying at 90°C. The dry compressive strengths of synthesized products from all the ashes were in the range 14-63 MPa suggesting their possible utilization as building materials.

A correlation between the amount of amorphous phase in the starting materials and the final strength after 7 days curing was less obvious to establish at higher concentration of sodium hydroxide. However the trend observed on the values of wet strength at lowest NaOH concentration were similar to the amount of amorphous phase in the starting materials and the sample that globally presented the best strengths also resulted from the more amorphous starting material. The geopolymers consisted of mixture of X-ray amorphous material with crystalline phases. Scanning electron microscopy showed a homogenously distributed mixture of lath-shaped and agglomerated morphologies, with a homogeneous distribution of Si, Al and O in the geopolymer matrix. The FTIR spectra of both the as-synthesized and heated geopolymers show two broad absorbance bands, between 820 -1250 cm^{-1} and 450-730 cm^{-1} assigned to the internal vibrations of Si-O-Si, and Si-O-Al respectively.

A Mössbauer spectroscopy study of the iron present in the volcanic ashes revealed a difference in the solubility of crystalline iron bearing-phases, sugesting that iron behavior during alkali activation relies on its chemical and mineralogical state in the starting materials and is not necessarily deleterious to geopolymer formation.

Extended studies on the more reactive ash showed that KOH promotes more thermally stable materials while NaOH promotes faster reaction rate and better strength. The largest particles only acted as reactive filler while smaller particles dissolved in the activating solution, forming the inorganic polymer matrices. Reducing the amount of coarse particles promoted better reactivity and better compressive strength development for specimens made with

NaOH. Both the curing conditions (temperature, wet or dry conditions) and the Na_2O/SiO_2 molar ratio were found to influence the development of the compressive strength. The addition of sand to produce a mortar reduced the compressive strength, but the resulting samples were still within the ASTM recommendations for building materials.

The geopolymer products were found to present a glass transition between 600-900°C and were relatively stable to heat (shrinking only slowly up to 900°C and retaining about 60% of their initial compressive strength after heating to 900°C). The compressive strengths of the heated materials and their thermal behavior suggest their potential suitability as low-grade refractories as well as in building applications.

However, further investigations in order to improve materials durability and properties by new formulations based on mixing volcanic ash with other materials need to be envisaged. A study on the suitability of volcanic ashes from other deposits as well as other type of aluminosilicate materials is also of interest. Finally the consideration of environmental concerns will be very relevant for a potential production of geopolymers for commercial purpose in Cameroon.

REFERENCES

1. Ahmaruzzaman. M, A review on the utilization of fly ash, Progress in Energy and Combustion Science, 36, **2010**, 327–363.

2. Akasaka M, ^{57}Fe Mössbauer Study of Clinopyroxenes in the Join $CaFe^{3+}$ $AlSiO_6$-$CaTiAl_2O_6$. Phys Chem Mineral 9, **1983**, 205-211.

3. Aliprandi G., Matériaux réfractaires et céramiques technique, Septima, Paris, **1979**, 612 p.

4. Andji J.Y.Y., Abba Toure A, Kra G, Jumas J.C, Yvon J, Blanchart P, Iron role on mechanical properties of ceramics with clays from Ivory Coast, Ceramics International 35, **2009**, 571–577.

5. Bancroft MG, Burns RG, Stone A J Applications of the Mössbauer effect to silicate mineralogy-II. Iron silicates of unknown and complex crystal structures. Geochim Cosmochim Acta 32, **l968,** 547 – 559.

6. Bancroft M G, Maddock AG, Burns RG, Application of the Mössbauer effect to silicate mineralogy-I. Iron silicates of known crystal structure. Geochim Cosmochim Acta 31, **1967**, 2219- 2246.

7. Barbosa F.F. Valeria, MacKenzie J.D. Kenneth, Thaumaturgo, C, Synthesis and characterisation of materials based on inorganic polymers of alumina and silica: sodium polysialate polymers, Internationl Journal of Inorganic Materials 2, **2000**, 309-317.

8. Barbosa F.F. Valeria, MacKenzie J.D. Kenneth, Thermal behaviour of inorganic geopolymers and composites derived from sodium polysialate, Materials Research Bulletin 38, **2003a**, 319-331.

9. Barbosa V.F.F., MacKenzie K.J.D., Synthesis and thermal behaviour of potassium sialate geopolymers, Materials Letters 57, **2003b,** 1477–1482.

10. Bell J.L., Driemeyer P.E., Kriven W.M., Formation of ceramics from metakaolin-based Geopolymers: Part I- Cs-Based Geopolymer, Journal of the American Ceramic Society, 92, 1, **2009a**, 1-8.

11. Bell J.L., Driemeyer P.E., Kriven W.M., Formation of Ceramics from Metakaolin-Based Geopolymers. Part II: K-Based Geopolymer, Journal of the American Ceramic Society, 92, 3, **2009b**, 607-615.

12. Berg L G, Demidenko B A, Remiznikova V A and Nizamov M S, 'Unfired finishing building materials based on kaolin'. Stroitel'nye Materialy, **1970**, 10, 22.

13. Bijocka C., Tusset J., Messi A., Perra J., Etude et evaluation de l'activité pouzzolanique des pouzzolanes de Djoungo (Cameroun). Ann. Fac. Sc. HSI., Chimie et Sciences de la terre, **1993**, 133-145.

14. Boutterin C., Davidovits J., Réticulation Géopolymérique (LTGS) et Matériaux de Construction, géopolymère, 1, **2003** 79-88.

15. Buchwald. A, Hohmann. M, Posern K, Brendler, E., The suitability of thermally activated illite/smectite clay as raw material for geopolymer binders, Applied Clay Science 46, **2009**, 300–304.

16. Cheng T. W, Chiu J .P, Fire-resistant geopolymer produced by granulated blast furnace slag, Miner. Eng. 16, **2003**, 205–210.

17. Cioffi R., Maffucci L., Santoro L., Optimization of geopolymer synthesis by calcination and polycondensation of a kaolinitic residue, Resources Conservation and Recycling, 40, **2003**, 27-28.

18. Dali Bondar, C.J. Lynsdale, Neil B. Milestone, N. Hassani, A.A. Ramezanianpour, Effect of type, form, and dosage of activators on strength of alkali-activated natural pozzolanas, Cement & Concrete Composites 33, **2011**, 251–260.

19. Davidovits J., 30 Years of Successes and Failures in Geopolymer Application. Market Trends and Potential Breakthroughs, Geopolymer Conference, October 28-29, Melbourne, Australia, **2002**.

20. Davidovits J. Geopolymer : inorganic polymeric new materials, journal of thermal analysis, 37, **1991**, 1633-1656.

21. Davidovits .J., Geopolymers: Man-Made Rock Geosynthesis and the Resulting Development of Very Early High Strength Cement, Materials Education, 16, **1994a**, 91-139.

22. Davidovits J. and James C., Low Temperature Geopolymeric Setting of Ceramics (LTGS)(IV): Dolomite presence is proof of LTGS in Cyprus Amphorae, Symposium on Archaeometry, Smithsonian Institution, Washington D.C, USA, Abstracts, **1984**, 24-25.

23. Davidovits J., Global Warming Impact on cement and Aggregates Industries, World Ressource Review, 6, 2, **1994b**, 263-276.

24. Davidovits. J., Geopolymer Chemistry and Application, 2nd edition, Institut Géopolymère, **2008**, 586 p.

25. Davidovits Joseph, Geopolymers of the First Generation: SILIFACE-Process, Geopolymer, **1988**, 1, 49-67.

26. Dedecek J., Tvaruzkova Z., Sobalik Z., Metal Ions as Probes for Characterization of Geopolymer Materials, Journal of the American Ceramic Society, 91, 9, **2008**, 3052-3057.

27. De Silva .P, Sagoe-Crenstil. K, Sirivivatnanon .V, Kinetics of geopolymerization: Role of Al_2O_3 and SiO_2, Cement and Concrete Research 37, **2007**, 512–518.

28. Dennis V. Perepelitsa, Mössbauer Spectroscopy of 57Fe, MIT Department of Physics, 2007.

29. Diaz. E.I, Allouche E.N., Eklund S., Factors affecting the suitability of fly ash as source material for geopolymers, Fuel, 89, **2010**, 992-996.

30. Dimitrios Panias, Ioanna P. Giannopoulou , Theodora Perraki, Effect of synthesis parameters on the mechanical properties of fly ash-based geopolymers, Colloids and Surfaces A: Physicochem. Eng. Aspects, 301, **2007**, 246–254.

31. Duxson P., Fernandez-Jimérez A., Provis J. L., Lukey, G.C. Palomo A., van Deventer J. S. J., Geopolymer technology: the current state of the art, Advances in geopolymer science and technology, 42, **2007a**, 2917- 2933.

32. Duxson P., Mallicoat S.W., Lukey G.C., Kriven W.M., van Deventer J.S.J., The effect of alkali and Si/Al ratio on the development of mechanical properties of metakaolin-based geopolymers, colloids and surfaces, 292, **2006a**, 8-20.

33. Duxson . P, The structure and thermal evolution of metakaolin geopolymers, ph.d Engineering Thesis, University of Melbourne, Australia, **2006**.

34. Duxson . P, Lukey G.C., van Deventer J.S.J., Thermal evolution of metakaolin geopolymers: Part 1 – Physical evolution, J. Non-Cryst. Sol, 352, **2006b**, 5541–5555.

35. Duxson Peter, Provis John L., Lukey Grant C., Mallicoat Seth W., Kriven Waltraud M., van Deventer Jannie S.J., Understanding the relationship between geopolymer composition, microstructure and mechanical properties, Colloids and Surfaces A: Physicochem. Eng. Aspects 269, **2005a**, 47–58.

36. Duxson Peter, Provis John L, Lukey Grant C, Separovic Frances, and van Deventer Jannie S. J, 29Si NMR Study of Structural Ordering in Aluminosilicate Geopolymer Gels, Langmuir, **2005b**, 21, 3028-3036.

37. Duxson P, Provis J.L,. Lukey G. C,. van Deventer J.S.J, The role of inorganic polymer technology in the development of ‘green concrete’, Cement and Concrete Research 37, **2007b**, 1590–1597.

38. Dyson D.J, X-Ray and Electron Diffraction Studies in Materials Sciences, MANEY, **2004**,364p

39. Elimbi A, Tchakoute H.K, Njopwouo D, Effects of calcination temperature of kaolinite clays on the properties of geopolymer cements, Construction and Building Materials, doi:10.1016/j.conbuildmat2010.12.055, **2011**.

40. Elimbi A., Tchakoute H.K., Kondoh M., Dika Manga J., Thermal behavior and characteristics of fired geopolymers produced from local Cameroonian metakaolin, Ceramics International, 40, 3, **2014,** 4515-4520.

41. Fernando Pacheco-Torgal, Joa˜o Castro-Gomes, Said Jalali, Alkali-activated binders: A review Part 1. Historical background, terminology, reaction mechanisms and hydration products, Construction and Building Materials, 22, **2008**, 1305–1314.

42. Greenwood NN, Gibb TC, Mössbauer Spectroscopy. Chapman and Hall, London, **1971** Ch 10.

43. Habert G, d'Espinose de Lacaillerie J.B, Roussel N, An environmental evaluation of geopolymer based concrete production: reviewing current research trends, Journal of Cleaner Production 19, **2011**, 1229-1238.

44. Izquierdo M., Querol .X, Davidovits J., Antenucci. D, H. Nugteren, Fernandez-Pereira .C, Coal fly ash-slag-based geopolymers: Microstructure and metal leaching, J. Hazardous Mater, 166, **2009**, 561–566.

45. Izquierdo Maria, Querol Xavier, Phillipart Charles , Antenucci Diano, Towler Mark, The role of open and closed curing conditions on the leaching properties of fly ash-slag-based geopolymers, Journal of Hazardous Materials, 176, **2010**, 623–628.

46. Jouenne C.A., Traité de céramique et matériaux, Septima, Paris, **2001**, 657 p.

47. Ka-Bik Yip Christina, The role of calcium in geopolymerisation, Ph.D Thesis, University of Melbourne, Melbourne, Australia, **2004**.

48. Kamseu E., Leonelli C.,. Perera D.S, Melo U.C., Lemougna P.N., Investigation of volcanic ash-based geopolymers as potential building materials, Interceram; 58, 2, **2009**, 136-140.

49. Karfa T., Frittage à basse température d'une argile kaolinitique du Burkina Faso. Transformations thermiques et réorganisations structurales. Thèse de Doctorat, Univ. De Limoges, France **2003**.

50. Khale .D, Chaudhary .R, Mechanism of geopolymerization and factors influencing its development: a review, J. Mater. Sci, 42, **2007**, 729–746.

51. Kolousek David, Brus Jiri, Urbanova Martina, Andertova Jana, Hulinsky Vaclav, Vorel Jindrich, Preparation, structure and hydrothermal stability of alternative (sodium silicate-free) geopolymers, J Mater Sci, 42, **2007**, 9267–927.

52. Komnitsas K., Zaharaki D., Geopolymereisation: a review and prospects for minerals industry, Minerals engineering, 20, **2007**, 1261-1277.

53. Kong L.Y. Daniel, G Jay., Sanjayan, Damage behavior of geopolymer composites exposed to elevated temperatures, Cement & Concrete Composites, 30, **2008**, 986–991.

54. Kong L.Y., Daniel, Sanjayan .G.Jay, Effect of elevated temperatures on geopolymer paste, mortar and concrete, Cem. Concr. Res, 40, **2010,** 334–339.

55. Kovalchuk G., Ferna´ndez-Jime´nez A., Palomo A., Alkali-activated fly ash: Effect of

thermal curing conditions on mechanical and microstructural development – Part II, Fuel, 86, **2007**, 315–322.

56. Lecomte. I, Henrist. C, Li´egeois. M, Maseri. F, Rulmont. A, Cloots. R, (Micro)-structural comparison between geopolymers, alkali-activated slag cement and Portland cement, Journal of the European Ceramic Society 26, **2006**, 3789–3797.

57. Lee W.K.W., van Deventer J.S.J., The interface between natural siliceous aggregates and geopolymers, Cement and concrete research, 34, **2003**, 195-206.

58. Lee William K., Solid-Gel Interactions in Geopolymers, Ph.D Thesis, University of Melbourne, Melbourne, Australia, **2002**.

59. Lemougna N. P, MacKenzie K. J.D., Melo U.F. C, Synthesis and thermal properties of inorganic polymers (geopolymers) for structural and refractory applications from volcanic ash, Ceramics International, 37, **2011**, 3011-3018.

60. Lemougna N. P, Réticulation géopolymérique à basse temperature de quelques aluminosilicates, Mémoire de D.E.A en Chimie Inorganique, Université de Yaoundé I, Yaoundé, Cameroun, **2008**.

61. Leonelli C., Kamseu E., Boccaccini D.N., Melo U.C., Rizzuti A., Billong N., Misselli P., Volcanic ash as alternative raw materials for traditional vitrified ceramic products, Advances in Applied Ceramics, 106 , 1, **2007**, 1-7.

62. MacKenzie K.J.D and Smith M.E, Multinuclear Solid-state NMR of Inorganic Materials, Pergamon Materials Series (Series Editor: R.W.CAHN), **2002**, 727 p.

63. MacKenzie K.J.D., O'Leary B., Inorganic polymers (geopolymers) containing acid–base indicators as possible colour-change humidity indicators, Materials Letters, 63, **2009**, 230–232.

64. MacKenzie J. D. Kenneth, Rahner Nils, Smith E Mark, Wong Alan, Calcium-containing inorganic polymers as potential bioactive materials, J Mater Sci, 45, **2010**, 999–1007.

65. MacKenzie K.J.D., Utilization of Non-Thermally Activated Clays in the Production of Geopolymers. Chapter 14 in "Geopolymers: structure, processing, properties and applications", Ed. J. Provis and J. van Deventer, Woodhead, Cambridge, **2009**, 294-314.

66. MacKenzie J. D. Kenneth, Smith E Mark., Wong Alan, A multinuclear MAS NMR study of calcium-containing aluminosilicate inorganic polymers, J. Mater. Chem, 17, **2007**, 5090–5096.

67. Meinhold R. H., MacKenzie K. J. D., Brown I. W. M., Thermal reactions of kaolinite studied by solid state 27-Al and 29- Si NMR, Journal of Materials Science Letters, 4, **1985**, 163-166.

68. Melo U. C. and Ndigui B., Activité pouzzolanique des déchets de briques et tuiles cuites, Silicate Industriel, 70, 1-2, **2004**, 11-18.

69. Miladinovic. Z, Zakrzewska. J, Kovacevic. B, Bacic. G, Monitoring of crystallization processes during synthesis of zeolite A by in situ ^{27}Al NMR spectroscopy, Materials Chemistry and Physics, 104, **2007,** 384–389.

70. Mysen BO, The structural behavior of ferric and ferrous iron in aluminosilicate glass near meta-aluminosilicate joins. Geochim Cosmochim Acta 70, **2006**, 2337–2353.

71. Nota di Paolo Ballirano, Adriana Maras e Francesco Burragato, dal Socio A. Mottana, Mineralogia-Sodalite from Vetralla (Roman potassic province) and Bancroft (Ontario, Canada), Rend. Fis Acc Linceis 9, 2, **1991**, 361-369.

72. Nugteren Henk, Secondary industrial minerals from coal fly ash and aluminium anodising waste solutions, PhD thesis, TuDelft University of Technology, Delft, Netherland, **2010**.

73. Ntep Gweth P., Dupuy J. J., Matip O., Fombutu Fogakoh A., Kalngui E., Ressources Minérales du Cameroun, Ministère des Mines, de l'Eau et de l'Energie, Yaoundé, Cameroun, **2001**.

74. Obonyo E, Kamseu E, Melo U C, Leonelli C, Advancing the Use of Secondary Inputs in Geopolymer Binders for Sustainable Cementitious Composites: A Review, Sustainability, doi:3390/su3020410.10, 3, **2011**, 410-423.

75. O'Connor J. Sean, MacKenzie J. D. Kenneth, Synthesis, characterisation and thermal behaviour of lithium aluminosilicate inorganic polymers, J Mater Sci, 45, **2010**, 3707–3713.

76. Wandji P. et Tchoua F.M., Le coefficient de Feret : application à la détermination des propriétés pouzzolaniques des projection volcaniques de Foumbot (Ouest Cameroun), Ann Fac Sc, Chim, vol. 2, **1988**, 201-216.

77. Perera S Dan, Cashion D John, Blackford G Mark, Zhang Zhaoming, Vance R. Eric, Fe speciation in geopolymers with Si/Al molar ratio of ~2, Journal of the European Ceramic Society, 27, **2007**, 2697–2703.

78. Provis J.L., Yong C.Z., Duxson P., van Deventer J.S.J., Correlating mechanical and thermal properties of sodium silicate-fly ash geopolymers, Colloids and surfaces A: physicochem.Eng. Aspects 336, **2009**, 57-63.

79. Provis John Lloyd, Modelling the Formation of Geopolymers, Ph.d Engineering Thesis, University of Melbourne, Melbourne, Australia, **2006**.

80. Radhi. H, Evaluating the potential impact of global warming on the UAE residential buildings – A contribution to reduce the CO_2 emissions, Building and Environment, **2009**, 44, 2451–2462.

81. Rahier . H, Denayer j. F., Van Mele. B, Low-temperature synthesized aluminosilicate glasses part IV modulated dsc study on the effect of particle size of metakaolinite on the production of inorganic polymer glasses, Journal of Materials Science 38, **2003**, 3131 – 3136.

82. Rahier. H, Van Mele B, Biesemans M, Wastiels.J, Wu. X, Low-temperature synthesized aluminosilicate glasses. Part I Low-temperature stoichiometry and structure of a model compound, Journal of Material science, 31,**1996a**, 71-79.

83. Rahier. H, Van Mele B, Wastiels.J, Low-temperature synthesized aluminosilicate glasses. Part II Rheological transformations during low-temperature cure and high-temperature properties of a model compound, Journal of Material science, 31, **1996b**, 80-85.

84. Rahier. H, Simon W, Van Mele B, M. Biesemans, Low-temperature synthesized aluminosilicate glasses. Part III Influence of the composition of the silicate solution on production, structure and properties, Journal of Material science, 32, **1997**, 2237-2247.

85. Rahier. H, Wullaert. B, Van Mele. B, Influence of the degree of dehydroxylation of kaolinite on the properties of aluminosilicate glasses, Journal of Thermal Analysis and Calorimetry, 62, **2000**, 417-427.

86. Rahier .H, Wastiels .J, Biesemans .M, Willlem .R , Van Assche .G, Van Mele .B, Reaction mechanism, kinetics and high temperature transformations of geopolymers, J Mater Sci, 42, **2007**, 2982–2996.

87. Ravikumar Deepak, Peethamparan Sulapha, Neithalath Narayanan, Structure and strength of NaOH activated concretes containing fly ash or GGBFS as the sole binder, Cement & Concrete Composites 32, **2010,** 399–410.

88. Rossano S, Behrens H, Wilke M Advanced analyses of 57Fe Mössbauer data of alumino-silicate glasses. Phys Chem Mineral 35, **2008**, 77–93.

89. Rowles. M R, Hanna J V, Pike K J, Smith M E, and O'Connor B H, 29Si, 27 Al, 1H and 23Na MAS Study of the bonding character in aluminosilicate Inorganic Polymers, Applied Magnetic Resonance, 22, **2007**, 663-689.

90. Ruscher Claus H., Mielcarek Elzbieta M., Wongpa Jakrapan, Jaturapitakkul Chai, Jirasit Fongjan and Lohaus Ludger, Silicate-, aluminosilicate and calciumsilicate gels for building materials: chemical and mechanical properties during ageing, Eur. J. Mineral, 23, **2011,** 111–124.

91. Rüscher C. H., Mielcarek E., Lutz W., Ritzmann A. and Kriven W. M., Weakening of Alkali-Activated Metakaolin During Aging Investigated by the Molybdate Method and Infrared Absorption Spectroscopy, J. Amer. Ceram. Soc., 93, **2010**, 2585-2590.

92. Sara L. Campbell and Javier M. G. Duarte, Using Mössbauer Spectroscopy to Measure Properties of Iron 57 Nuclei, MIT Department of Physics , **2008.**

93. Schmückera Martin, MacKenzie J.D Kenneth., Microstructure of sodium polysialate siloxo geopolymer, Ceramics International 31, **2005**, 433–437.

94. Shi C,. Fernández Jiménez A, Palomo A , New cements for the 21st century: The

pursuit of an alternative to Portland cement, Cement and Concrete Research 41, **2011**, 750–763.

95. Sigg J., Les produits de terre cuites, Septima, Paris, **1991**, 494 P.

96. Sindhunata, A conceptual model of geopolymerisation, Ph.D Thesis, University of Melbourne, Melbourne, Australia, **2006**.

97. Singh P. S., Trigg M., Burgar I., Bastow T., Geopolymer formation processes at room temperature studied by ^{29} Si and ^{27}Al MAS-NMR, 396, **2005**, 392-402.

98. Singh P.S., Bastow T., Trigg M., Outstanding problems posed by nonpolymeric particulates in the synthesis of a well-structured geopolymeric material, Cement and Concrete Research, 34, **2004**, 1943-1947.

99. Sofi M., van Deventer J. S. J., Mendis P. A., Lukey G.C. Engineering properties of inorganic polymer concretes, Cement and Concrete Research, 37, **2007**, 251-257.

100. Spiering B, Seifert FA, Iron silicate glasses of granitic composition: a Mössbauer spectroscopic study. Contrib Miner Petrol 90, 1985, 63-73.

101. Subaer, Influence of aggregate on the microstructure of geopolymer, Ph.D Thesis, Curtin University of Technology, Western Australia, **2004**.

102. Sumajouw M. D.J., Rangan B. V., Low-calcium fly ash-based geopolymer concrete: reinforced beams and columns, Research Report GC 3, Faculty of Engineering, Curtin University of Technology, Perth, Australia, 2**006**.

103. Swanepoel J.C., Strydom C.A., Utilisation of fly ash in a geopolymeric material, Applied Geochemistry, vol. 17, **2002**, 1143-1148.

104. Tailby J., MacKenzie K.J.D., Structure and mechanical properties of aluminosilicate geopolymer composites with Portland cement and its constituent minerals, Cem. Concrete Res. 40, **2010**, 787-794.

105. Temuujin J., van Riessen A., MacKenzie K.J.D., Preparation and characterisation of fly ash based geopolymer mortars, Construction and Building Materials, 24, **2010**, 1906–1910.

106. Temuujin J., Williams R.P., van Riessen A., Effect of mechanical activation of fly ash on the properties of geopolymer cured at ambient temperature, J. Mater. Proc. Technol. 209, **2009**, 5276–5280.

107. Thompson A, Rancourt DG, Chadwick OA, Chorover J, Iron solid-phase differentiation along a redox gradient in basaltic soils. Geochim Cosmochim Acta 75, 2011, 119–133.

108. van Cromphaut C, de Resende VG, De Grave E, Van Alboom A, Vandenberghe RE, Klingelhöfer G, Characterisation of the magnetic iron phases in Clovis Class rocks in Gusev crater from the MER Spirit Mössbauer spectrometer, Geochim Cosmochim Acta

71, 2007, 4814–4822.

109. van Jaarsveld J.G.S and van Deventer J.S.J, The potential use of geopolymeric materials to immobilize toxic metals: Part I. Theory and applications, Minerals Engineering, vol 10, no. 7, **1996**, 659-669.

110. van Jaarsveld J.G.S., Van Deventer J.S.J., Lukey G.C. The effect of composition and temperature on the properties of fly ash-and kaolinite-based géopolymers, Chemical Engineering journal, vol 89, **2002**, 63-73.

111. van Jaarsveld J.G.S., van Deventer J.S.J., Lukey G.C., The characterization of source materials in fly ash-based geopolymers, Materials Letters, vol. 57, **2003**, 1272-1280.

112. Verdolotti L., Iannace S., Lavorgna M., Lamanna R., Geopolymerization reaction to consolidate incoherent pozzolanaic soil, J. Mater. Sci. 43, **2008**, 865–873.

113. Wallah S. E., Rangan B. V., Low-calcium fly ash-based geopolymer concrete: long-term properties, Research Report GC 2, Faculty of Engineering, Curtin University of Technology, Perth, Australia, **2006**.

114. Wandji Pierre et Tchoua Felix, Les projections volcaniques de Foumbot (Ouest-Cameroun): Pétrogarphie et Géochimie, Syllabus, Série Sciences, 1, **1989**, 5-33.

115. Wang H., Li H., Yan F., Synthesis and tribological behaviour of metakaolinite-based geopolymer composites, Materials letters, 59, **2005**, 3976-3981.

116. Xu Hua, Geopolymerisation of aluminosilicate minerals, Ph.D engineering Thesis, University of Melbourne, Melbourne, Australia, **2002**.

117. Xu Hua, van Deventer J.S.J., The geopolymerisation of alumino-silicate minerals, International journal of mineral processing, 59, **2000**, 247-266.

118. Zhang Bo, MacKenzie K. J. D., Bigley C., Ryan M.J., BrownI.W.M. Phase Development of NaOH Activated Blast Furnace Slag Geopolymers Cured at 90°C, American Institute of Physics, 978-0-7354-0688-9/09, **2009**.

119. Zuhua. Z, Xiao. Y, Huajun .Z, Yue. C, Role of water in the synthesis of calcined kaolin-based geopolymer, Applied Clay Science 43, **2009**, 218–223.

ANNEXES

I : Weight loss during the curing process at 90°C

Time / Composition	1 day	2day	3day	6day	7day
	Weight loss (%)				
Va-K	6,82	8,68	10,16	13,02	13,65
Va-K0.18	5,24	6,75	7,94	10,63	11,15
Va-K-Sil	6,85	8,94	10,77	12,12	14,29
Va-Na	2,58	4,74	6,81	11,57	12,38
Va-NaSil	2,56	4,13	5,32	8,08	8,45
Va-Na+K	4,32	6,41	8,06	12,56	13,28
Va-Na+Ksil	5,26	8,78	11,21	12,46	13,74

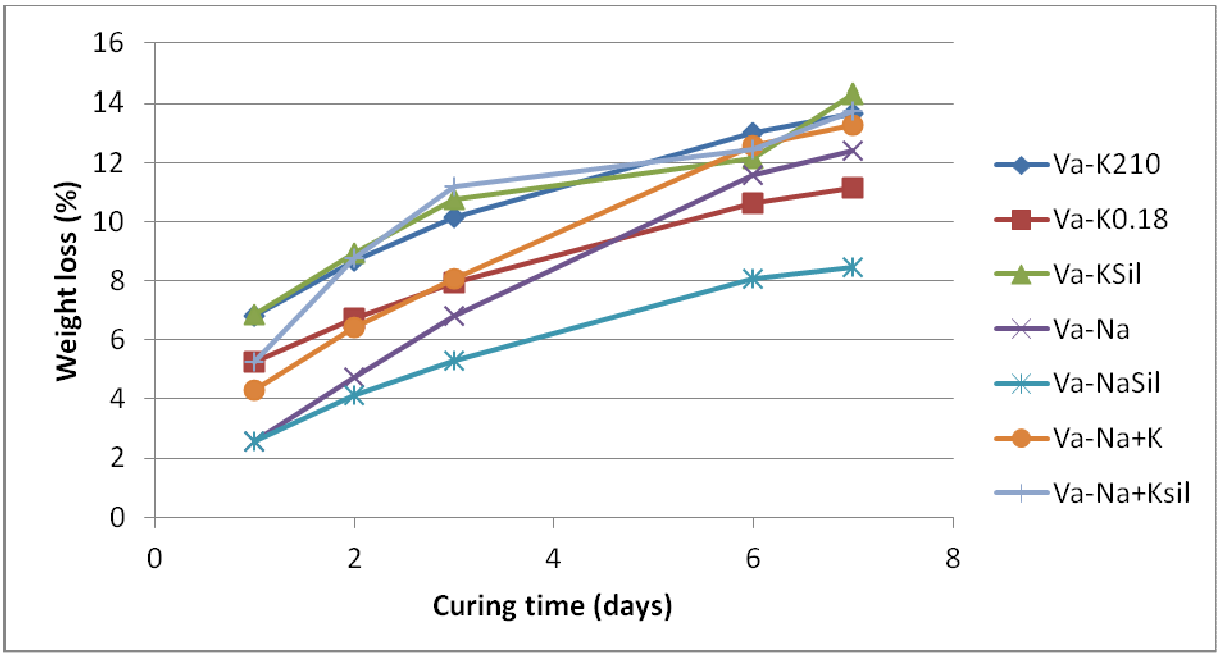

Observation: The mass of water represents about 16% (210g/1330g) of the total mass of the initial geopolymer mixture for Va-Na specimen and about 15 % (210g/1378g) for K specimen. After seven days curing, the remaining water is about 3% of the specimen mass for Va-Na versus about 1.5% for Va-K.

II: X-Ray indexing of volcanic ashes

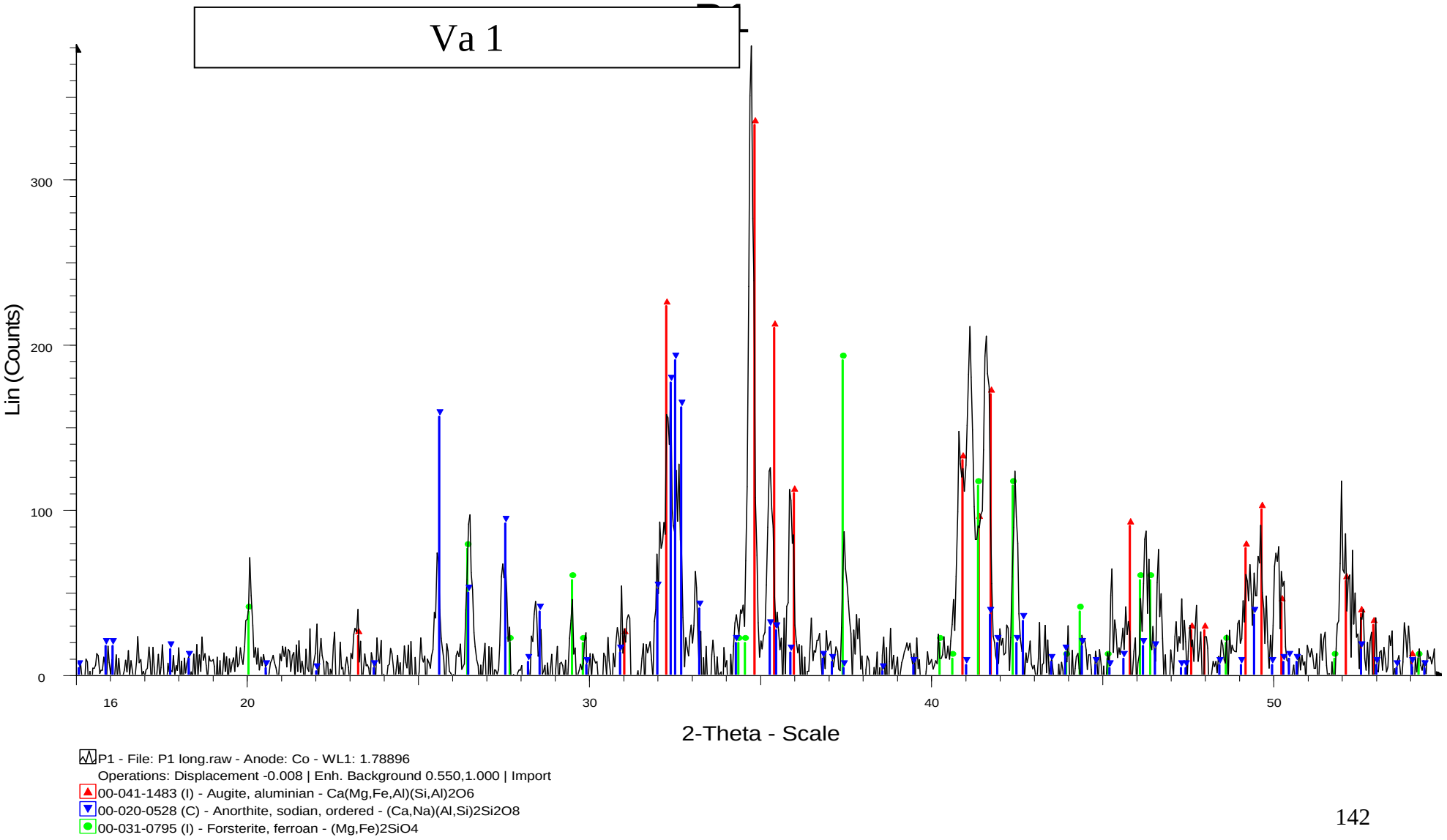

Va 2

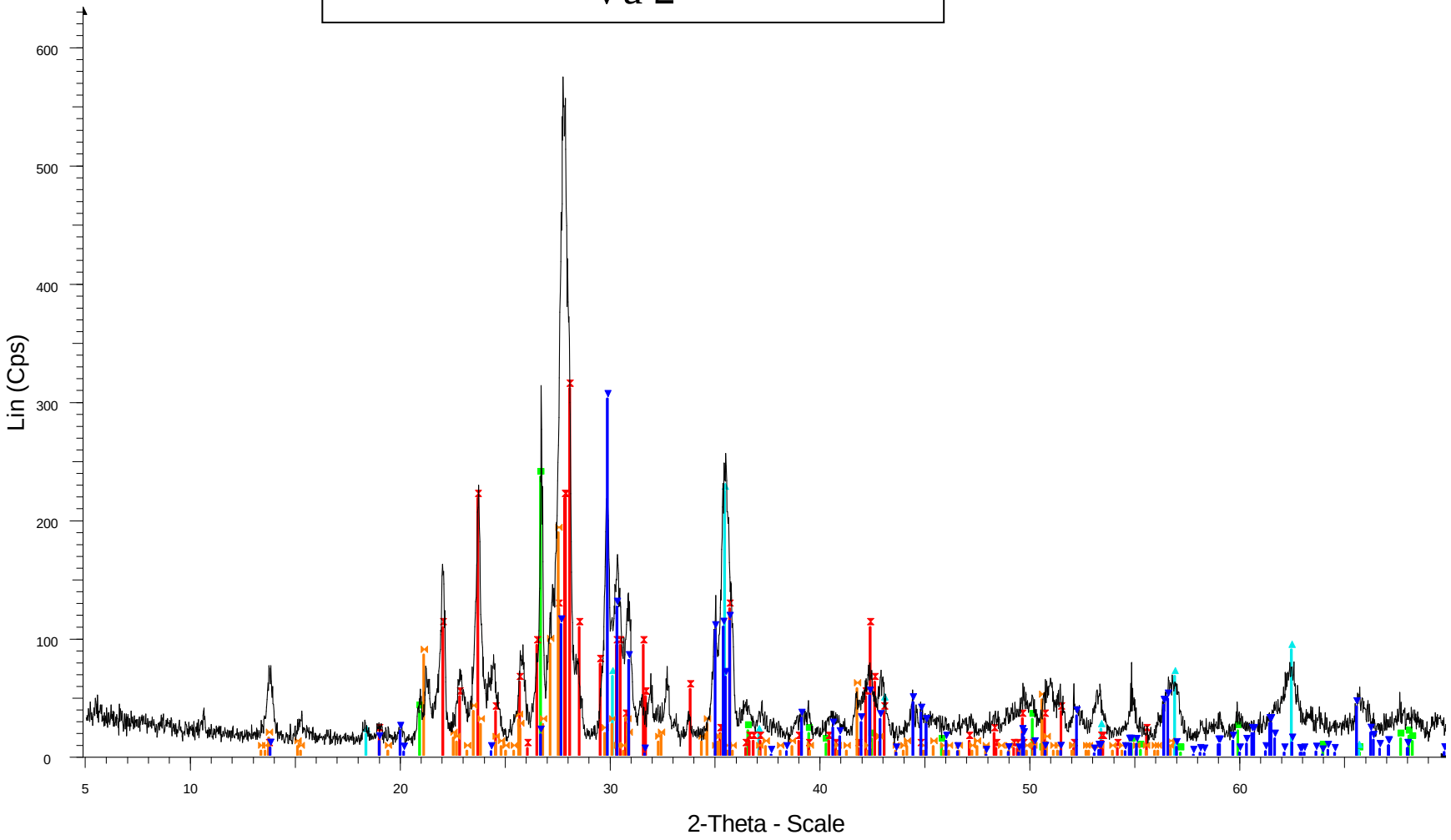

Sample11 - Step: 0.020 °- Step time: 1.2 s - Anode : Cu - WL1: 1.5406 - Company: ULB Matières et Matériaux - Creation: 19/12/2011 10:54:32

00-046-1045 (*) - Quartz, syn - SiO2 - Hexagonal - a 4.91344 - b 4.91344 - c 5.40524 - alpha 90.000 - beta 90.000 - gamma 120.000 - Primitive - P3221 (154) - 3 - 113.010

01-070-3753 (C) - Augite - (CaMg0.74Fe0.25)Si2O6 - Monoclinic - a 9.75000 - b 8.90100 - c 5.27400 - alpha 90.000 - beta 106.000 - gamma 90.000 - Base-centered - C2/c (15) - 4 - 439.972

00-019-0629 (*) - Magnetite, syn - Fe+2Fe2+3O4 - Cubic - a 8.39600 - b 8.39600 - c 8.39600 - alpha 90.000 - beta 90.000 - gamma 90.000 - Face-centered - Fd-3m (227) - 8 - 591.858

00-018-1202 (I) - Anorthite, sodian, intermediate - (Ca,Na)(Si,Al)4O8 - Triclinic - a 8.17600 - b 12.86500 - c 7.10200 - alpha 93.450 - beta 116.100 - gamma 90.500 - Base-centered - C-1 (0) - 4 - 669.111

00-019-0932 (I) - Microcline, intermediate - KAlSi3O8 - Triclinic - a 8.56000 - b 12.97000 - c 7.21000 - alpha 90.300 - beta 116.100 - gamma 89.000 - Base-centered - C-1 (0) - 4 - 718.739

Va 3

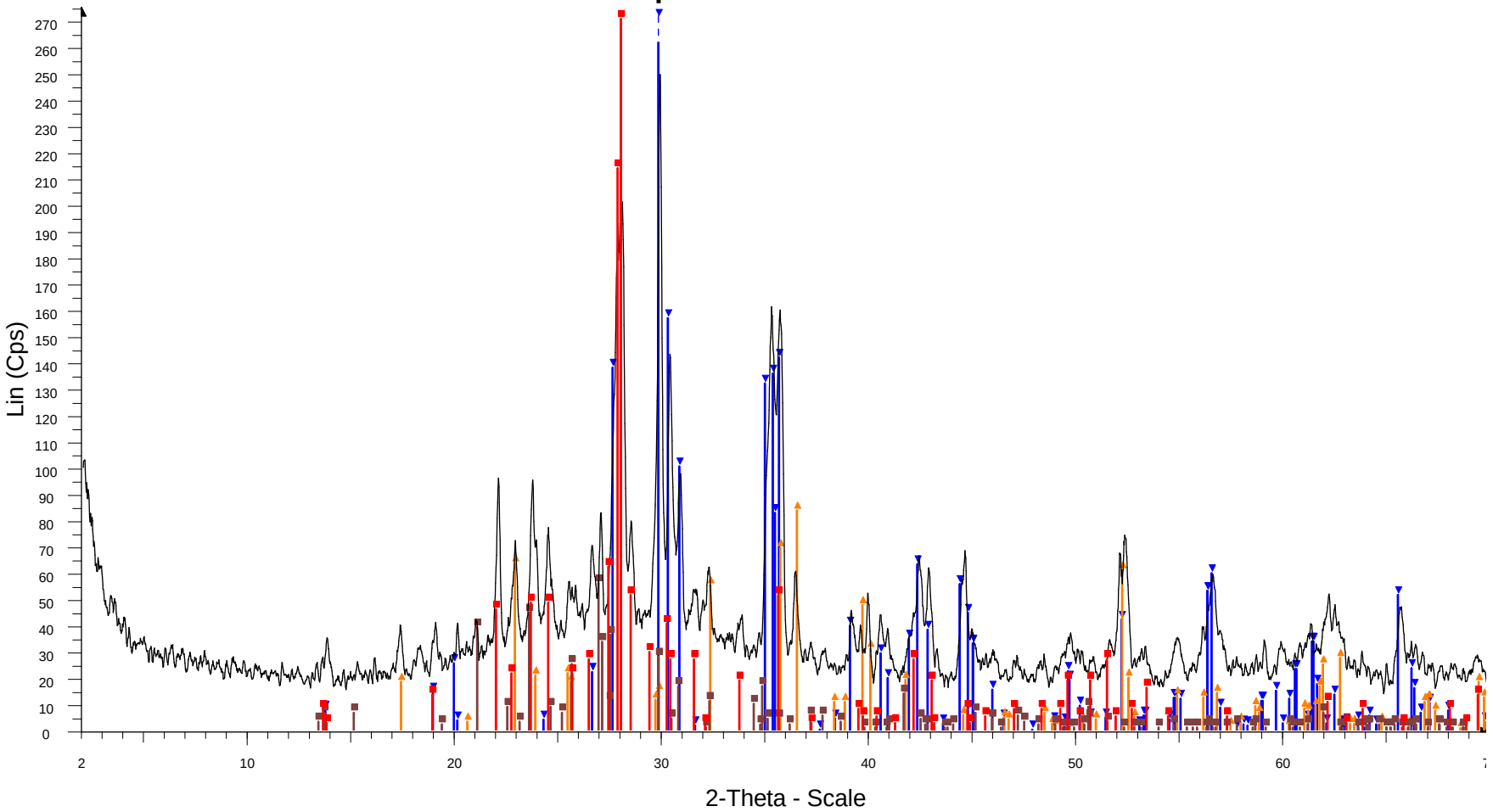

Sample9 Cendres - Step: 0.020 °- Step time: 1.2 s - Anode: Cu - WL1: 1.5406 - Generator kV: n.a. - Generator mA: n.a. - Divergence slit: n.a. - Company: ULB Matières et Matériaux - Creation: 17/08/2011 16:34:53

00-041-1481 (I) - Anorthite, sodian, disordered - (Ca,Na)(Si,Al)4O8 - Triclinic - a 8.18130 - b 12.87400 - c 7.09700 - alpha 93.378 - beta 115.968 - gamma 90.776 - Primitive - P-1 (2) - 4 - 670.218

01-070-3753 (C) - Augite - (CaMg0.74Fe0.25)Si2O6 - Monoclinic - a 9.75000 - b 8.90100 - c 5.27400 - alpha 90.000 - beta 106.000 - gamma 90.000 - Base-centered - C2/c (15) - 4 - 439.972

00-034-0189 (*) - Forsterite, syn - Mg2SiO4 - Orthorhombic - a 5.98170 - b 10.19780 - c 4.75530 - alpha 90.000 - beta 90.000 - gamma 90.000 - Primitive - Pmnb (62) - 4 - 290.074

00-031-0966 (*) - Orthoclase - KAlSi3O8 - Monoclinic - a 8.55600 - b 12.98000 - c 7.20500 - alpha 90.000 - beta 116.010 - gamma 90.000 - Base-centered - C2/m (12) - 4 - 719.122

Va 4

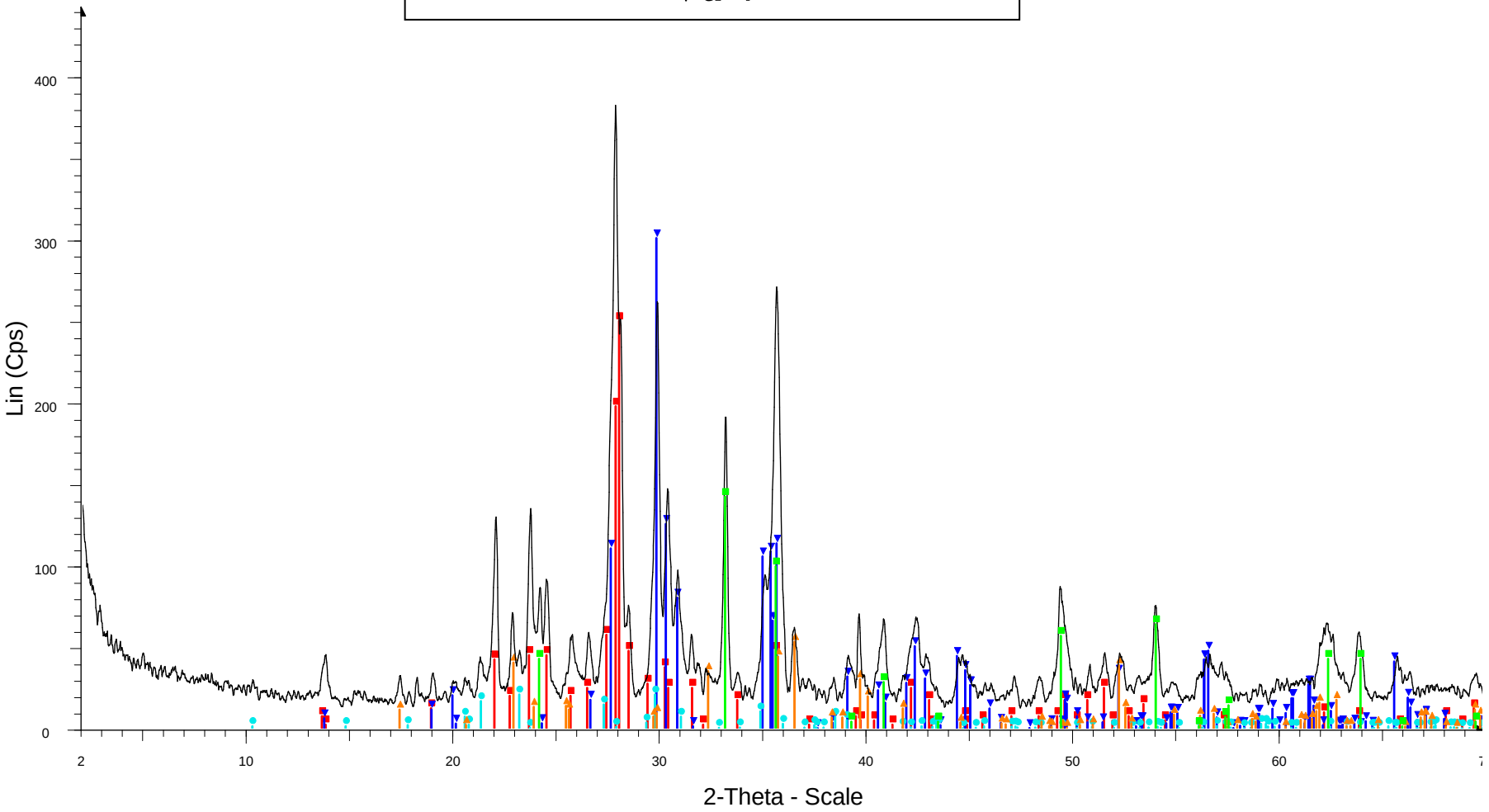

Sample10 Cendres - Step: 0.020 °- Step time: 1.2 s - Anode: Cu - WL1: 1.5406 - Generator kV: n.a. - Generator mA: n.a. - Divergence slit: n.a. - Company: ULB Matières et Matériaux - Creation: 18/08/2011 9:23:16

00-041-1481 (I) - Anorthite, sodian, disordered - (Ca,Na)(Si,Al)4O8 - Triclinic - a 8.18130 - b 12.87400 - c 7.09700 - alpha 93.378 - beta 115.968 - gamma 90.776 - Primitive - P-1 (2) - 4 - 670.218

01-070-3753 (C) - Augite - (CaMg0.74Fe0.25)Si2O6 - Monoclinic - a 9.75000 - b 8.90100 - c 5.27400 - alpha 90.000 - beta 106.000 - gamma 90.000 - Base-centered - C2/c (15) - 4 - 439.972

00-035-0424 (*) - Nepheline, syn - NaAlSiO4 - Hexagonal - a 9.97800 - b 9.97800 - c 8.33000 - alpha 90.000 - beta 90.000 - gamma 120.000 - Primitive - P63 (173) - 8 - 718.228

00-034-0189 (*) - Forsterite, syn - Mg2SiO4 - Orthorhombic - a 5.98170 - b 10.19780 - c 4.75530 - alpha 90.000 - beta 90.000 - gamma 90.000 - Primitive - Pmnb (62) - 4 - 290.074

00-033-0664 (*) - Hematite, syn - Fe2O3 - Rhombo.H.axes - a 5.03560 - b 5.03560 - c 13.74890 - alpha 90.000 - beta 90.000 - gamma 120.000 - Primitive - R-3c (167) - 6 - 301.926

III: Atomic and weight composition of points selected during SEM analyses

III-1: **Figure III-1-10**: Microstructure of synthesized products at Na_2O/Al_2O_3 of 1.5: *A) 250 magnification, showing area of geopolymer matrix and undisolved particles;*

pt= point

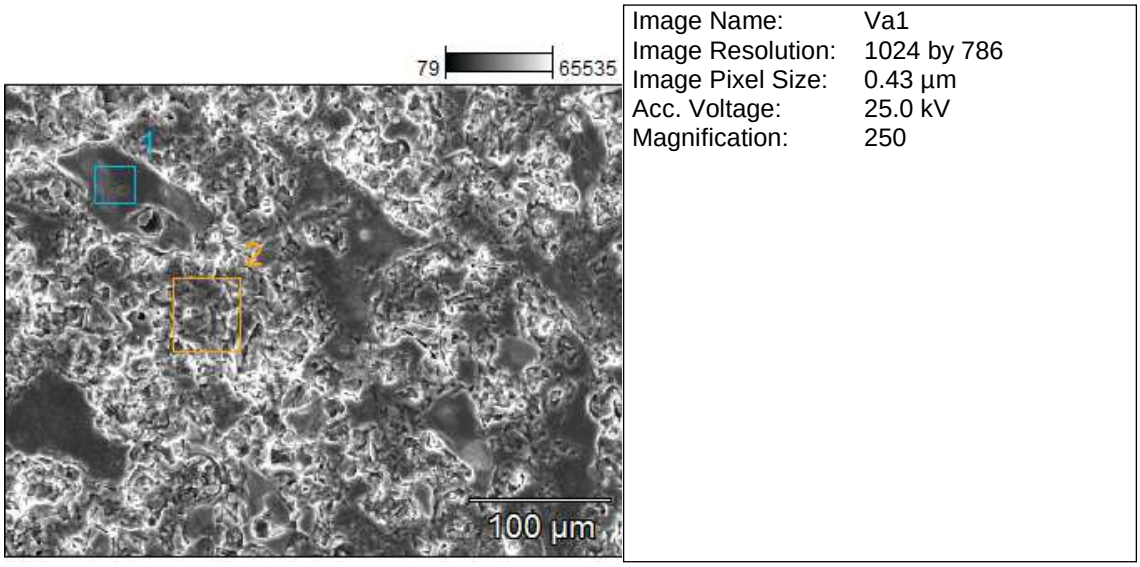

Weight %

	O-K	Na-K	Mg-K	Al-K	Si-K	P-K	Cl-K	K-K	Ca-K	Ti-K	Fe-K
Va1_pt1	35.9	8.5	3.2	7.3	21.6	0.3	0.1	1.4	11.1	2.1	8.5
Va1_pt2	41.0	14.0	1.8	6.3	17.4	0.3		1.4	8.1	1.9	7.7

Weight % Error (+/- 1 Sigma)

	O-K	Na-K	Mg-K	Al-K	Si-K	P-K	Cl-K	K-K	Ca-K	Ti-K	Fe-K
Va1_pt1	+/-0.5	+/-0.1	+/-0.1	+/-0.1	+/-0.1	+/-0.0	+/-0.0	+/-0.1	+/-0.1	+/-0.0	+/-0.1
Va1_pt2	+/-0.3	+/-0.2	+/-0.1	+/-0.1	+/-0.1	+/-0.0		+/-0.1	+/-0.1	+/-0.1	+/-0.1

Atom %

	O-K	Na-K	Mg-K	Al-K	Si-K	P-K	Cl-K	K-K	Ca-K	Ti-K	Fe-K
Va1_pt1	52.1	8.6	3.1	6.3	17.8	0.2	0.1	0.8	6.4	1.0	3.5
Va1_pt2	56.7	13.5	1.6	5.1	13.7	0.2		0.8	4.5	0.9	3.0

Atom % Error (+/- 1 Sigma)

	O-K	Na-K	Mg-K	Al-K	Si-K	P-K	Cl-K	K-K	Ca-K	Ti-K	Fe-K
Va1_pt1	+/-0.7	+/-0.1	+/-0.1	+/-0.1	+/-0.1	+/-0.0	+/-0.0	+/-0.0	+/-0.1	+/-0.0	+/-0.1
Va1_pt2	+/-0.4	+/-0.2	+/-0.1	+/-0.1	+/-0.1	+/-0.0		+/-0.0	+/-0.1	+/-0.0	+/-0.1

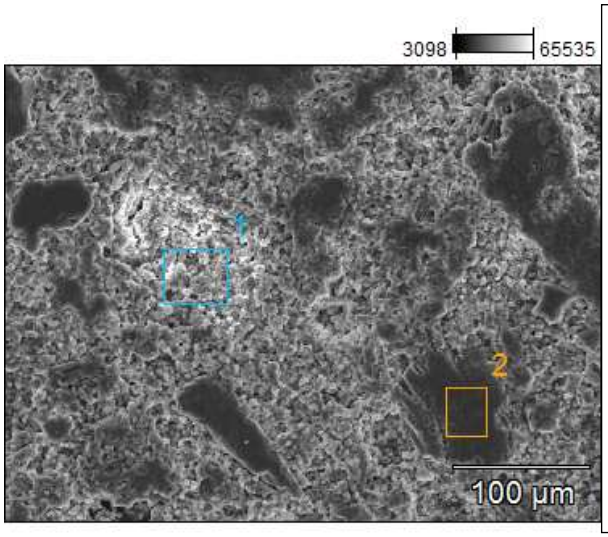

Image Name:	Va2
Image Resolution:	1024 by 786
Image Pixel Size:	0.43 µm
Acc. Voltage:	25.0 kV
Magnification:	250

Weight %

	O-K	Na-K	Mg-K	Al-K	Si-K	K-K	Ca-K	Ti-K	Mn-K	Fe-K
Va2(2)_pt1	44.8	8.6		4.4	33.9	4.8	1.2	0.4		2.0
Va2(2)_pt2	37.5	1.1	6.7	4.2	22.6		18.1	1.9	0.2	7.7

Weight % Error (+/- 1 Sigma)

	O-K	Na-K	Mg-K	Al-K	Si-K	K-K	Ca-K	Ti-K	Mn-K	Fe-K
Va2(2)_pt1	+/-0.3	+/-0.1		+/-0.1	+/-0.1	+/-0.1	+/-0.0	+/-0.0		+/-0.1
Va2(2)_pt2	+/-0.2	+/-0.1	+/-0.1	+/-0.1	+/-0.1		+/-0.1	+/-0.0	+/-0.0	+/-0.1

Atom %

	O-K	Na-K	Mg-K	Al-K	Si-K	K-K	Ca-K	Ti-K	Mn-K	Fe-K
Va2(2)_pt1	59.1	7.9		3.4	25.5	2.6	0.6	0.2		0.8
Va2(2)_pt2	55.0	1.1	6.5	3.7	18.9		10.6	0.9	0.1	3.2

Atom % Error (+/- 1 Sigma)

	O-K	Na-K	Mg-K	Al-K	Si-K	K-K	Ca-K	Ti-K	Mn-K	Fe-K
Va2(2)_pt1	+/-0.4	+/-0.1		+/-0.0	+/-0.1	+/-0.0	+/-0.0	+/-0.0		+/-0.0
Va2(2)_pt2	+/-0.3	+/-0.1	+/-0.1	+/-0.1	+/-0.1		+/-0.0	+/-0.0	+/-0.0	+/-0.0

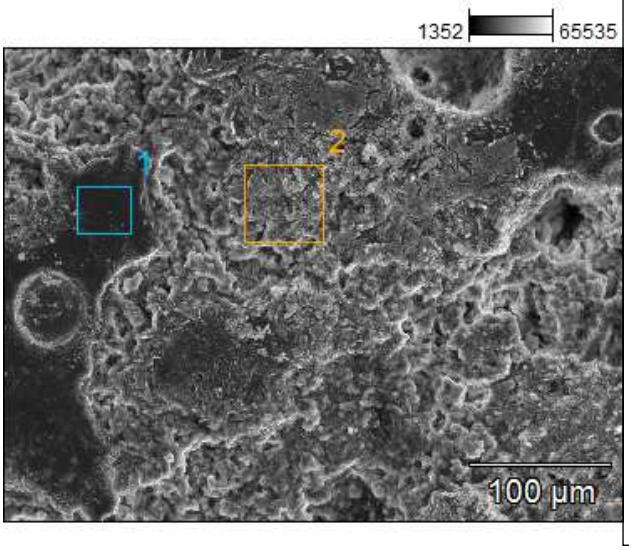

Image Name:	Va3
Image Resolution:	1024 by 786
Image Pixel Size:	0.43 µm
Acc. Voltage:	25.0 kV
Magnification:	250

Weight %

	O-K	Na-K	Mg-K	Al-K	Si-K	P-K	Cl-K	K-K	Ca-K	Ti-K	Fe-K
Va3_pt1	29.5	5.8	2.3	9.8	25.4	0.5	0.1	2.1	9.5	3.1	11.8
Va3_pt2	29.6	25.1	0.7	6.2	18.2	0.3	0.1	1.2	8.5	2.0	8.0

Weight % Error (+/- 1 Sigma)

	O-K	Na-K	Mg-K	Al-K	Si-K	P-K	Cl-K	K-K	Ca-K	Ti-K	Fe-K
Va3_pt1	+/-0.5	+/-0.1	+/-0.1	+/-0.1	+/-0.2	+/-0.0	+/-0.0	+/-0.1	+/-0.1	+/-0.1	+/-0.2
Va3_pt2	+/-0.5	+/-0.2	+/-0.1	+/-0.1	+/-0.1	+/-0.0	+/-0.0	+/-0.0	+/-0.1	+/-0.0	+/-0.1

Atom %

	O-K	Na-K	Mg-K	Al-K	Si-K	P-K	Cl-K	K-K	Ca-K	Ti-K	Fe-K
Va3_pt1	45.6	6.2	2.4	9.0	22.4	0.4	0.1	1.3	5.9	1.6	5.2
Va3_pt2	43.1	25.4	0.7	5.4	15.1	0.3	0.1	0.7	4.9	1.0	3.3

Atom % Error (+/- 1 Sigma)

	O-K	Na-K	Mg-K	Al-K	Si-K	P-K	Cl-K	K-K	Ca-K	Ti-K	Fe-K
Va3_pt1	+/-0.7	+/-0.1	+/-0.1	+/-0.1	+/-0.1	+/-0.0	+/-0.0	+/-0.0	+/-0.1	+/-0.0	+/-0.1
Va3_pt2	+/-0.7	+/-0.2	+/-0.1	+/-0.1	+/-0.1	+/-0.0	+/-0.0	+/-0.0	+/-0.1	+/-0.0	+/-0.1

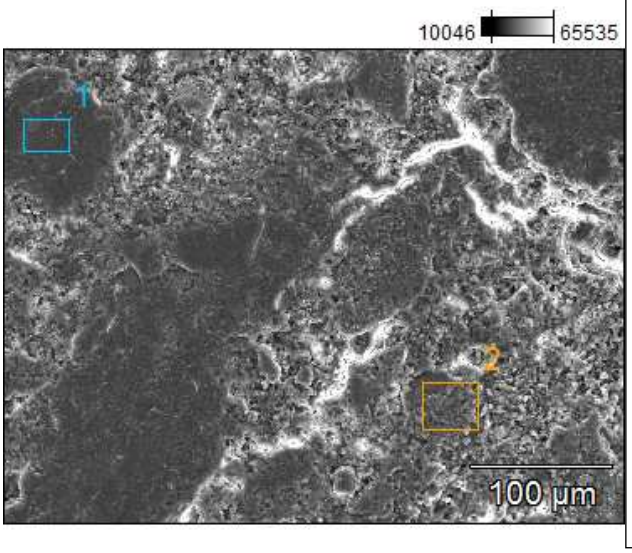

Image Name:	Va4
Image Resolution:	1024 by 786
Image Pixel Size:	0.43 µm
Acc. Voltage:	25.0 kV
Magnification:	250

Weight %

	O-K	Na-K	Mg-K	Al-K	Si-K	P-K	Cl-K	K-K	Ca-K	Ti-K	Mn-K	Fe-K
Va4_pt1	32.6	6.1	2.4	9.6	26.2	0.5	0.1	1.5	9.5	2.4	0.1	9.1
Va4_pt2	35.8	12.1	2.2	6.3	22.8	0.5		1.2	8.2	2.3	0.1	8.6

Weight % Error (+/- 1 Sigma)

	O-K	Na-K	Mg-K	Al-K	Si-K	P-K	Cl-K	K-K	Ca-K	Ti-K	Mn-K	Fe-K
Va4_pt1	+/-0.2	+/-0.1	+/-0.0	+/-0.1	+/-0.1	+/-0.0	+/-0.0	+/-0.0	+/-0.1	+/-0.0	+/-0.0	+/-0.1
Va4_pt2	+/-0.2	+/-0.1	+/-0.1	+/-0.1	+/-0.1	+/-0.0		+/-0.0	+/-0.1	+/-0.0	+/-0.0	+/-0.1

Atom %

	O-K	Na-K	Mg-K	Al-K	Si-K	P-K	Cl-K	K-K	Ca-K	Ti-K	Mn-K	Fe-K
Va4_pt1	48.6	6.3	2.3	8.5	22.3	0.4	0.1	0.9	5.6	1.2	0.1	3.9
Va_pt2	51.4	12.1	2.0	5.3	18.6	0.3		0.7	4.7	1.1	0.1	3.5

Atom % Error (+/- 1 Sigma)

	O-K	Na-K	Mg-K	Al-K	Si-K	P-K	Cl-K	K-K	Ca-K	Ti-K	Mn-K	Fe-K
Va4_pt1	+/-0.4	+/-0.1	+/-0.0	+/-0.1	+/-0.1	+/-0.0	+/-0.0	+/-0.0	+/-0.0	+/-0.0	+/-0.0	+/-0.0
Va4_pt2	+/-0.3	+/-0.1	+/-0.1	+/-0.1	+/-0.1	+/-0.0		+/-0.0	+/-0.0	+/-0.0	+/-0.0	+/-0.0

III-2: Figure III-2-8: SEM micrographs. a) Va-Na, b) Va-K

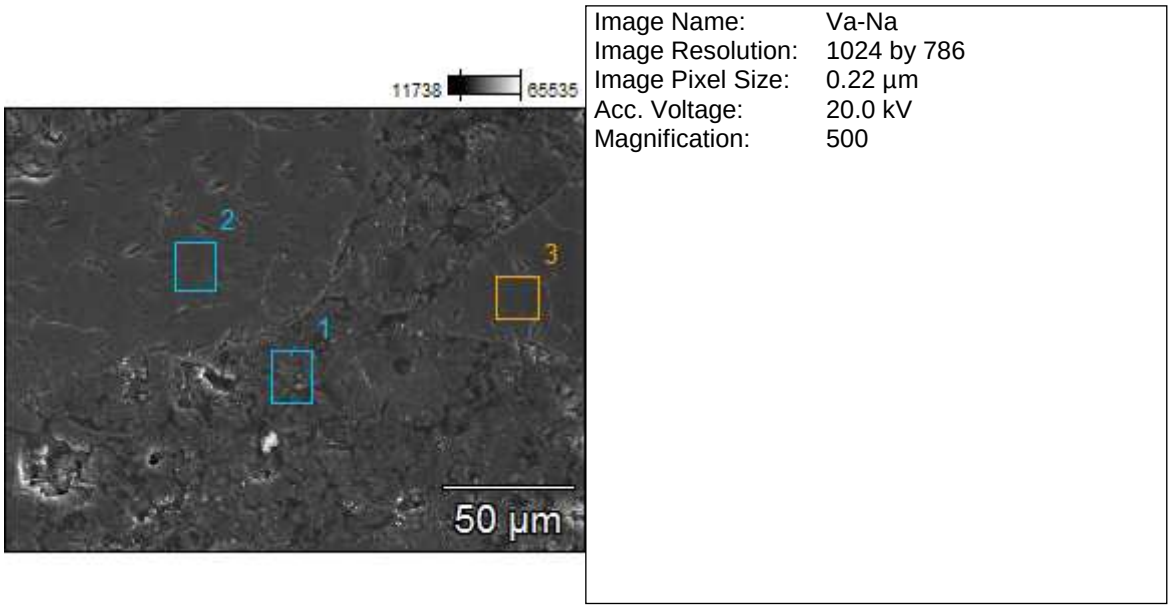

Weight %

	O-K	Na-K	Mg-K	Al-K	Si-K	P-K	K-K	Ca-K	Ti-K	Mn-K	Fe-K
Va-Na_pt1	20.44	18.13	0.90	10.11	25.08	0.52	2.37	10.28	2.30		9.87
Va-Na_pt2	11.95	0.51	34.10		33.08		0.15	0.41		0.31	19.51
Va-Na _pt3	17.76	1.62	8.46	6.12	30.72			26.07	1.79	0.27	7.20

Weight % Error (+/- 1 Sigma)

	O-K	Na-K	Mg-K	Al-K	Si-K	P-K	K-K	Ca-K	Ti-K	Mn-K	Fe-K
Va-Na _pt1	+/-0.21	+/-0.13	+/-0.12	+/-0.15	+/-0.10	+/-0.05	+/-0.05	+/-0.13	+/-0.06		+/-0.21
Va-Na _pt2	+/-0.29	+/-0.06	+/-0.17		+/-0.14		+/-0.03	+/-0.04		+/-0.07	+/-0.24
Va-Na _pt3	+/-0.20	+/-0.09	+/-0.06	+/-0.12	+/-0.14			+/-0.15	+/-0.05	+/-0.06	+/-0.17

Atom %

	O-K	Na-K	Mg-K	Al-K	Si-K	P-K	K-K	Ca-K	Ti-K	Mn-K	Fe-K
Va-Na _pt1	32.52	20.07	0.95	9.54	22.72	0.43	1.54	6.53	1.22		4.50
Va-Na _pt2	20.08	0.59	37.73		31.67		0.10	0.27		0.15	9.39
Va-Na _pt3	30.24	1.92	9.48	6.18	29.80			17.72	1.02	0.13	3.51

Atom % Error (+/- 1 Sigma)

	O-K	Na-K	Mg-K	Al-K	Si-K	P-K	K-K	Ca-K	Ti-K	Mn-K	Fe-K
Va-Na _pt1	+/-0.33	+/-0.14	+/-0.13	+/-0.14	+/-0.09	+/-0.04	+/-0.03	+/-0.09	+/-0.03		+/-0.10
Va-Na _pt2	+/-0.48	+/-0.07	+/-0.18		+/-0.13		+/-0.02	+/-0.02		+/-0.03	+/-0.12
Va-Na _pt3	+/-0.35	+/-0.11	+/-0.07	+/-0.12	+/-0.13			+/-0.10	+/-0.03	+/-0.03	+/-0.08

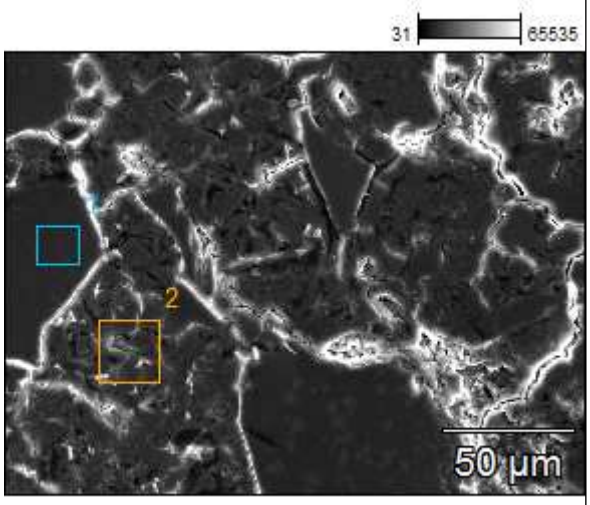

Image Name:	Va-K
Image Resolution:	1024 by 786
Image Pixel Size:	0.22 µm
Acc. Voltage:	20.0 kV
Magnification:	500

Weight %

	O-K	Na-K	Mg-K	Al-K	Si-K	P-K	K-K	Ca-K	Ti-K	Mn-K	Fe-K
Va-K_pt1	14.87		30.56		30.03		0.54	0.55		0.36	23.09
Va-K _pt2	18.24	4.65	3.02	9.07	22.73	0.45	16.74	11.07	1.76		12.27

Weight % Error (+/- 1 Sigma)

	O-K	Na-K	Mg-K	Al-K	Si-K	P-K	K-K	Ca-K	Ti-K	Mn-K	Fe-K
Va-K _pt1	+/-0.28		+/-0.16		+/-0.14		+/-0.04	+/-0.04		+/-0.07	+/-0.27
Va-K _pt2	+/-0.24	+/-0.08	+/-0.06	+/-0.13	+/-0.09	+/-0.04	+/-0.15	+/-0.17	+/-0.06		+/-0.22

Atom %

	O-K	Na-K	Mg-K	Al-K	Si-K	P-K	K-K	Ca-K	Ti-K	Mn-K	Fe-K
Va-K _pt1	25.10		33.95		28.87		0.37	0.37		0.18	11.16
Va-K _pt2	31.77	5.64	3.46	9.38	22.56	0.41	11.93	7.70	1.02		6.13

Atom % Error (+/- 1 Sigma)

	O-K	Na-K	Mg-K	Al-K	Si-K	P-K	K-K	Ca-K	Ti-K	Mn-K	Fe-K
Va-K _pt1	+/-0.47		+/-0.17		+/-0.13		+/-0.03	+/-0.03		+/-0.03	+/-0.13
Va-K _pt2	+/-0.42	+/-0.09	+/-0.07	+/-0.14	+/-0.09	+/-0.04	+/-0.11	+/-0.12	+/-0.03		+/-0.11

LIST OF PUBLICATIONS AND COMMUNICATIONS FROM THE THESIS

Refereed international journal papers

1. **P.N. Lemougna**, U.F. Chinje Melo, M.P. Delplancke, H. Rahier, **Influence of the chemical and mineralogical composition on the reactivity of volcanic ashes during geopolymers synthesis**, Ceramics International, DOI 10.1016/j.ceramint.2013.06.072.

2. **Patrick N. Lemougna,** U.F. Chinje Melo, M.P. Delplancke, H. Rahier, **Influence of the activating solution's composition on the stability and thermomechanical properties of volcanic ash-based geopolymers,** Construction and Building Materials, 48, 2013, 278–286.

3. **Patrick N. Lemougna**, Kenneth J. D. MacKenzie, Guy N. L. Jameson, H. Rahier, U. F. Chinje Melo, **The role of iron in the formation of inorganic polymers (geopolymers) from volcanic ash: a ^{57}Fe Mössbauer spectroscopy study**, J Mater Sci, 48, 2013, pp5280–5286.

4. **Patrick N. Lemougna**, Kenneth J.D. MacKenzie, U.F. Chinje Melo, **Synthesis and thermal properties of inorganic polymers (geopolymers) for structural and refractory applications from volcanic ash**, Ceram. Int. 37, 2011, pp 3011-3018.

Refereed international conferences

- Patrick N. Lemougna, Kenneth J.D. MacKenzie, U.F. Chinje Melo, Development of low-energy building materials and refractories from Cameroonian volcanic ash: presented at the 9th International Conference of the Pacific Rim Ceramic Societies (PACRIM 9), in July 10-14, 2011 in Cairns, Australia.

- P. Lemougna, U.F. Chinje Melo, M.P. Delplancke, H. Rahier, Influence of the activating solution's composition on products stability and thermomechanical properties of volcanic ash-based geopolymers: presented at the 36th International Conference & Exposition on Advanced Ceramics & Composites (ICACC) in January 22-27, 2012 in Daytona Beach, Florida, USA

- P.N Lemougna; E. Kamseu; U.C. Melo, Volcanic ash based geopolymer: a potential opportunity for environmentally-friendly building materials in Cameroon: presented at the 4th edition of EG@ conference on training, research, innovation and development, in December 4-6, 2012 at National Polytechnic School, Yaoundé, Cameroon.